Hyperspectral Remote Sensing of Vegetation:

Knowledge Gain and Knowledge Gap After 40 years of Research


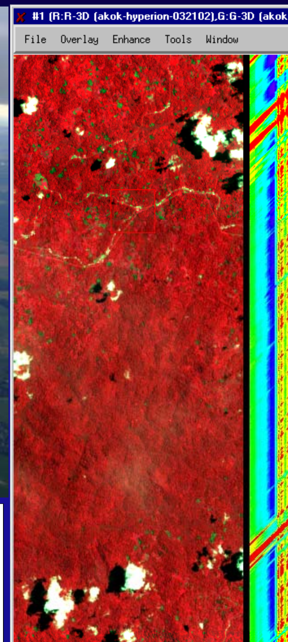


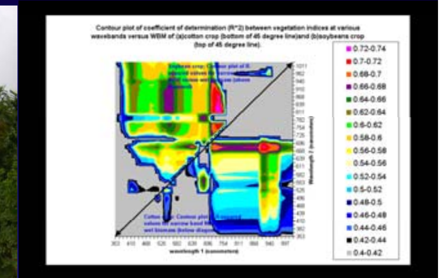

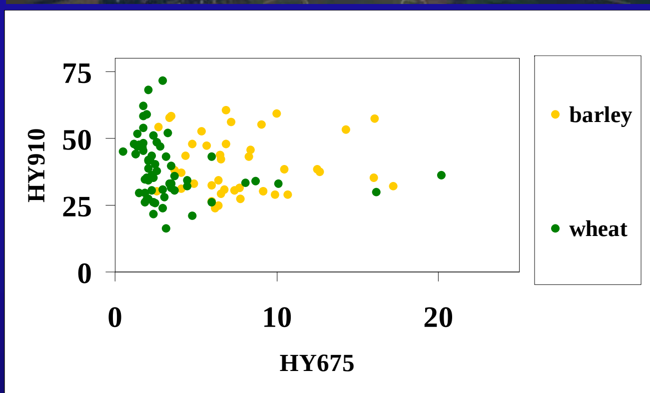

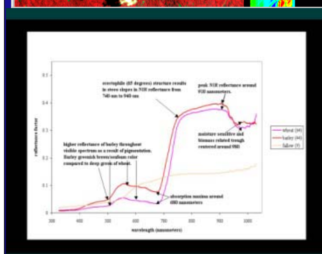
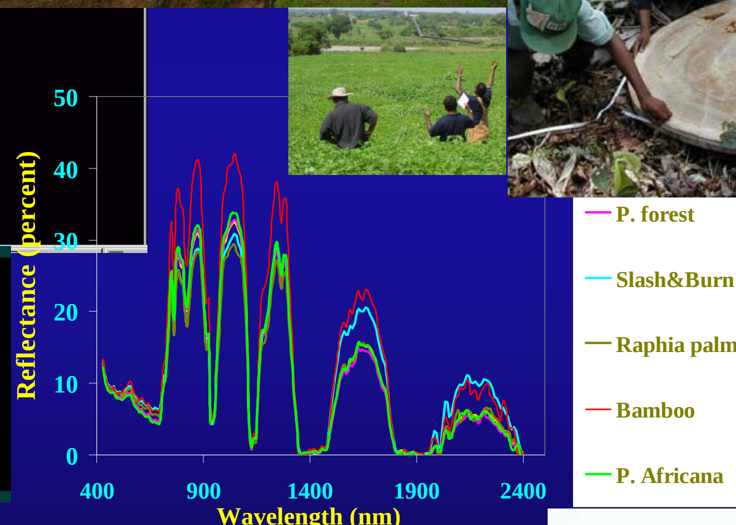



Prasad S. Thenkabail

Research Geographer, U.S. Geological Survey (USGS)

Landsat Science Team Meeting

USGS EROS Data Center, Sioux Falls, SD, USA. August 16-18, 2011

U.S. Geological Survey
U.S. Department of Interior

*"More Data (e.g., spectral, spatial, temporal, radiometric) is good.
Better understanding of data for application of interest is better.
However, current knowledge gap in understanding data and it's uncertainty is far greater than we want to admit"*
- A Thought for the lecture.

Hyperspectral Remote Sensing Vegetation
References Pertaining to this Presentation

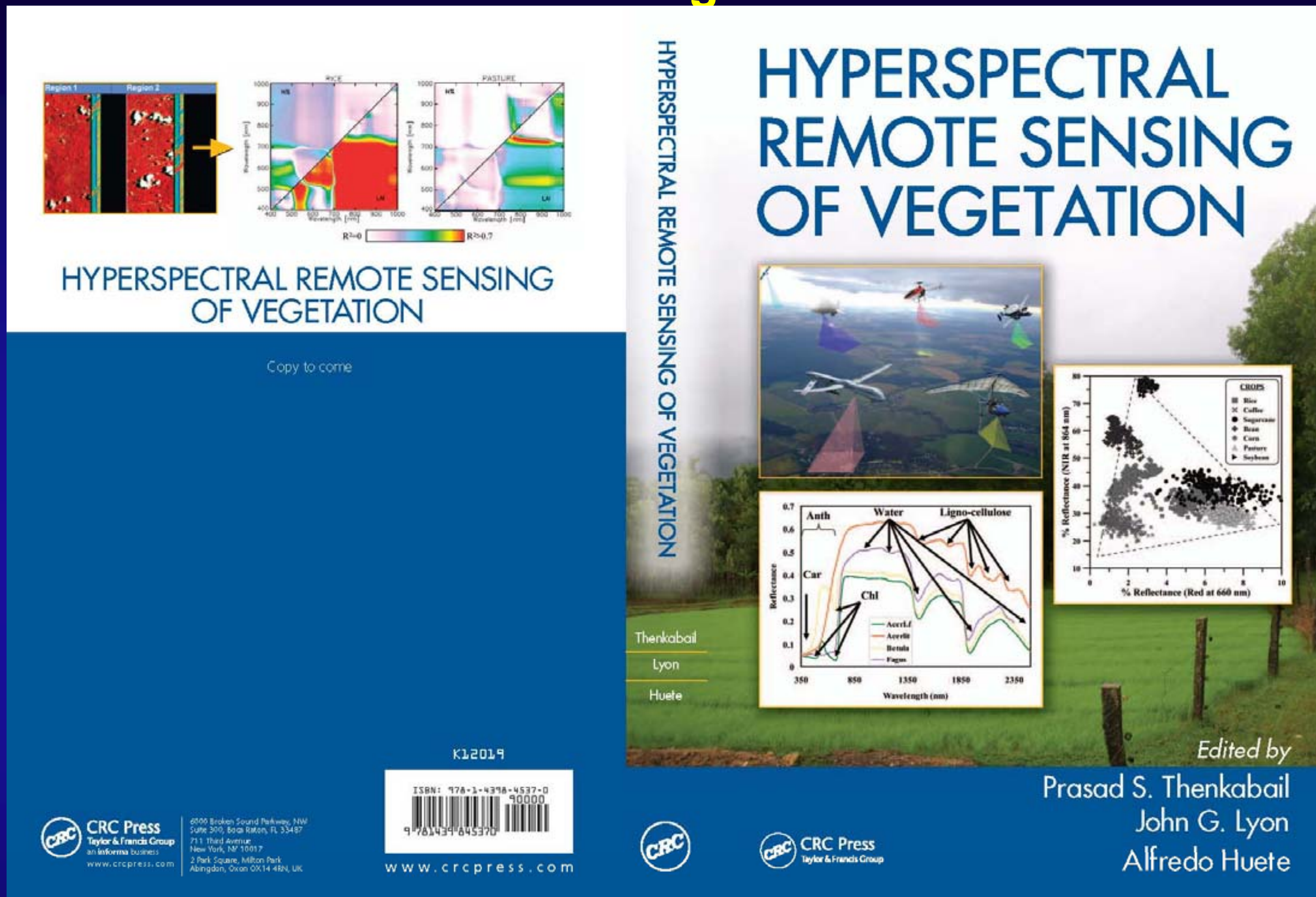

Thenkabail, P.S., Lyon, G.J., and Huete, A. 2011. Book entitled: "Hyperspectral Remote Sensing of Vegetation". 28 Chapters. CRC Press- Taylor and Francis group, Boca Raton, London, New York. Pp. 700+ (80+ pages in color). To be published by October 31, 2011.

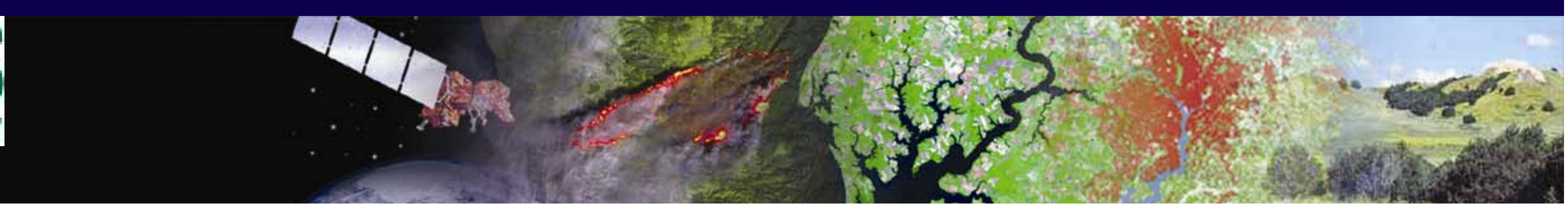

Importance of
Hyperspectral Sensors (Imaging Spectrometry) in
Study of Vegetation

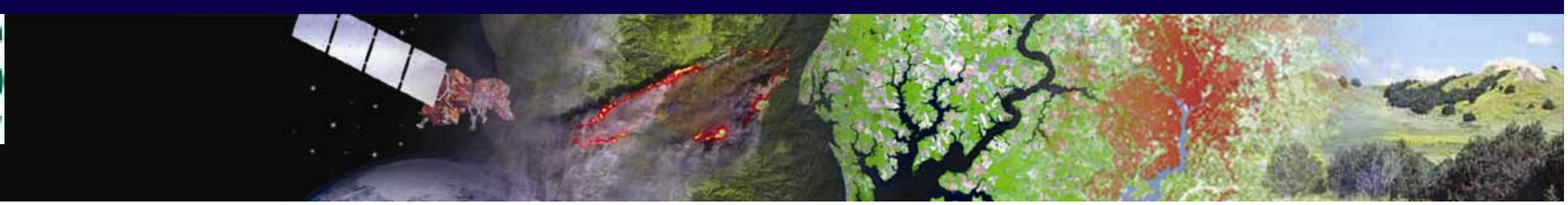

science for a changing world
U.S. Geological Survey
U.S. Department of Interior

Hyperspectral Remote Sensing of Vegetation

Importance of Hyperspectral Sensors (Imaging Spectroscopy) in Study of Vegetation

More specifically…………..hyperspectral Remote Sensing, originally used for detecting and mapping minerals, is increasingly needed for to characterize, model, classify, and map agricultural crops and natural vegetation, specifically in study of:

(a)Species composition (e.g., *chromolenea odorata vs. imperata cylindrica*);
(b)Vegetation or crop type (e.g., soybeans vs. corn);
(c)Biophysical properties (e.g., LAI, biomass, yield, density);
(d)Biochemical properties (e.g, Anthrocyanins, Carotenoids, Chlorophyll);
(e)Disease and stress (e.g., insect infestation, drought),
(f)Nutrients (e.g., Nitrogen),
(g)Moisture (e.g., leaf moisture),
(h)Light use efficiency,
(i)Net primary productivity and so on.

……….in order to increase accuracies and reduce uncertainties in these parameters……..

Hyperspectral Remote Sensing of Vegetation

Spectral Wavelengths and their Importance in the Study of Vegetation Biochemical properties

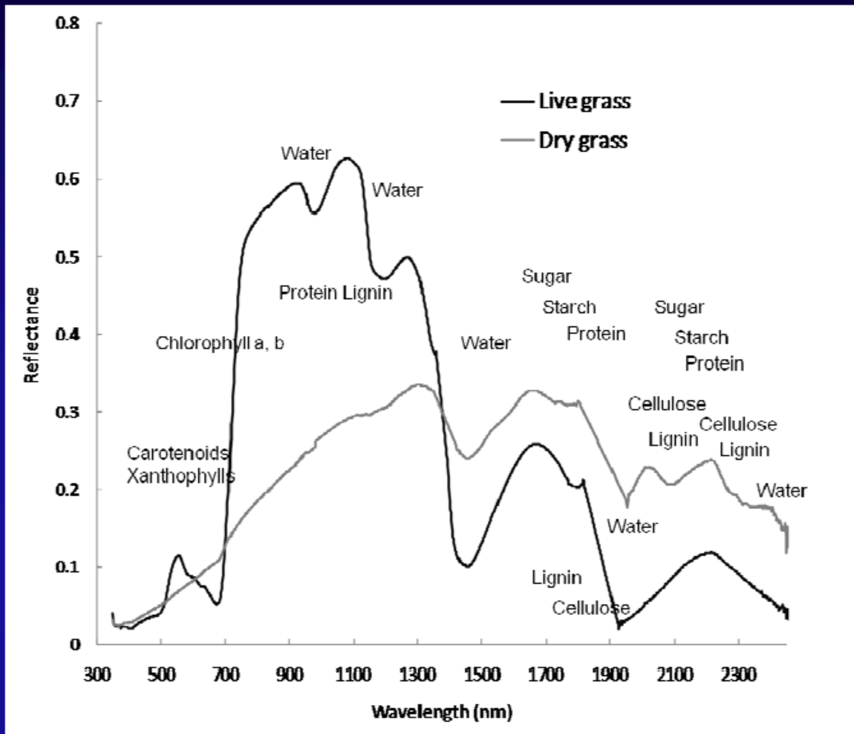

The reflectance spectra with characteristic absorption features associated with plant biochemical constitutents for live and dry grass (Adapted from Hill [13]).

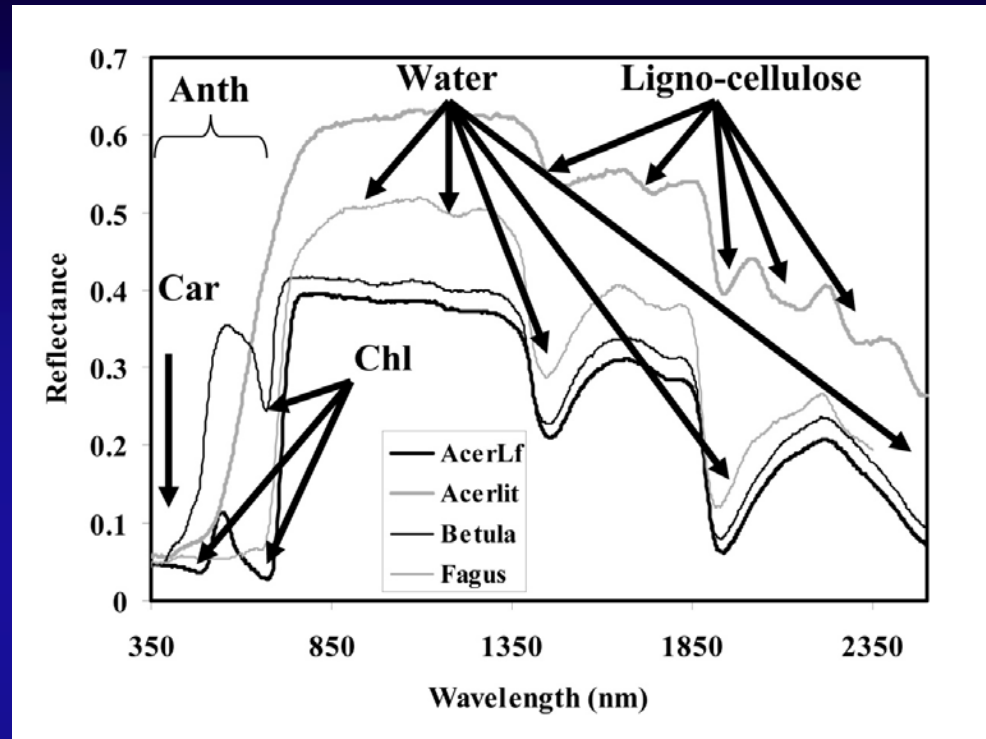

Reflectance spectra of leaves from a senesced birch (Betula), ornamental beech (Fagus) and healthy and fully senesced maple (AcerLf, Acerlit) illustrating Carotenoid (Car), Anthocyanin (Anth), Chlorophyll (Chl), Water and Ligno-cellulose absorptions.

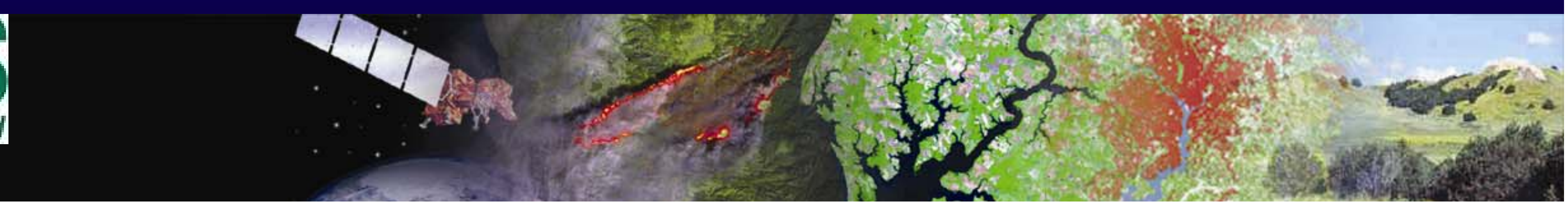

Definition of
Hyperspectral Sensors (Imaging Spectrometry) in
Study of Vegetation

Hyperspectral Remote Sensing of Vegetation

Definition of Hyperspectral Data

A. consists of hundreds or thousands of narrow-wavebands (as narrow as 1; but generally less than 5 nm) along the electromagnetic spectrum;

B. it is important to have narrowbands that are contiguous for strict definition of hyperspectral data; and not so much the number of bands alone (Qi et al. in Chapter 3, Goetz and Shippert).

…………Hyperspectral Data is fast emerging to provide practical solutions in characterizing, quantifying, modeling, and mapping natural vegetation and agricultural crops.

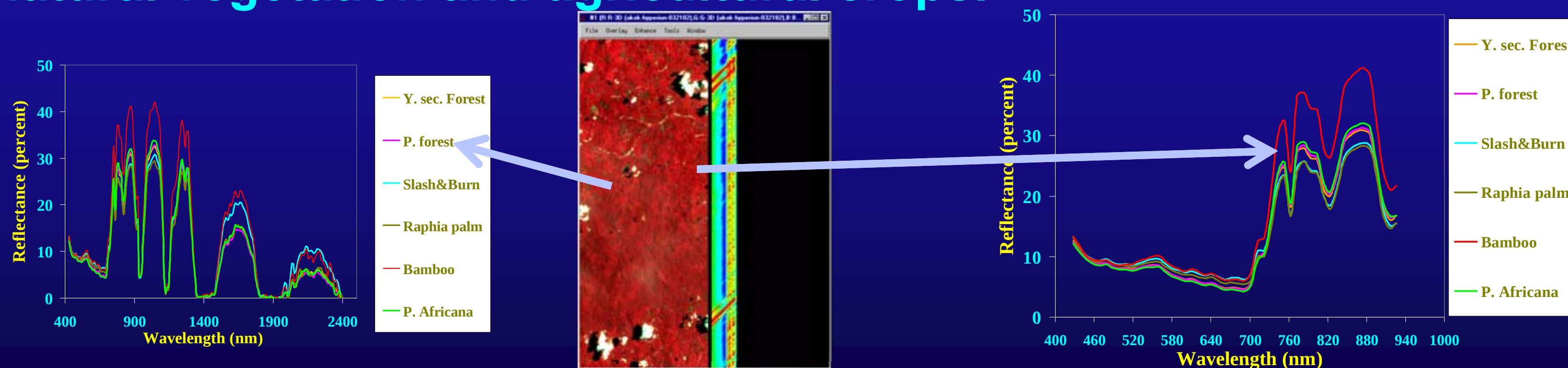

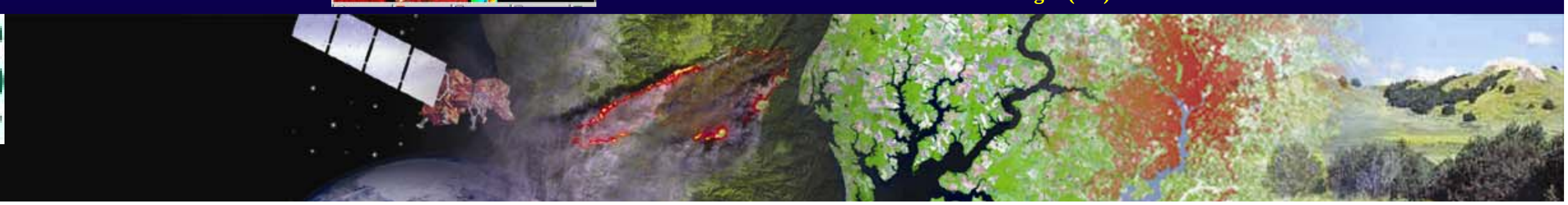

Hyperspectral Remote Sensing of Vegetation
Truck-mounted Hyperspectral sensors

The advantage of airborne, ground-based, and truck-mounted sensors are that they enable relatively cloud free acquisitions that can be acquired on demand anywhere; over the years they have also allowed careful study of spectra in controlled environments to advance the genre.

(a) (b) (c)

Truck-mounted Hyperspectral Data Acquisition example

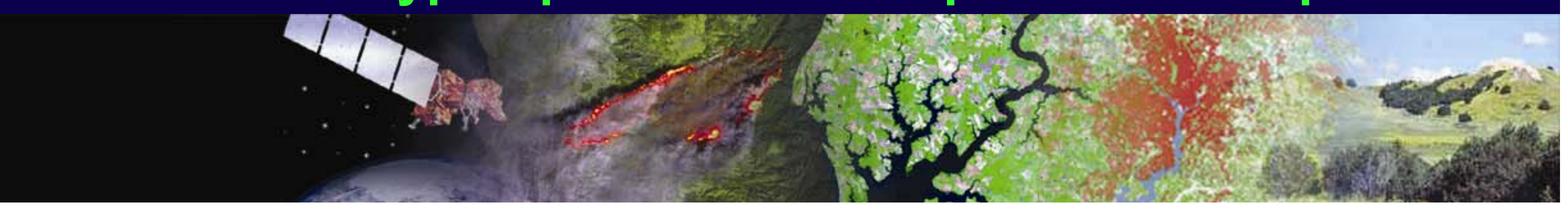

Hyperspectral Remote Sensing of Vegetation

Spaceborne Hyperspectral Imaging Sensors: Some Characteristics

Instrument (Satellite)	Altitude, km	Pixel Size, m	Number Bands	Spectral Range, nm	Spectral Resolution, nm	IFOV, µrad	Swath, km
HSI (SIMSA)	523	25	220	430-2400	20	47.8	7.7
FTHSI (MightySatII)	565	30	256	450-1050	10-50	50	13
Hyperion (EO-1)	705	30	220	400-2500	10	42.5	7.5
CHRIS (PROBA)	580	25	19	400-1050	1.25-11.0	43.1	17.5
COIS (NEMO)	605	30	210	400-2500	10	49.5	30
ARIES-1 (ARIES-1)	500	30	32 32 32	400–1100 2000-2500 1000-2000	22 16 31	60	15
UKON-B	400	20	256	400-800	4-8	50	15
Warfighter-1 (OrbView-4)	470	8	200 80	450-2500 3000-5000	11	20	5
EnMAP	675	30	92 108	420-1030 950-2450	5-10 10-20	30	30
HypSEO (MITA)	620	20	~210	400-2500	10	40	20
MSMI (SUNSAT)	660	15	~200	400-2350	10	22	15
PRISMA	695	30	250	400-2500	<10	40	30
ARTEMIS (TacSat-3)	425	4	400	400-2500	5	70	~10
HyspIRI	~700	60	>200	380-2500	10	80	145
SUPERSPEC (MYRIADE)	720	20	8	430-910	20	30	120
VENµS	720	5.3	12	415-910	16-40	8	27.5
Global Imager (ADEOS-2)	802	250-1000	36	380-1195	10-1000	310-1250	1600
WFIS (like MODIS)	705	1400	630	400-1000	1-5	2000	2400

Existing hyperspectral spaceborne missions:
1. Hyperion (USA's NASA),
2. PROBA (Europe's ESA;'s), and

There are some twenty spaceborne hyperspectral sensors

The advantages of spaceborne systems are their capability to acquire data: (a) continuously, (b) consistently, and (c) over the entire globe. A number of system design challenges of hyperspectral data are discussed in Chapter 3 by Qi et al. Challenges include cloud cover and large data volumes.

The 4 near future hyperspectral spaceborne missions:
1. PRISMA (Italy's ASI's),
2. EnMAP (Germany's DLR's), and
3. HISUI (Japanese JAXA);
4. HyspIRI (USA's NASA).

will all provide 30 m spatial resolution hyperspectral images with a 30 km swath width, which may enable a provision of high temporal resolution, multi-angular hyperspectral observations over the same targets for the hyperspectral BRDF characterization of surface.

The multi-angular hyperspectral observation capability may be one of next important steps in the field of hyperspectral remote sensing.

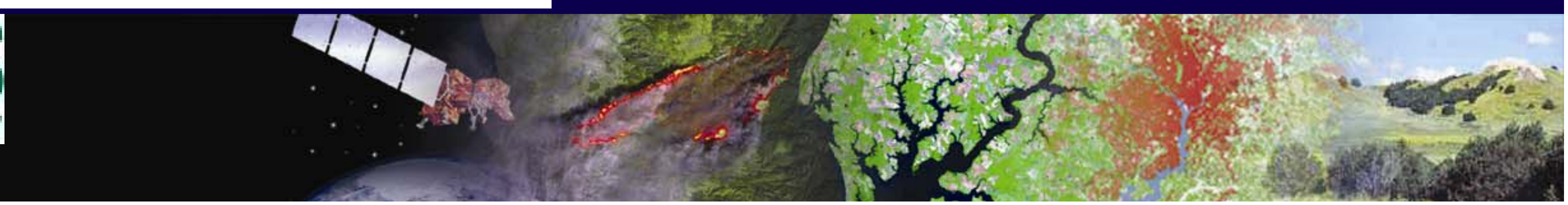

Hyperspectral Remote Sensing of Vegetation

Earth and Planetary Hyperspectral Remote Sensing Instruments

		Hyperspectral Instrument	Spectral Range (nm)	# of Channels	Spectral Bandpass	Spatial Resolution	Operational Dates
Earth							
		AVIRIS[1]	380 - 2500	224	10 nm	4 - 20 m	1989 - present
		ProSpecTIR-VS[2]	400 - 2450	256	2.3 - 20 nm	1 - 10 m	~2000 - present
	Airborne	HyMap[3]	400 - 2500	128	15 nm	2 - 10 m	~1997 - present
		CASI[4]	400 - 1000	288	2 - 12 nm	0.5 - 10 m	~1990 - present
		SFSI[5]	1230 - 2380	230	10 nm	0.5 - 10 m	1990 - present
	Spaceborne	EO-1 Hyperion[6]	400 - 2500	220	10 nm	30 m	2001 - present
Mercury		MESSENGER MASCS[7]	220 - 1450	768	0.2 - 0.5 nm	1 - 650 km	2004 - present
Moon		Chandrayaan-1 Moon Mineralogy Mapper[8]	400 - 2900	260	10 nm	70 - 140 m	2008 - 2009
Mars		Mars Express OMEGA[9]	350 - 5100	352	7 - 20 nm	300 m - 4.8 km	2003 - present
		Mars Reconnaissance Orbiter CRISM[10]	362 - 3920	545	6.55 nm	15.7 m - 200 m	2005 - present
Jupiter		Galileo NIMS[11]	700 - 5200	1 - 408	12.5 & 25 nm	50 - 500 km	1989 - 2003
Saturn		Cassini VIMS[12]	300 - 5100	352	7 & 14 nm	10 - 20 km	1997 - present

1 - Airborne Visible Infrared Imaging Spectrometer (http://aviris.jpl.nasa.gov)
2 - Spectral Technology and Innovative Research Corporation Hyperspectral Imaging Spectrometer (http://www.spectir.com/assets/Images/Capabilities/ProspecTIR%20specs.pdf)
3 - HyVista Corporation Hyperspectral Mapper, developed by Integrated Spectronics (http://www.hyvista.com/main.html and http://www.intspec.com)
4 - Compact Airborne Spectrographic Imager (http://www.geomatics-group.co.uk/GeoCMS/Products/CASI.aspx)
5 - SWIR Full Spectrum Imager (http://www.borstad.com/sfsi.html)
6 - Hyperion (http://eo1.gsfc.nasa.gov/Technology/Hyperion.html)
7 - Mercury Atmospheric and Surface Composition Spectrometer (http://www.messenger-education.org/instruments/mascs.htm)
8 - M^3 (http://moonmineralogymapper.jpl.nasa.gov/INSTRUMENT/)
9 - Observatoire pour la Minéralogie, l'Eau, les Glaces et l'Activité (http://sci.esa.int/science-e/www/object/index.cfm?fobjectid=34826&fbodylongid=1598)
10 - Compact Reconnaissance Imaging Spectrometer for Mars (http://crism.jhuapl.edu/)
11 - Near-Infrared Mapping Spectrometer (http://www2.jpl.nasa.gov/galileo/instruments/nims.html)
12 - Visual and Infrared Mapping Spectrometer (http://wwwvims.lpl.arizona.edu/)

See chapter 27, Vaughan et al.

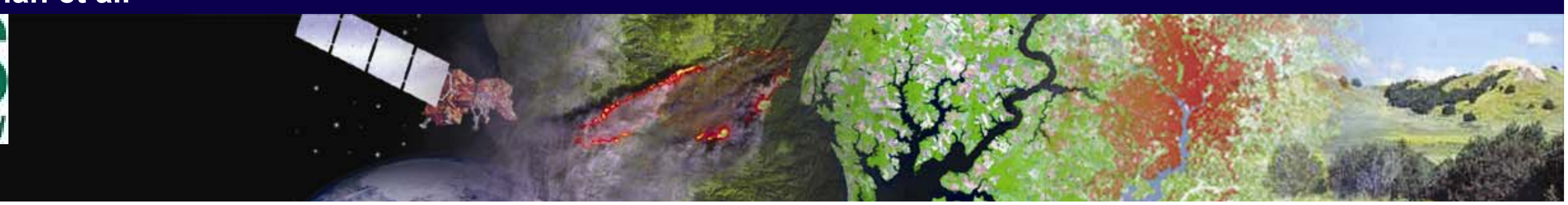

Comparison of Hyperspectral Data with Data from Other Advanced Sensors

Hyperspectral, Hyperspatial, and Advanced Multi-spectral Data

Satellite/Sensor or pixels	spatial resolution (meters)	spectral bands (#)	data points per hectare
Earth Observing-1			
Hyperion	30	196 (400-2500 nm)	11.1
ALI	10 m (P), 30 m (M)	1, 9	100, 11.1
IKONOS 2 SpaceImaging	1 m (P), 4 m (M)	4	10000, 625
QUICKBIRD Digital Globe	0.61 m (P), 2.44 m (M)	4	16393, 4098
Terra: Earth Observing System (EOS)			
ASTER	15 m, 30 m, 90 m (VNIR,SWIR,TIR)	4,6,5	44.4,11.1,1.26
MODIS	250-1000 m	36	0.16, 0.01
Landsat-7 ETM+	15 m (P), 30 m (M)	7	44.4,11.1
Landsat-4, 5 TM	30 m (M)	7	11.1
SPOT-1,2,3, 4,5 HRV	2.5 m. 5m, 10 m (P/M), 20 m (M)	4	
1600,400,100,25			
IRS-1C LISS	5 m (P), 23.5 m (M)	3	400, 18.1
IRS-1D LISS	5 m (P), 23.5 m (M)	3	400, 18.1

USGS
science for a changing world

U.S. Geological Survey
U.S. Department of Interior

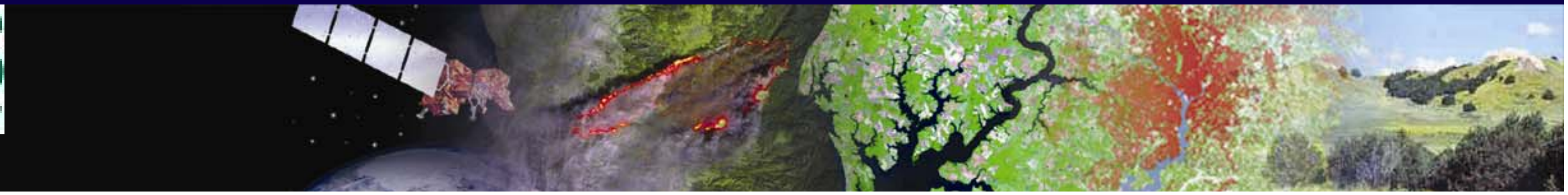

Hyperion Data from EO-1 (e.g., in Rainforests of Cameroon)

Hyperspectral Data Cube Providing Near-continuous data of 100's of Wavebands

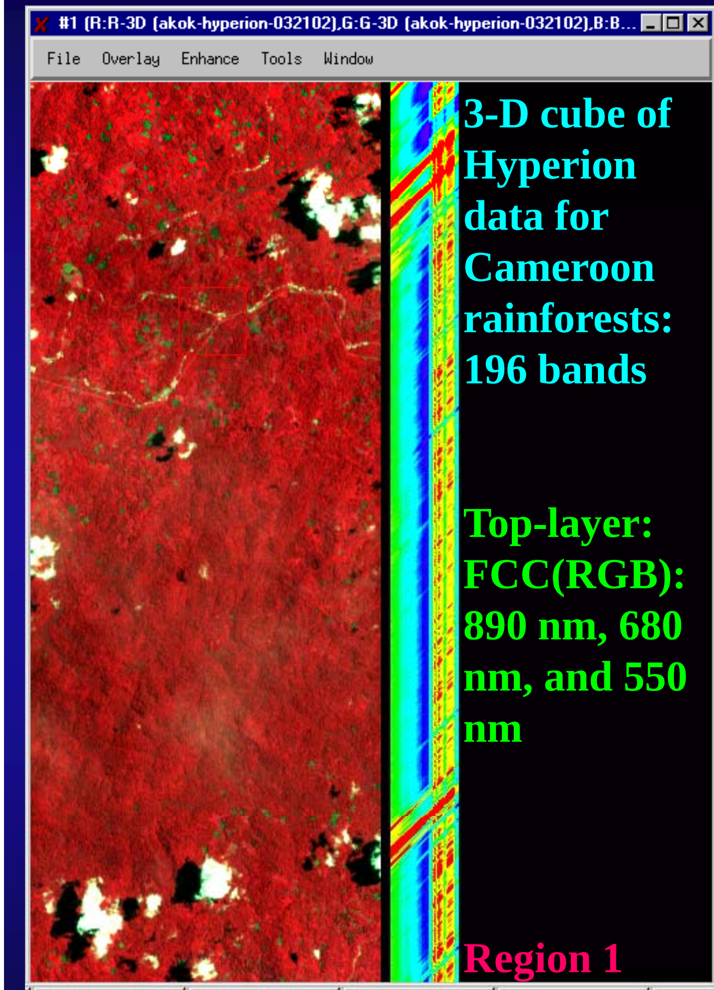

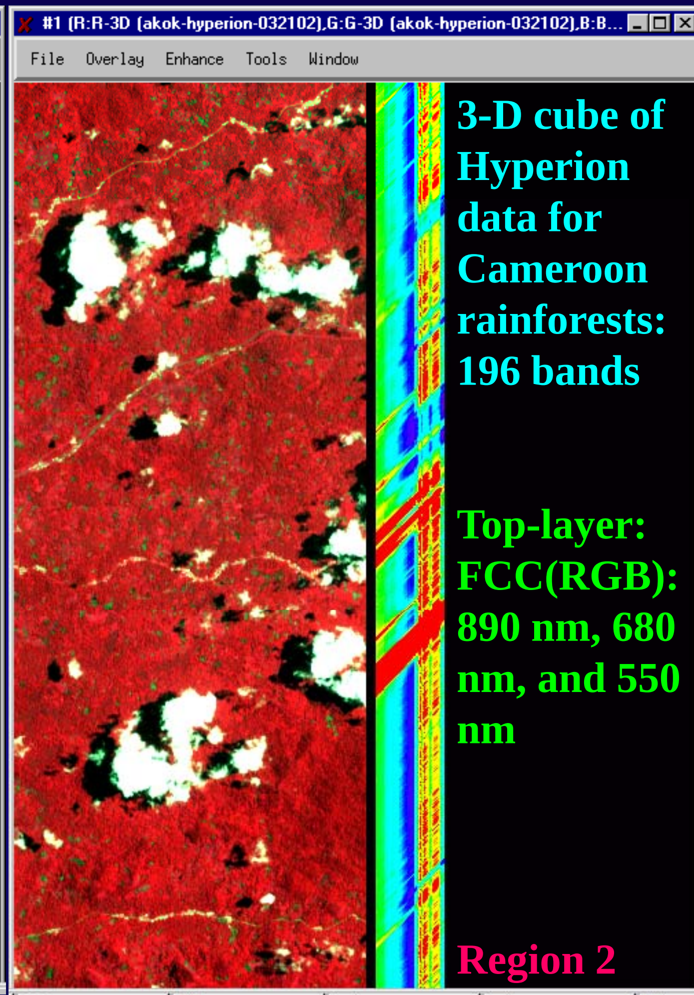

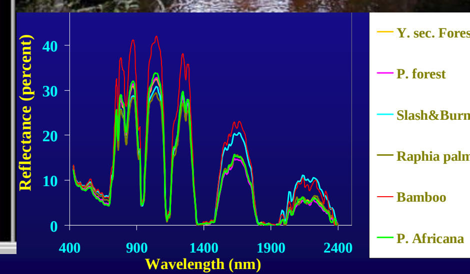

USGS
science for a changing world
U.S. Geological Survey
U.S. Department of Interior

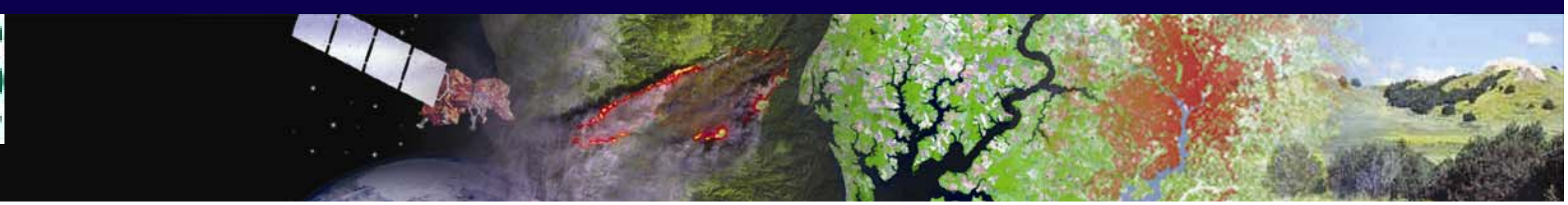

Hyperion Narrow-Band Data from EO-1 Vs. ETM+ Broad-band Data

Hyperspectral Data Provides Numerous Ways of Looking at Data

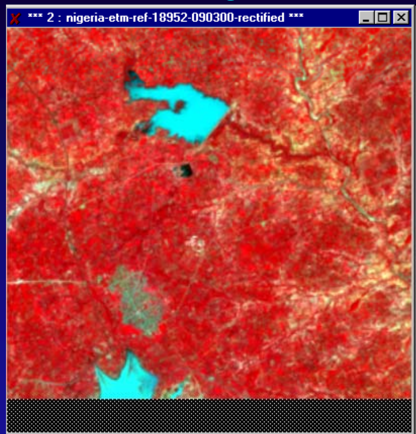

ETM+:4,3,2

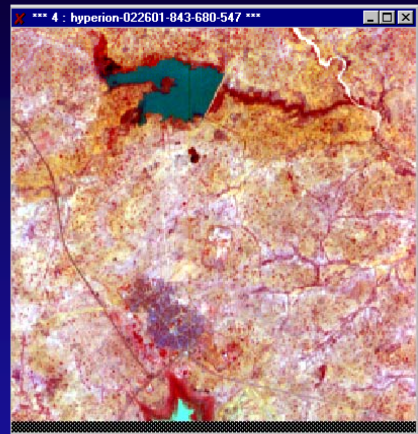

Hyperion:843, 680, 547

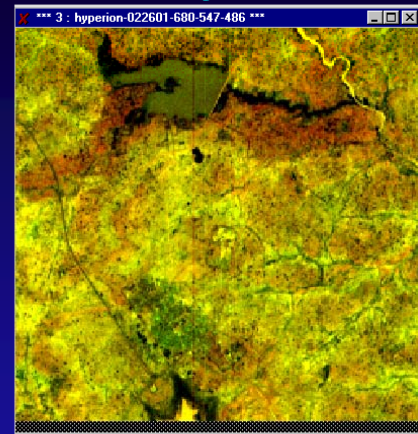

Hyperion: 680, 547, 486

Hyperion:905, 680, 547

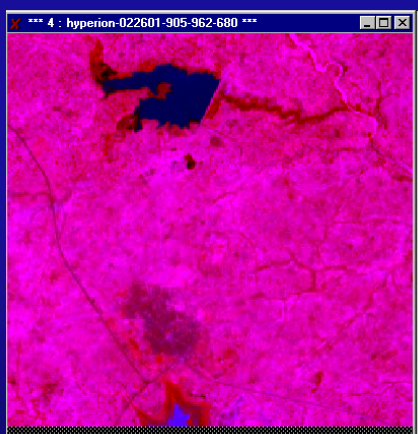

Hyperion:905, 962, 680

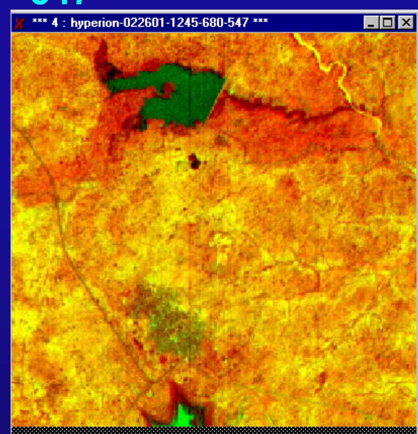

Hyperion:1245, 680, 547

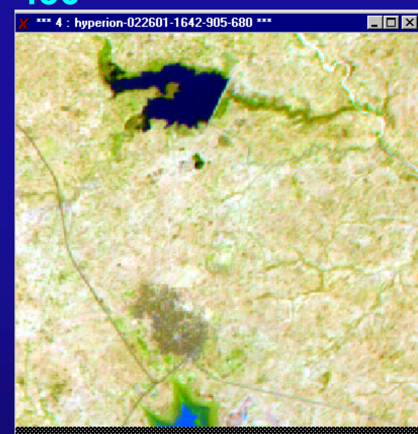

Hyperion:1642, 905, 680

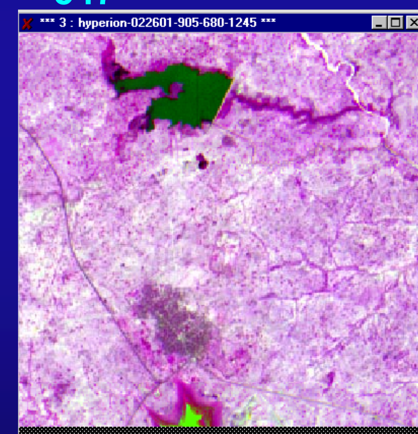

Hyperion:904,680,1245

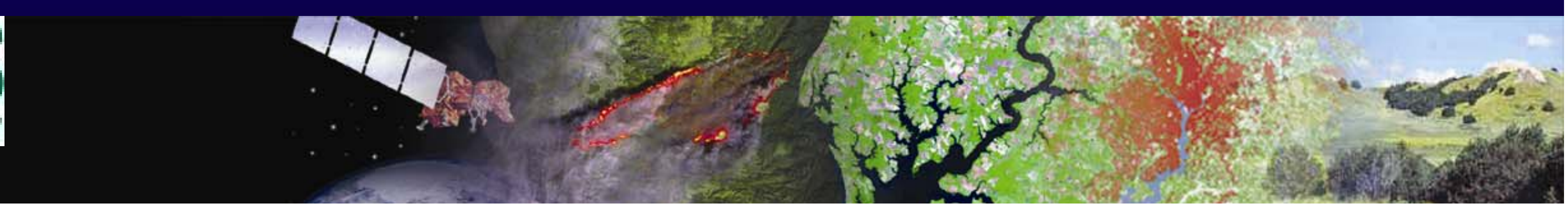

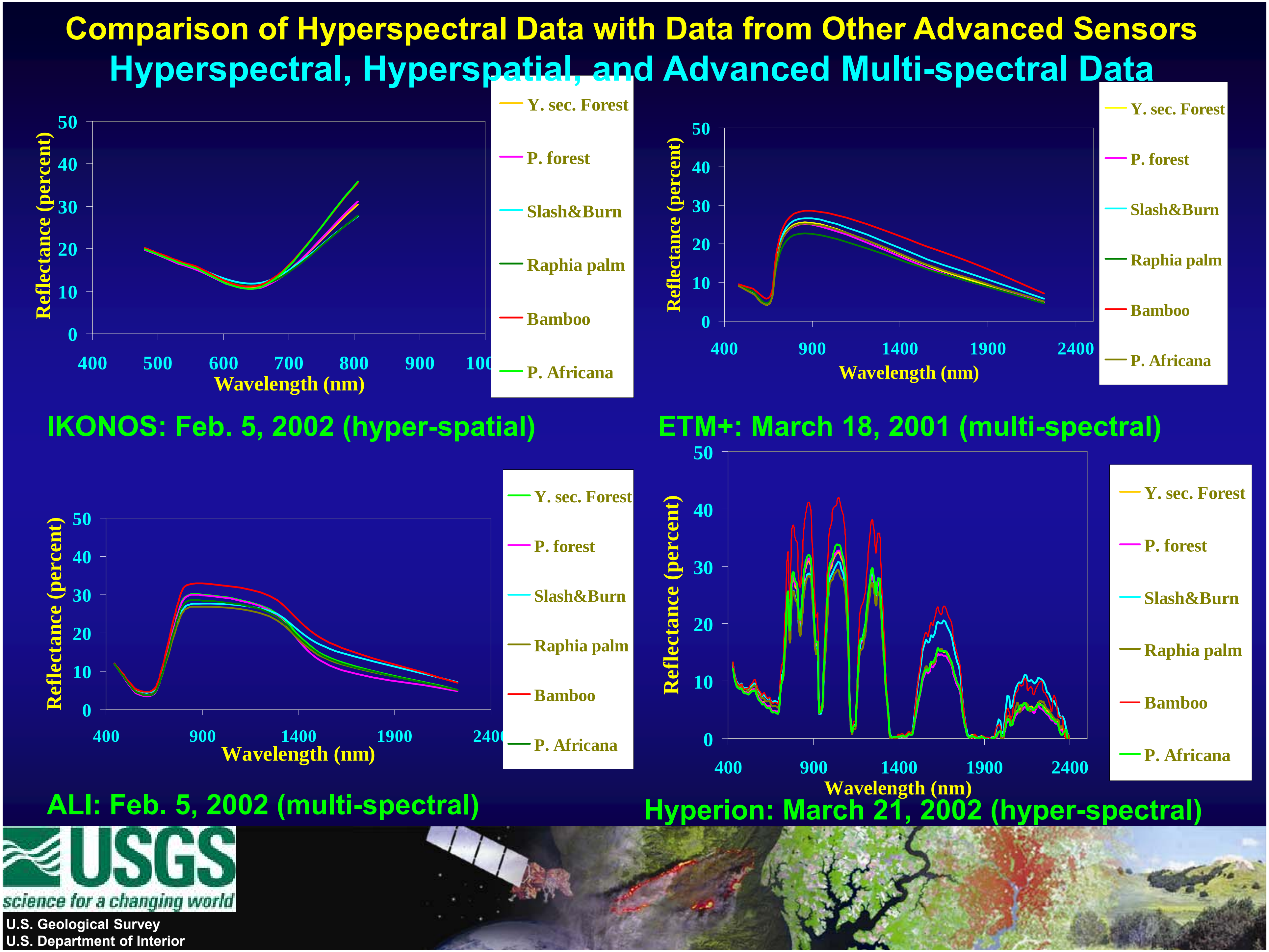
Comparison of Hyperspectral Data with Data from Other Advanced Sensors
Hyperspectral, Hyperspatial, and Advanced Multi-spectral Data
Reflectance (percent)
Wavelength (nm)
Y. sec. Forest
P. forest
Slash&Burn
Raphia palm
Bamboo
P. Africana
IKONOS: Feb. 5, 2002 (hyper-spatial)
ETM+: March 18, 2001 (multi-spectral)
ALI: Feb. 5, 2002 (multi-spectral)
Hyperion: March 21, 2002 (hyper-spectral)
USGS
science for a changing world
U.S. Geological Survey
U.S. Department of Interior

Hyperspectral Data Characteristics

Spectral Wavelengths and their Importance in Vegetation Studies

Hyperspectral Remote Sensing of Vegetation

Typical Hyperspectral Signatures of Certain Land Components

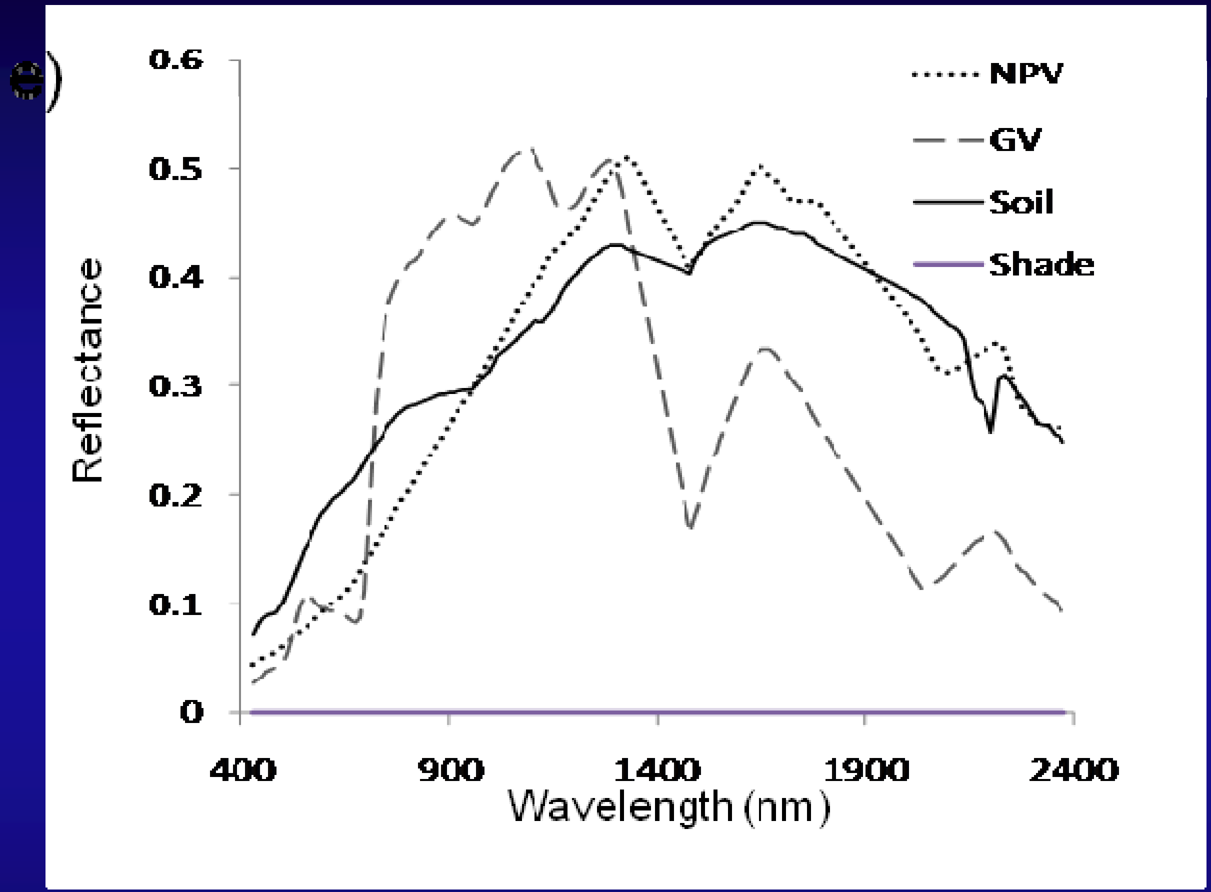

Fraction images of a pasture property in the Amazon derived from EO-1 Hyperion imagery. <u>Four endmembers</u>: (a) nonphotosynthetic vegetation (NPV); (b) green vegetation (GV); (c) Soil; and (d) Shade.

See chapter 9, Numata et al.

Hyperspectral Data on Tropical Forests
Factors Influencing Spectral Variation over Tropical Forests

1. Biochemistry (e.g., plant pigments, water, and structural carbohydrates):
Leaf reflectance in the visible spectrum is dominated by absorption features created by plant pigments, such as:

- chlorophyll a (chl-a): absorps in 410-430 nm and 600-690 nm;
- chlorophyll b (chl-b): absorps in 450-470 nm;
- carotenoids (e.g., β-carotene and lutein): peak absorption in wavebands <500 nm; and
- anthocyanins.
- Lignin, cellulose, protein, Nitrogen: relatively low reflectance and strong absorption in SWIR bands by water that masks other absorption features

……………However, dry leaves do not have strong water absorption and reveal overlapping absorptions by carbon compounds, such as lignin and cellulose, and other plant biochemicals, including protein nitrogen,starch, and sugars.

Note: see chapter 18, Clark et al.

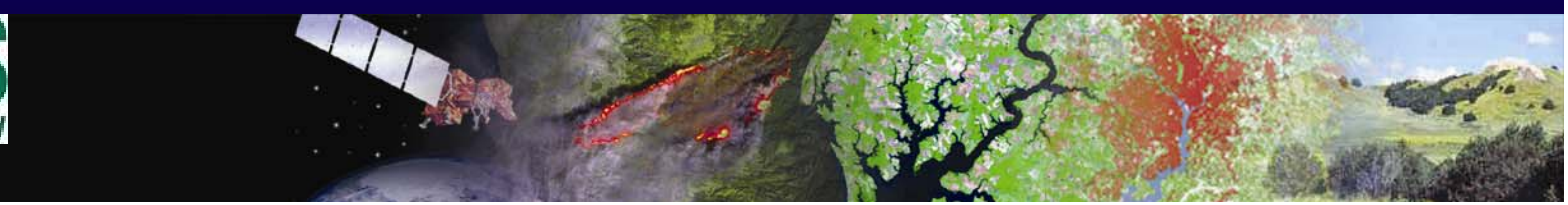

Hyperspectral Data on Tropical Forests

Factors Influencing Spectral Variation over Tropical Forests

2. Structure or biophysical (e.g., leaf thickness and air spaces): of leaves, and the scaling of these spectral properties due to volumetric scattering of photons in the canopy;

3. Nonphotosynthetic tissues (e.g., bark, flowers, and seeds); and

4. Other photosynthetic canopy organisms (e.g., vines, epiphytes, and epiphylls) can mix in the photon signal and vary depending on a complex interplay of species, structure, phenology, and site differences,

……………………………..currently, none of which are well understood.

Note: see chapter 18, Clark et al.

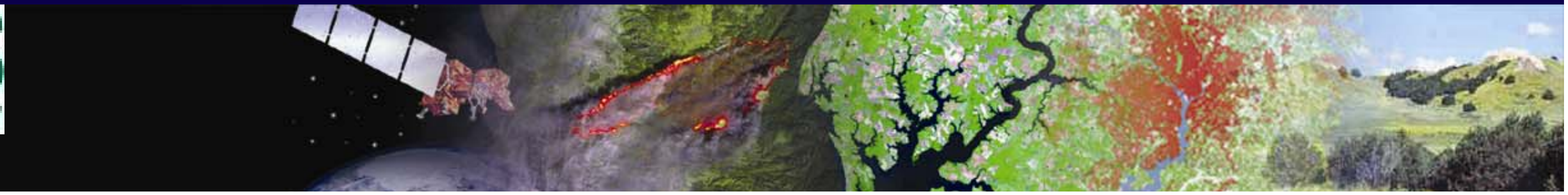

Hyperspectral Data on Tropical Forests

Individual Tree Crown Delineation: Illustrated for 2 species

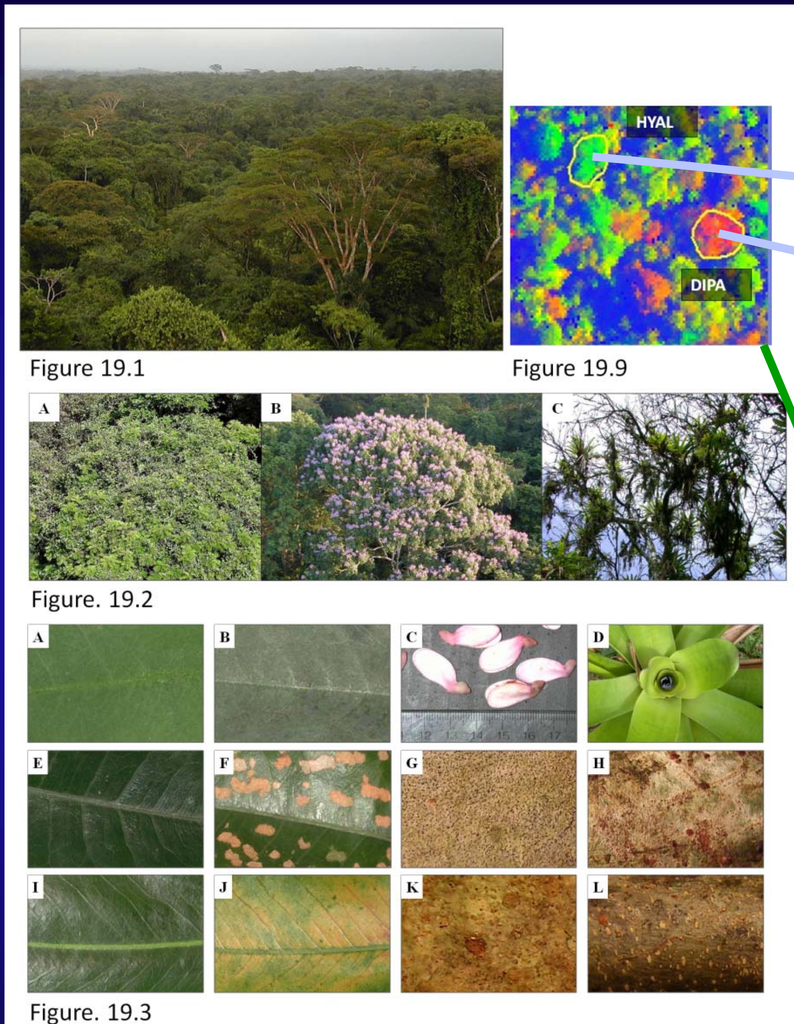

Figure 19.1

Figure 19.9

Figure. 19.2

Figure. 19.3

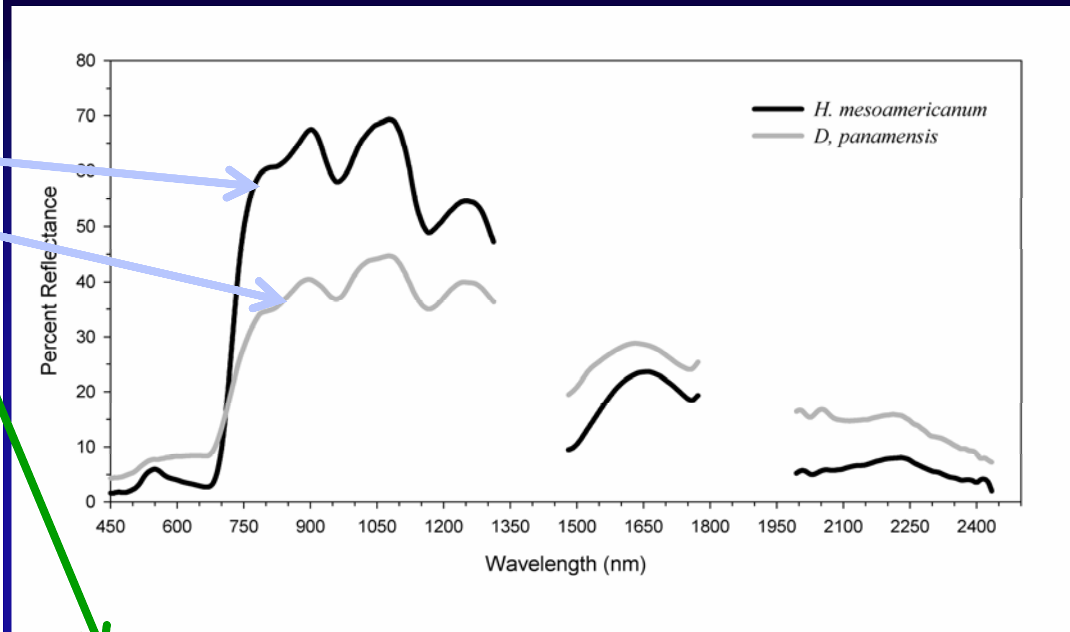

"Fractional abundance of green vegetation (green), non-photosynthetic vegetation (red) and photometric shade (blue) from a spectral mixture analysis.

Individual tree crowns delineated with visual interpretation: *Dipteryx panamensis (DIPA) and Hyeronima alchorneoides (HYAL)."*

Note: see chapter 18, Clark et al.

USGS
science for a changing world

U.S. Geological Survey
U.S. Department of Interior

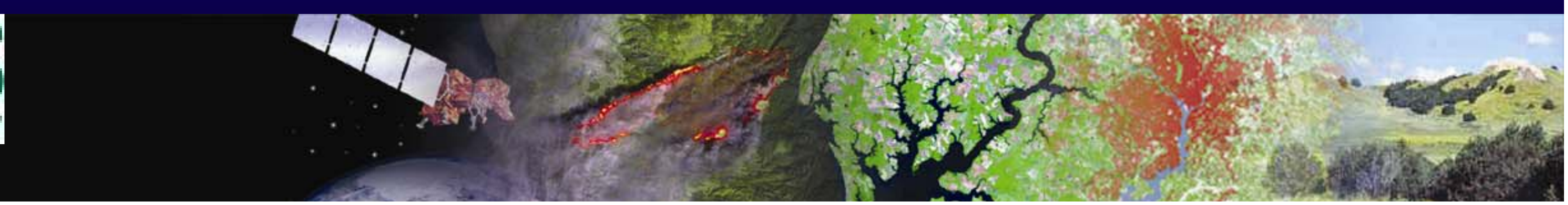

Hyperspectral Data on Vegetation from

A Forest-Margin Benchmark Area

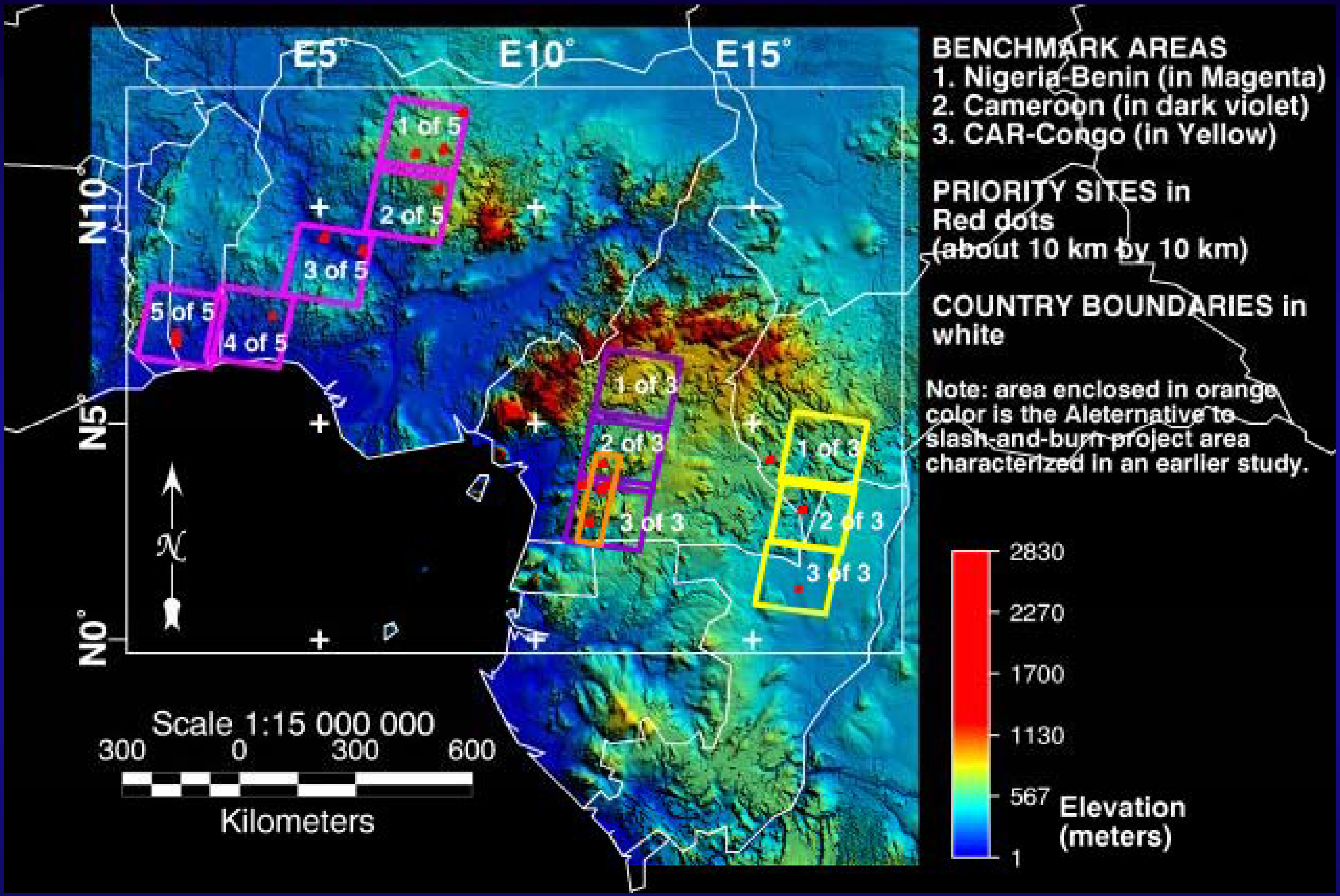

<u>African savannas and Rainforests</u>: Wide range of vegetation including forest and savanna vegetation and agricultural crops studies using Hyperion and Spectroradiometer data.

USGS
science for a changing world
U.S. Geological Survey
U.S. Department of Interior

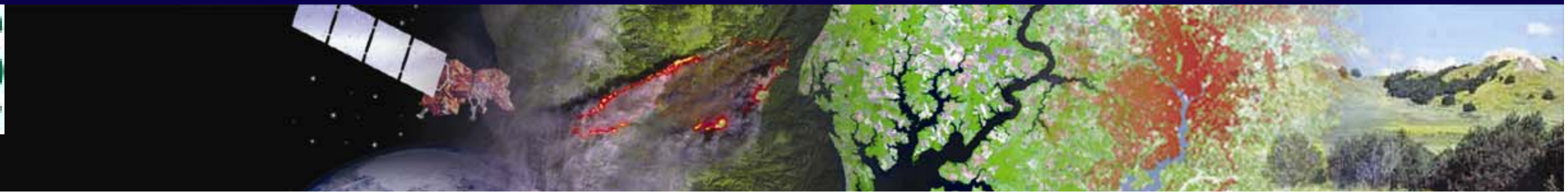

Hyperspectral Data of Two Dominant Weeds

Chromolaena Odorata in African Rainforests vs. *Imperata Cylindrica* in African Savannas

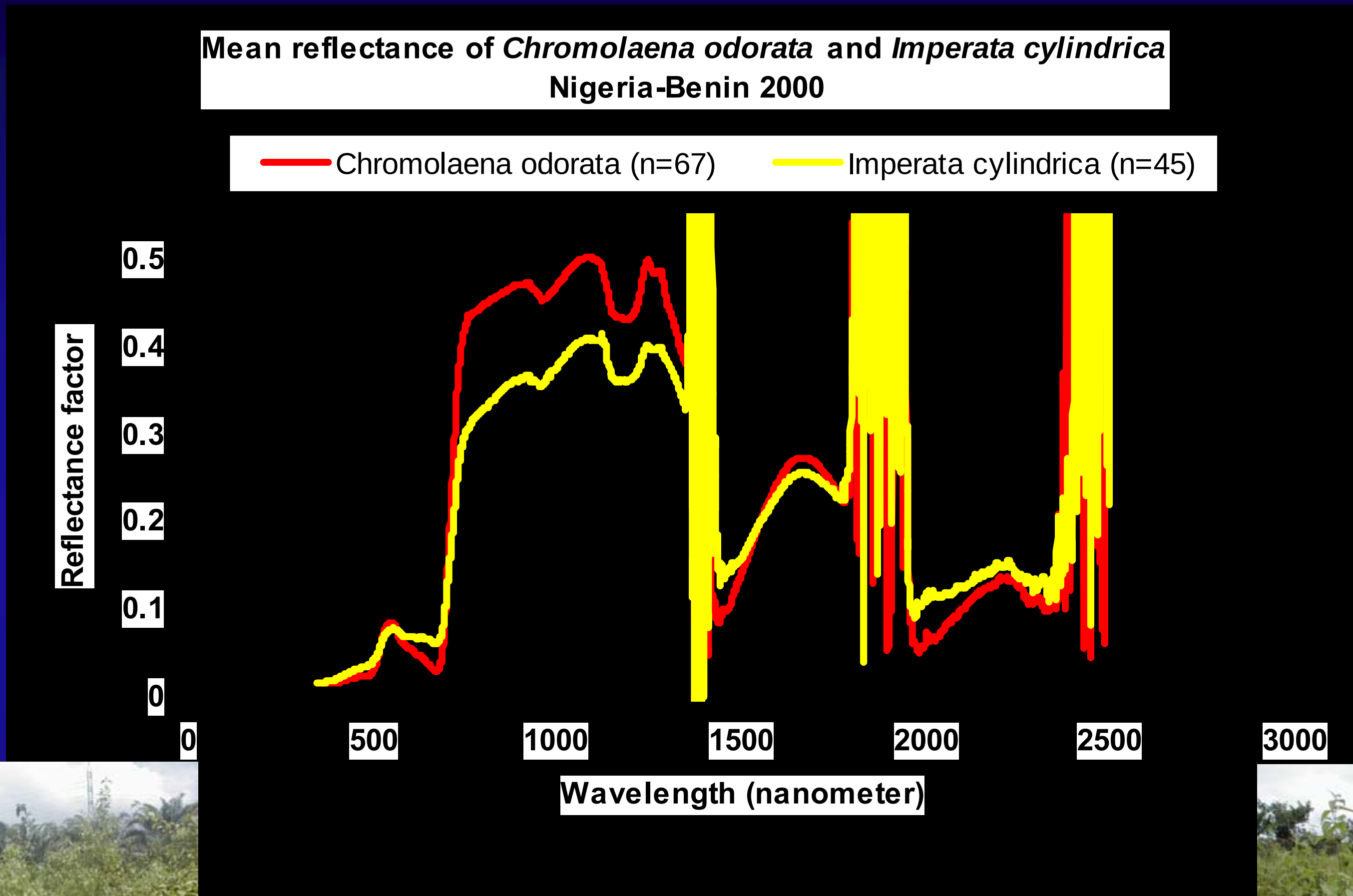

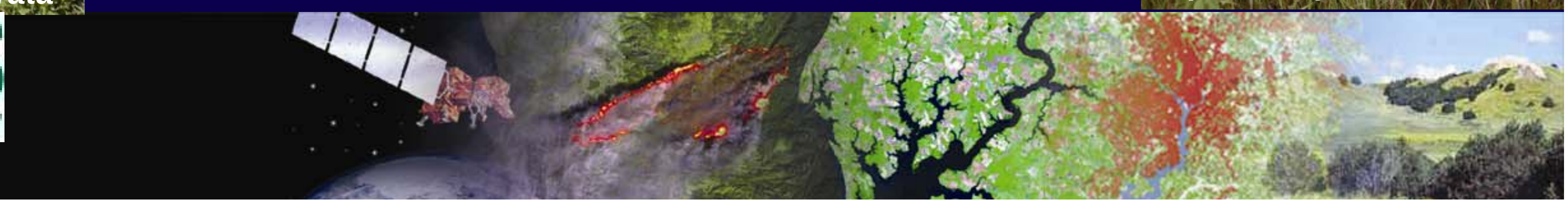

USGS
science for a changing world

U.S. Geological Survey
U.S. Department of Interior

Hyperspectral Data Gathered for the Following Rainforest Vegetation

using Hyperion EO-1 Data and Field-based Measurements of Biophysical Characteristics

USGS
science for a changing world

U.S. Geological Survey
U.S. Department of Interior

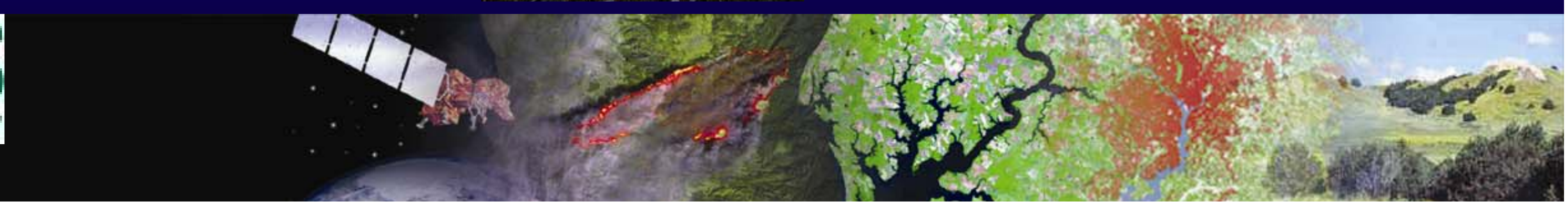

Hyperspectral Remote Sensing of Vegetation

Mega file Data Cube (MFDC) of Hyperion Sensor onboard EO-1

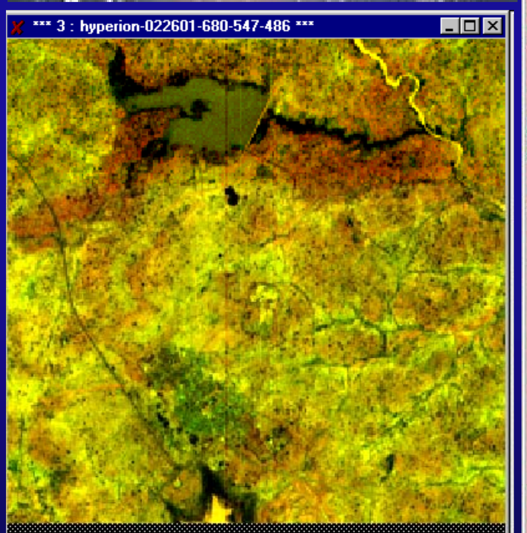

FCC (RGB): 680, 547, 486

e.g., MFDC of African Rainforests in Cameroon

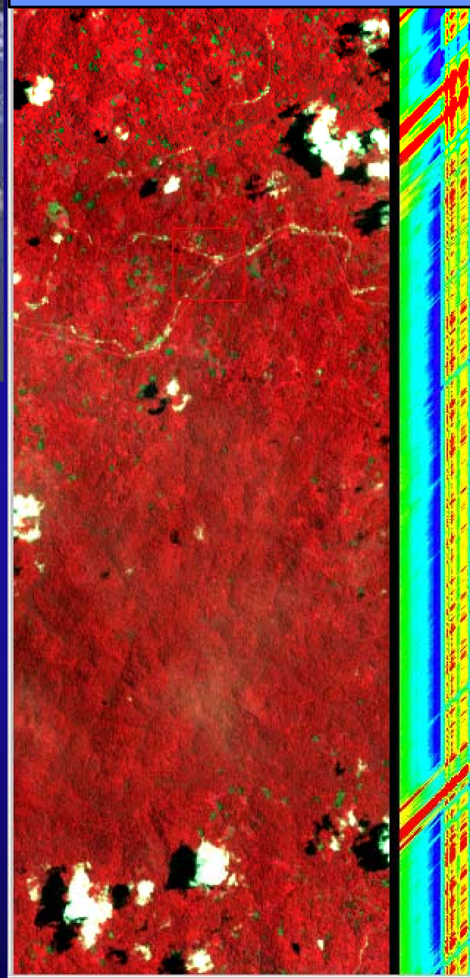

Hyperion: VNIR reflectance

(Mean spectral plots of landuse/landcover types)

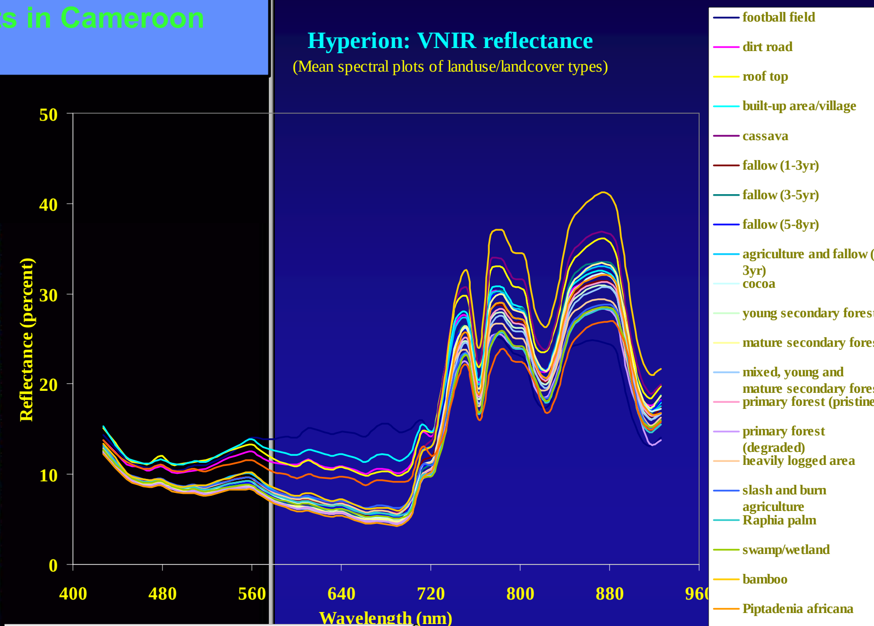

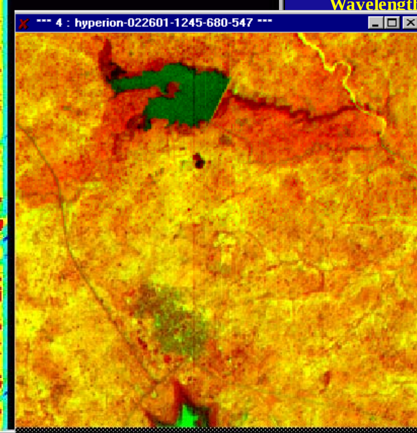

FCC (RGB): 1245, 680, 547

Hyperion has 220 bands in 400-2500 nm

Note: Currently NASA is planning a next Spaceborne Hyperspectral mission called: HyspIRI

USGS

science for a changing world

U.S. Geological Survey

U.S. Department of Interior

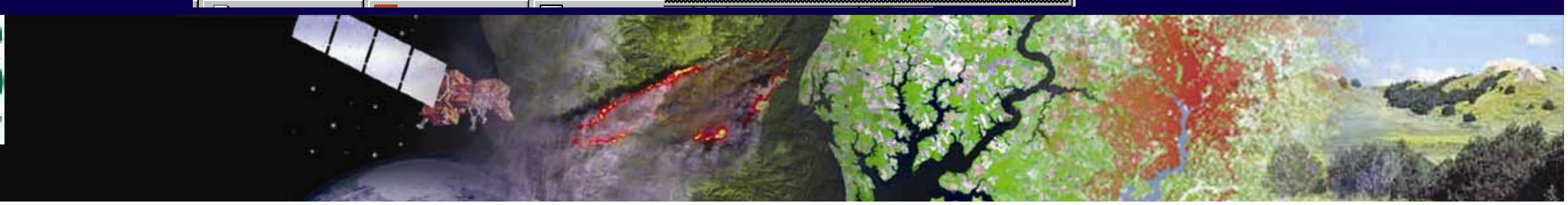

Hyperspectral Data Gathered for the Following Rainforest Vegetation

using Hyperion EO-1 Data

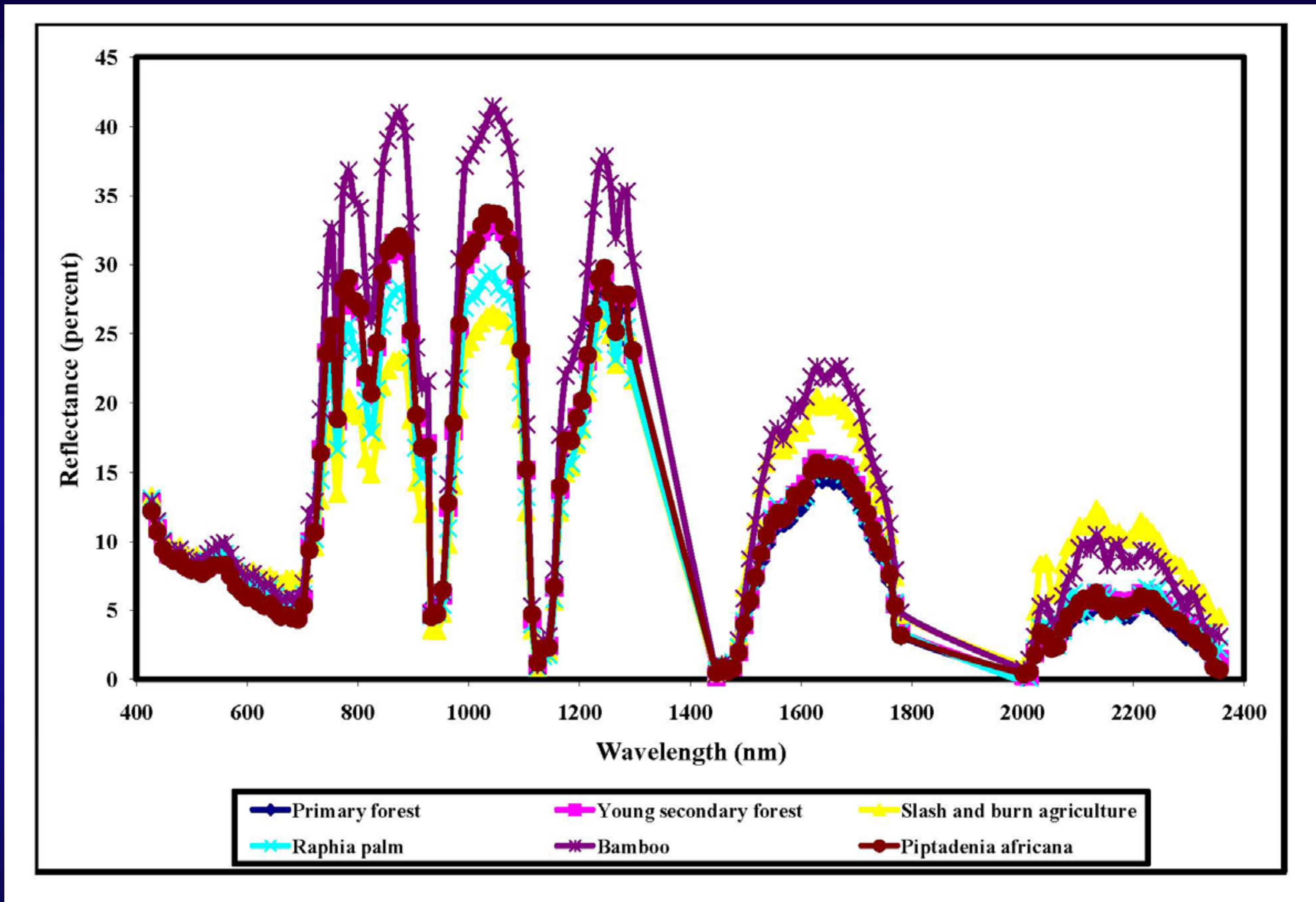

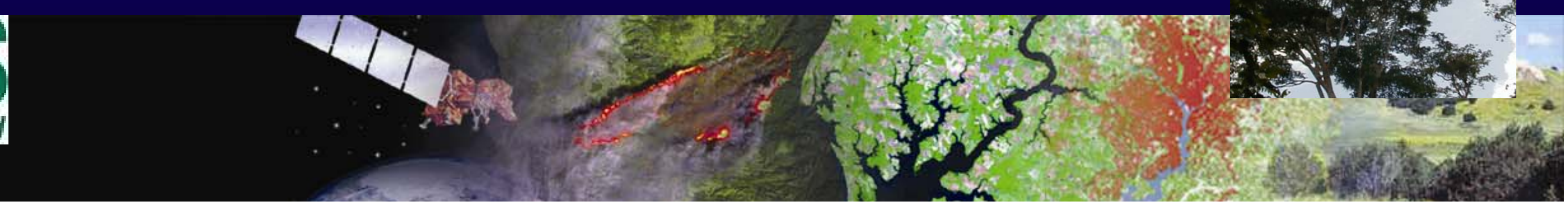

science for a changing world

U.S. Geological Survey
U.S. Department of Interior

Hyperspectral Data Gathered for the Following Rainforest Vegetation

using Hyperion EO-1 Data

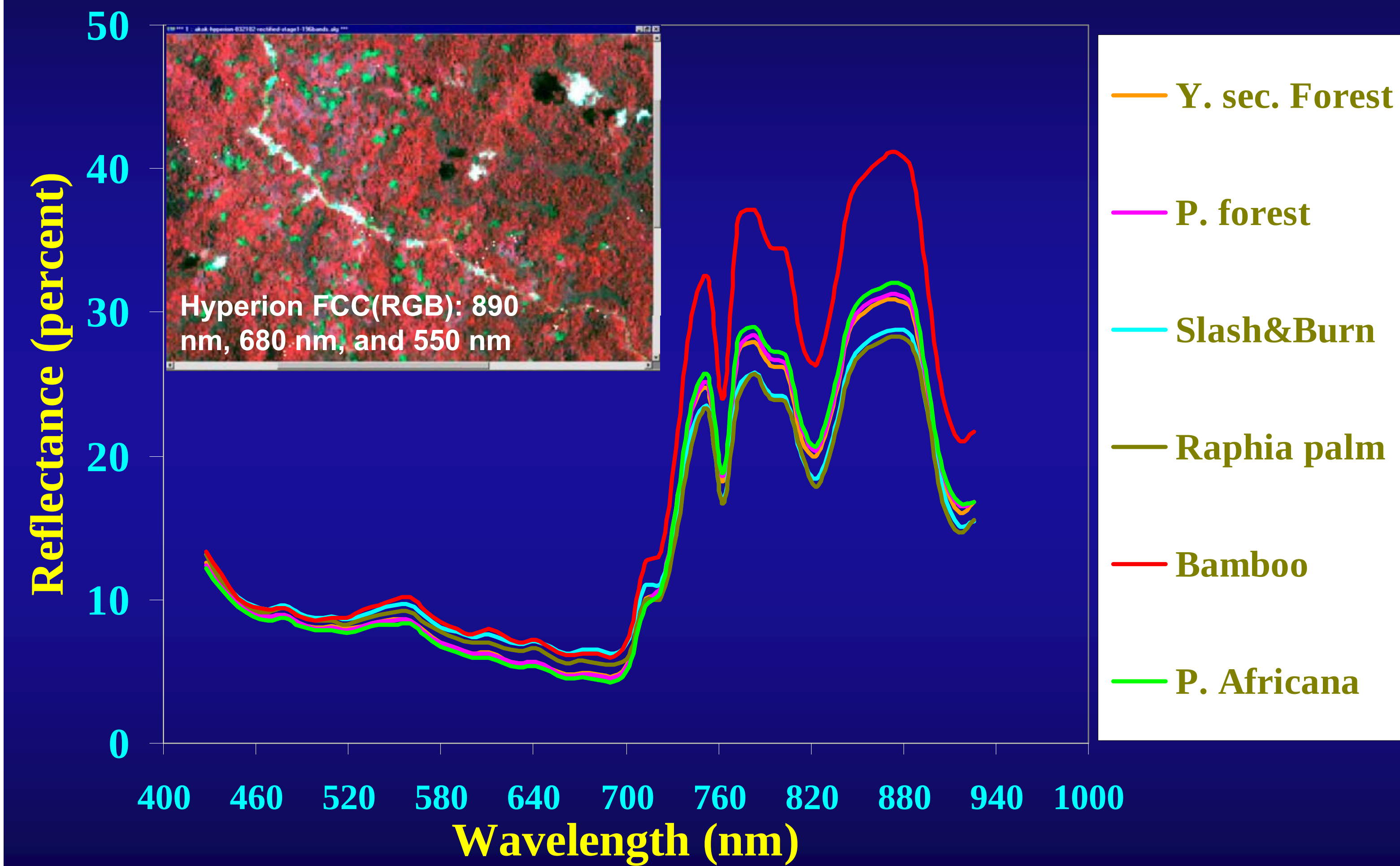

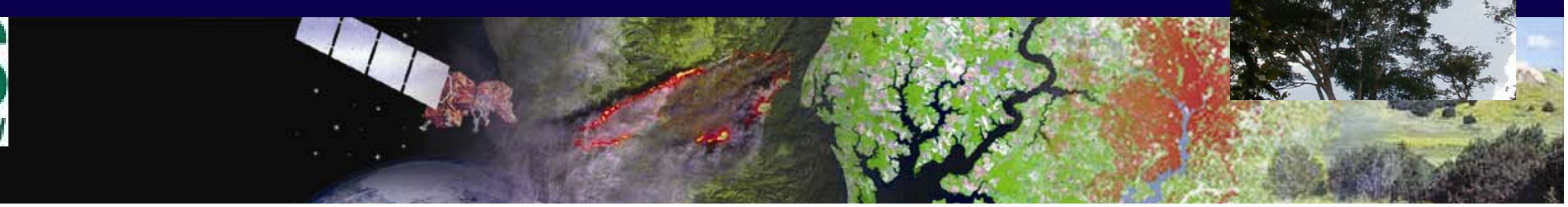

Hyperspectral Data of Vegetation Species and Agricultural Crops

Illustrations for Numerous Vegetation Species from African Savannas

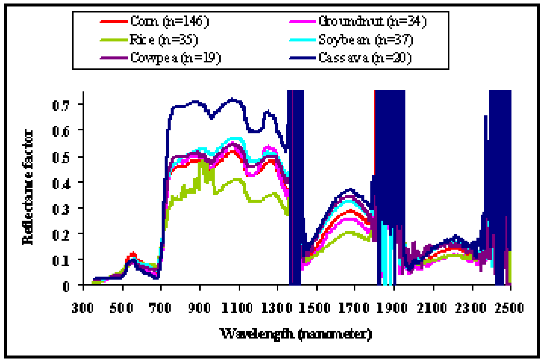

a. Crop species

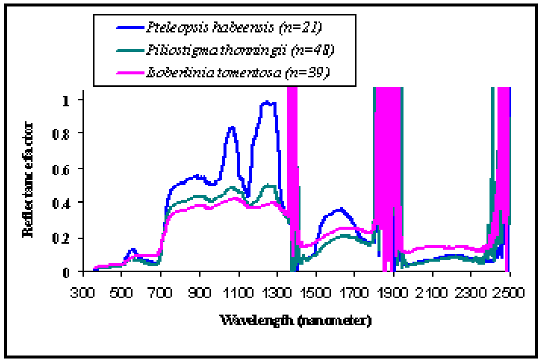

b. Shrub species

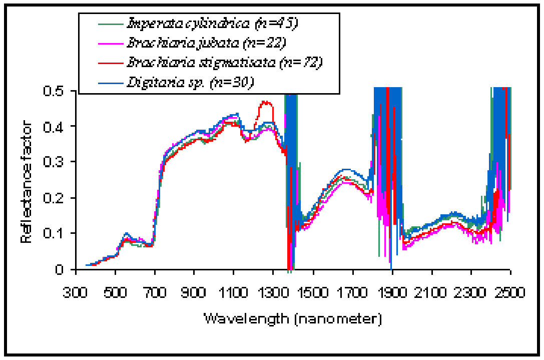

c. Grass species

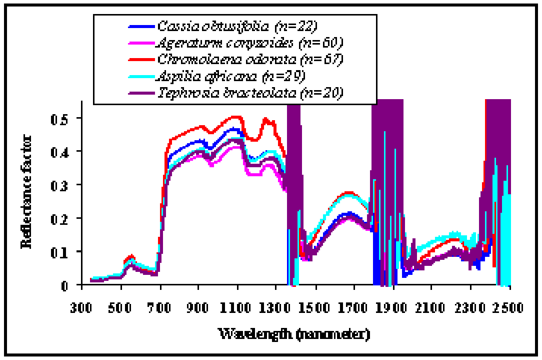

d. Weed species

USGS
science for a changing world

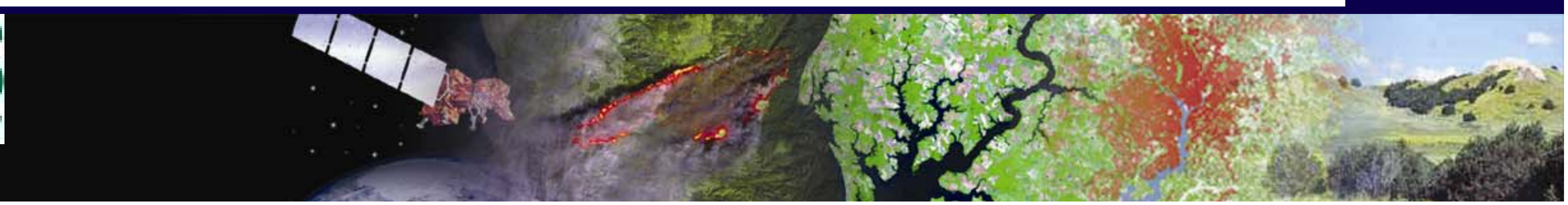

Hyperspectral Data on Vegetation from

A Desert-Margin Benchmark Area

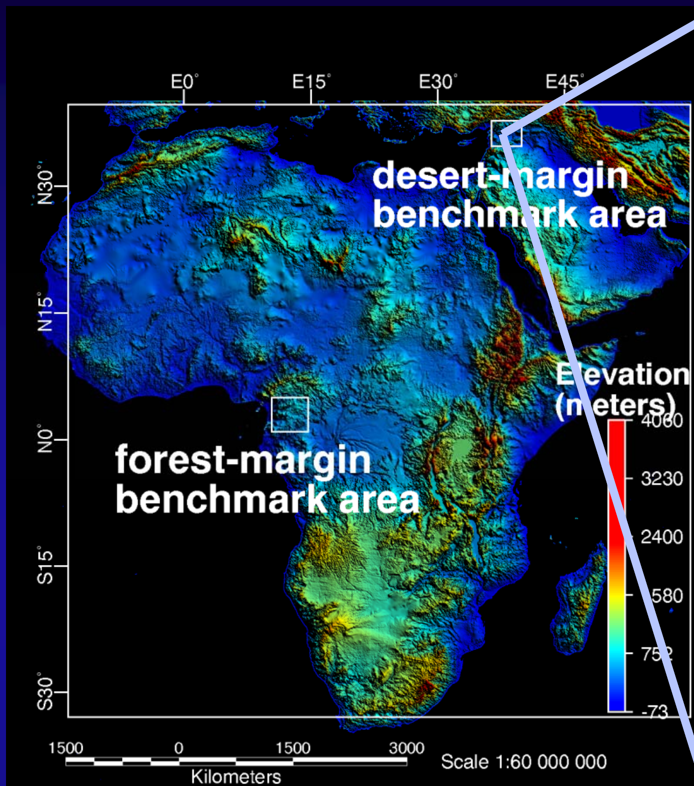

Forest-margin: Rainforest vegetation characteristics studied using Hyperion Spaceborne Hyperspectral Data

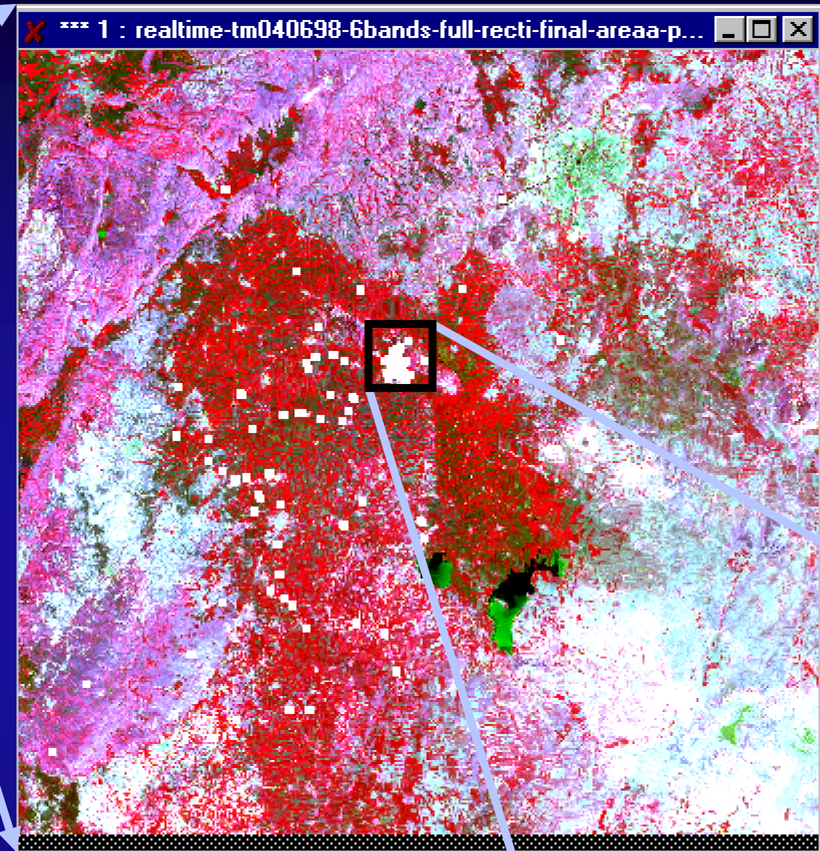

About 50 km by 50 km (part of Landsat-5 TM Path: 174, Row: 35)

Desert-margin: Agricultural cropland vegetation characteristics studied using Hand-held Spectroradiometer Hyperspectral Data

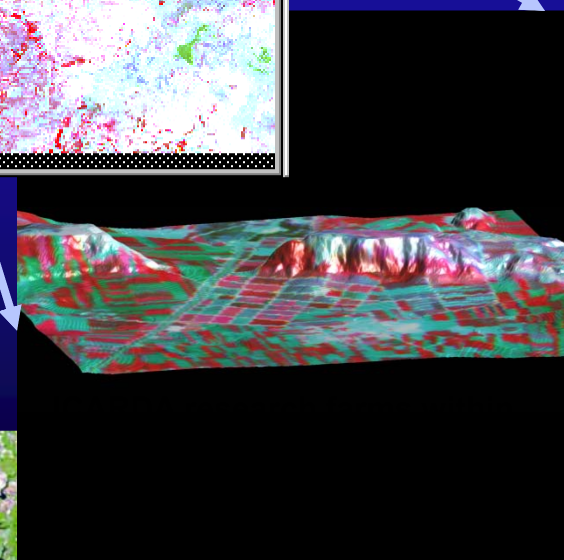

Wheat Crop Versus Barley Crop Versus Fallow Farm

Hyperspectral narrow-band Data for an Erectophile (65 degrees) canopy Structure

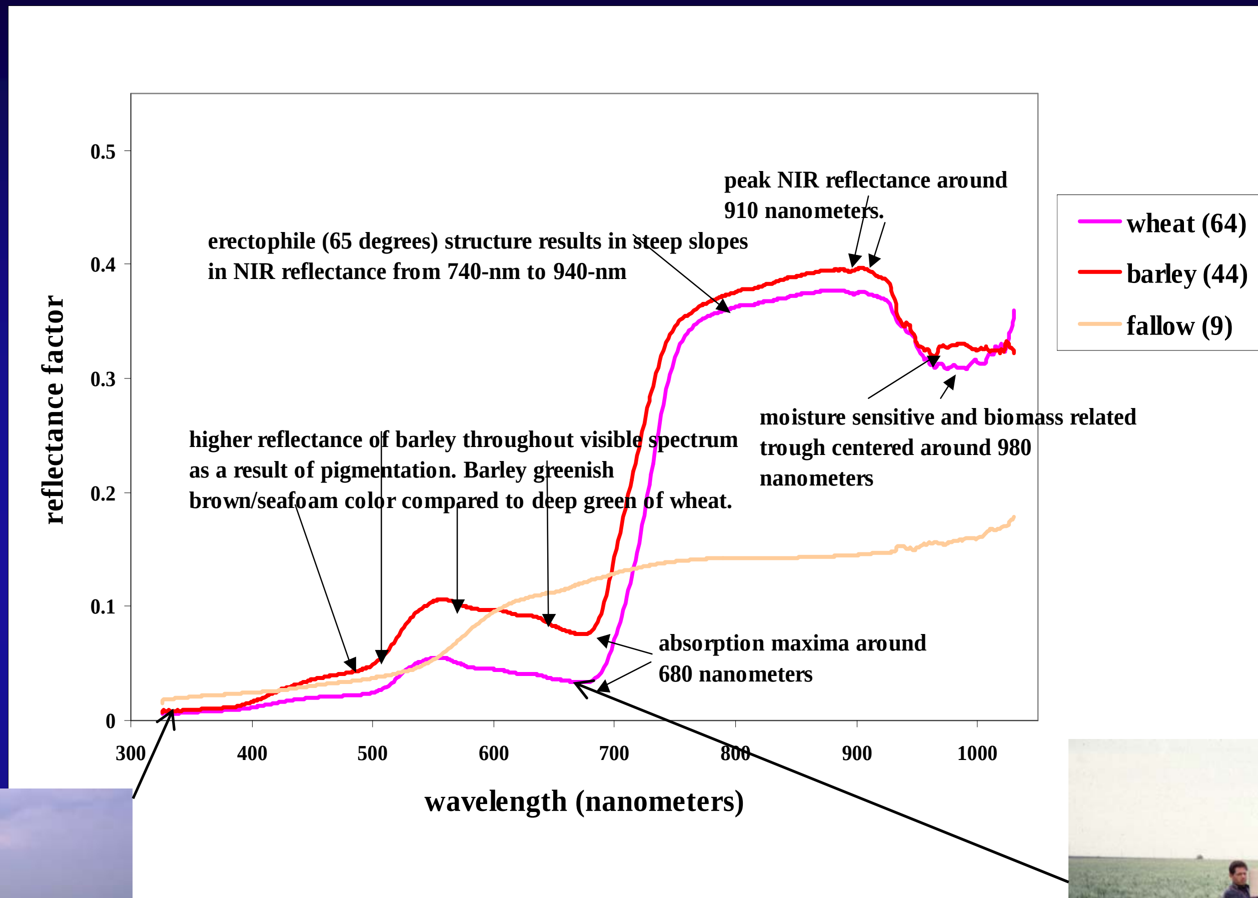

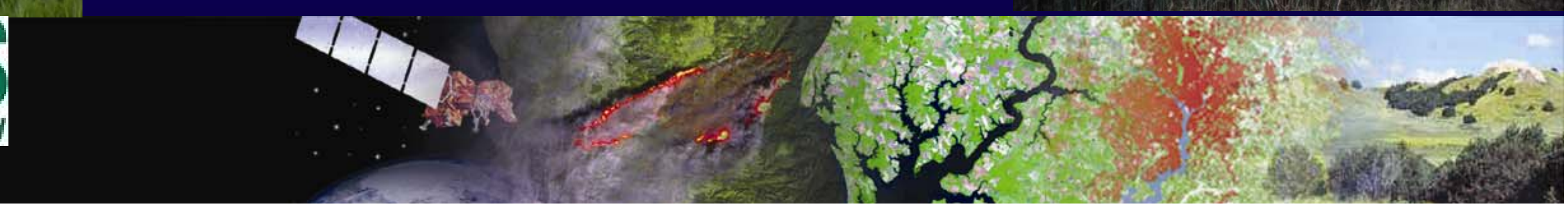

USGS
science for a changing world
U.S. Geological Survey
U.S. Department of Interior

Hyperspectral Remote Sensing of Vegetation

Spectral Wavelengths and their Importance in the Study of Vegetation Structure

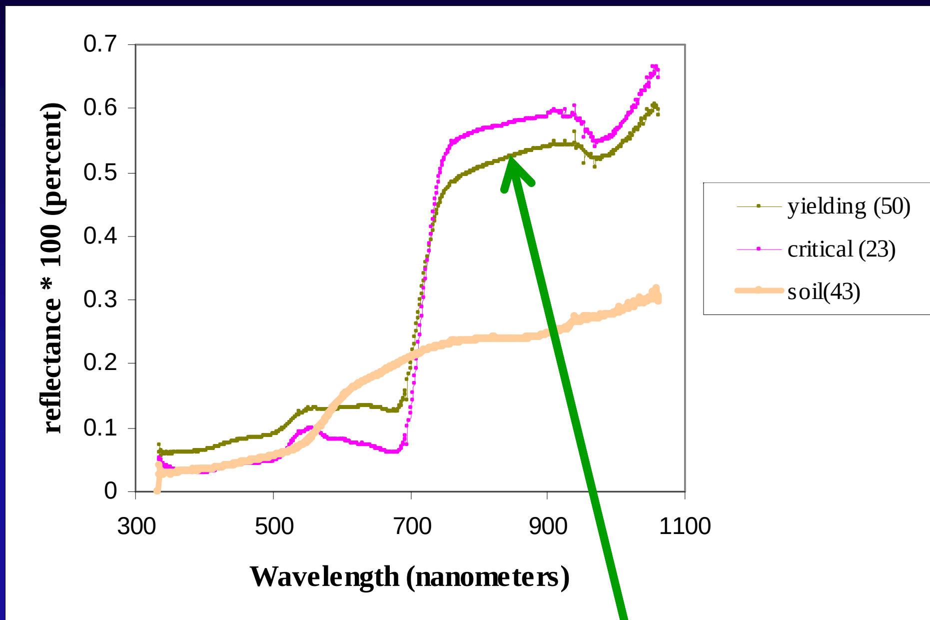

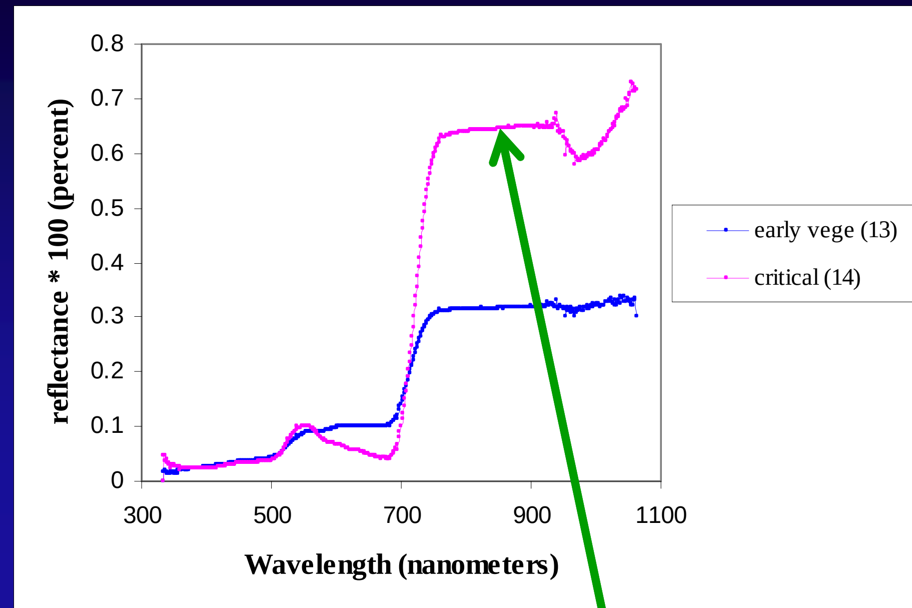

USGS
science for a changing world

Hyperspectral Remote Sensing of Vegetation

Spectral Wavelengths and their Importance in the Study of Vegetation over Time

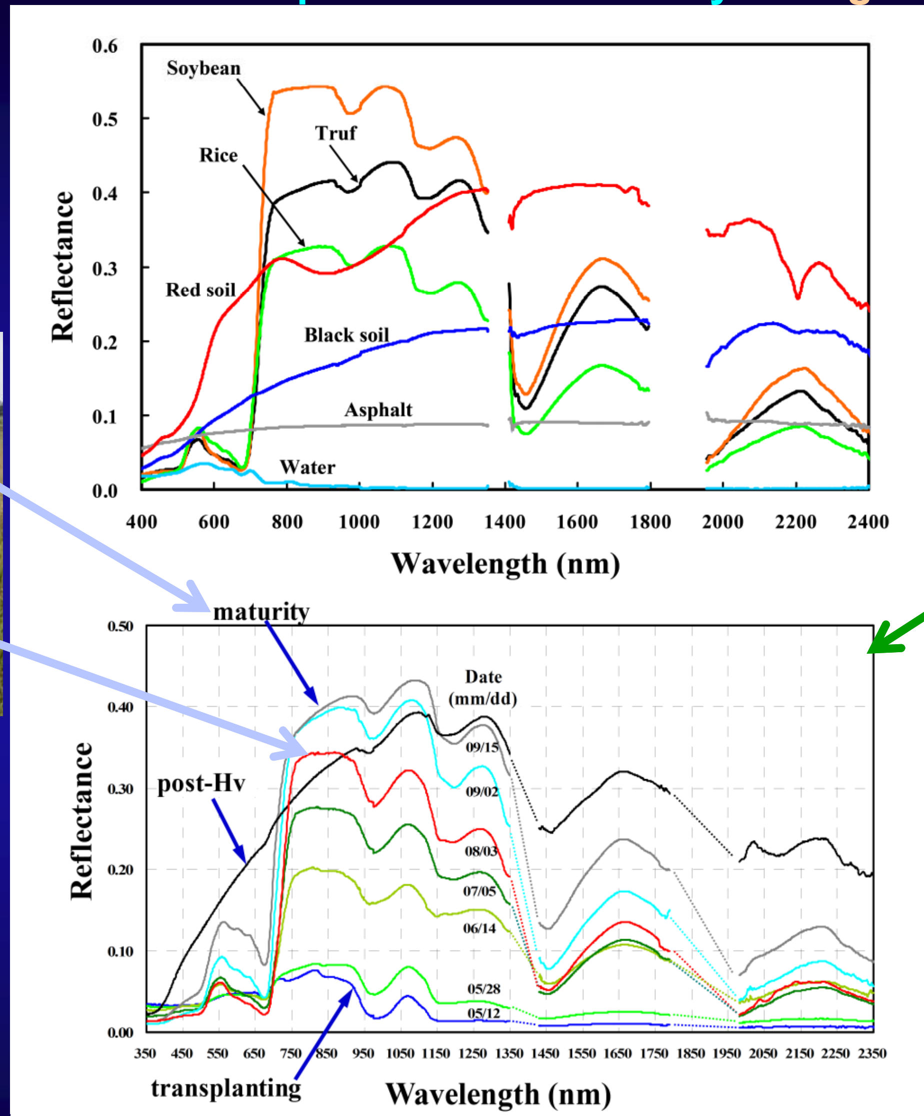

Typical reflectance spectra in agro-ecosystem surfaces (upper), and seasonal changes of spectra in a paddy rice field (lower).

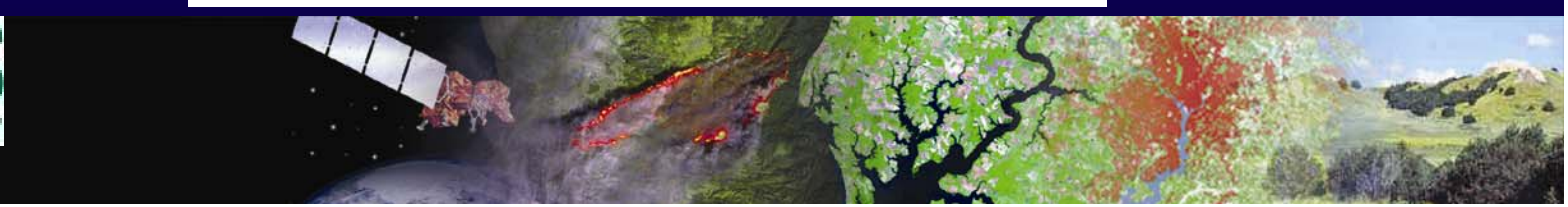

Hyperspectral Remote Sensing of Vegetation

Spectral Wavelengths and their Importance in the Study of Vegetation Stress

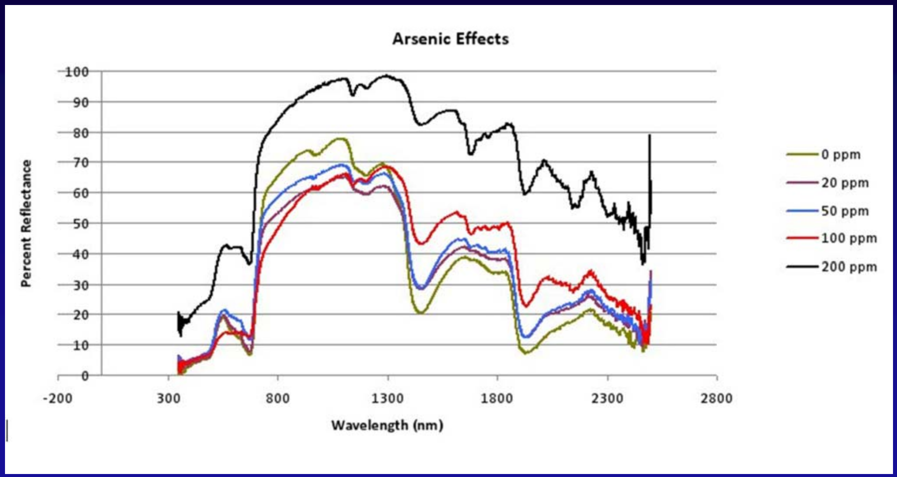

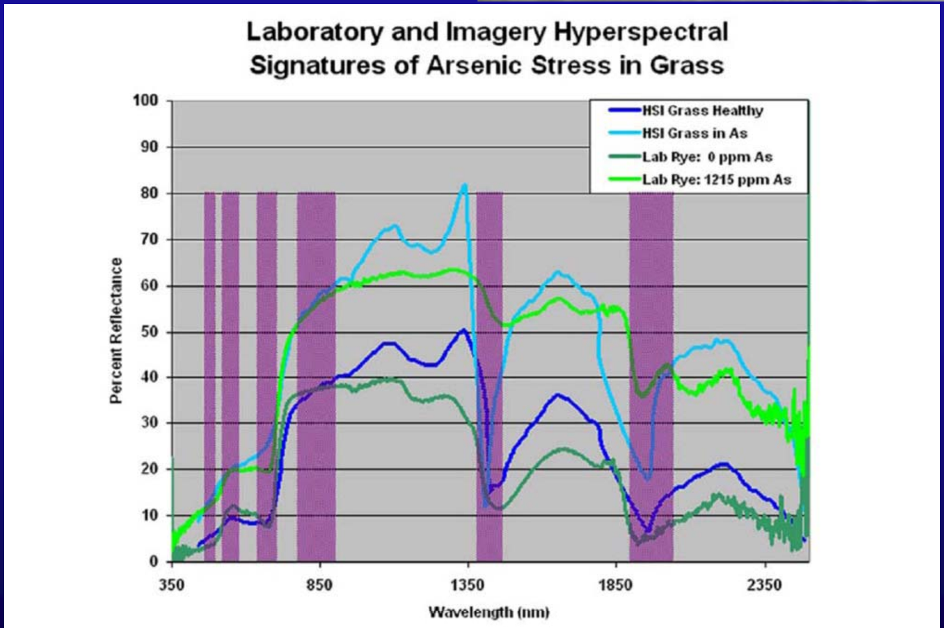

See chapter 23

Hyperspectral Remote Sensing of Vegetation

Spectral Wavelengths and their Importance in the Study of Vegetation in different Growth Stages

Figure 3a. Cotton in critical growth stage.

(a) Cotton (critical)

Figure 3c. Soybeans in critical growth stage.

(b) Soybeans (early)

Figure 3e. Potato in early growth stage.

(c) Potato (early)

Figure 3b. Cotton in yielding/harvest

(a) Cotton (flowering/senescing)

Figure 3d. Soybeans in flowering growth stage.

(b) Soybeans (critical)

Figure 3f. Potato in late growth stage.

(c) Potato (mid-vegetative)

Data was Gathered at Various Growth Stages

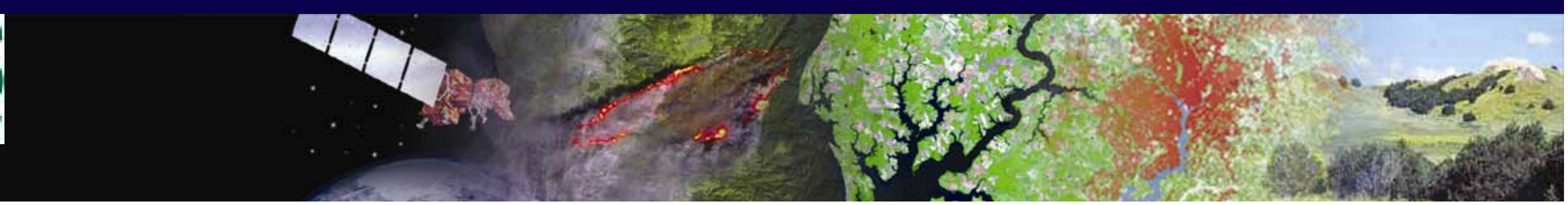

Hyperspectral Remote Sensing of Vegetation

Spectral Wavelengths and their Importance in the Study of Vegetation in different Growth Stages

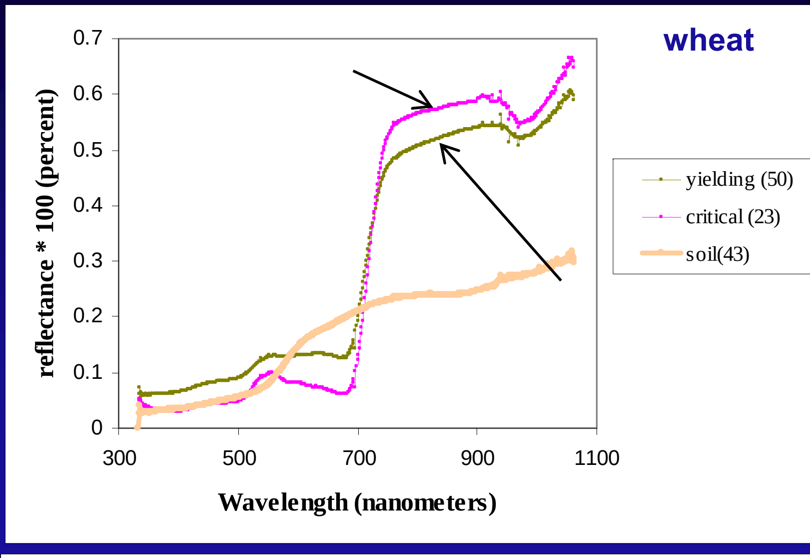

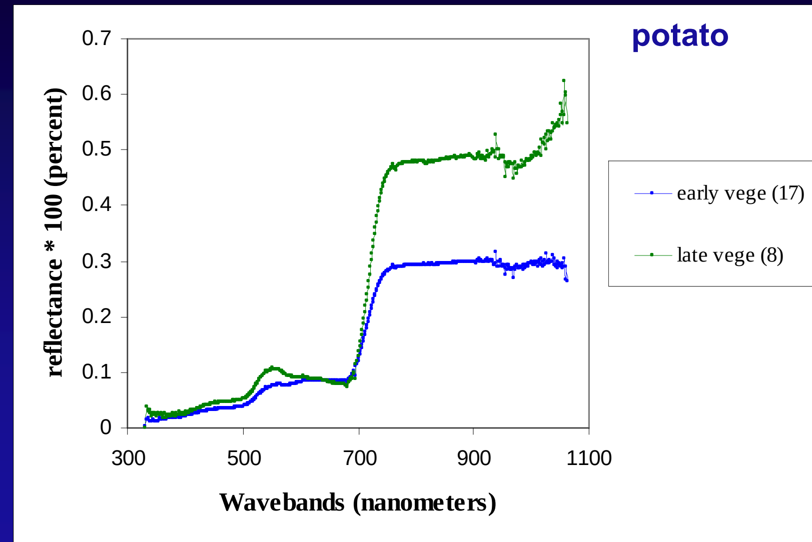

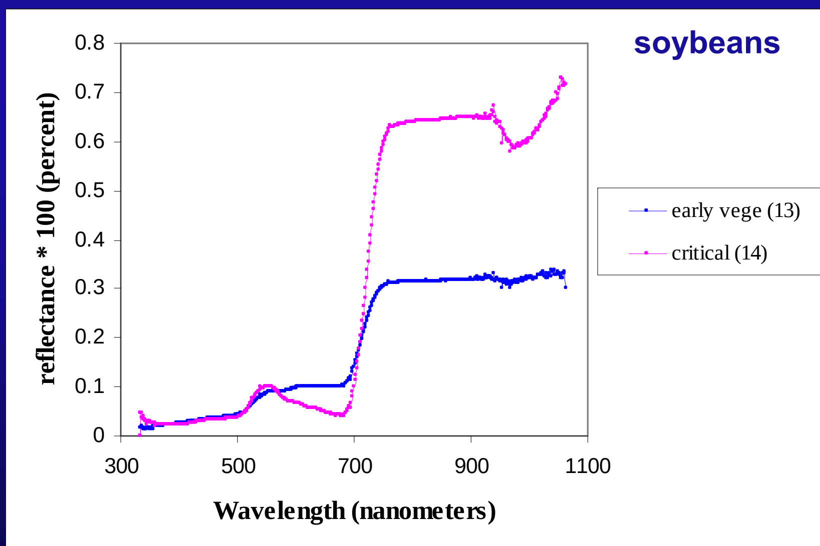

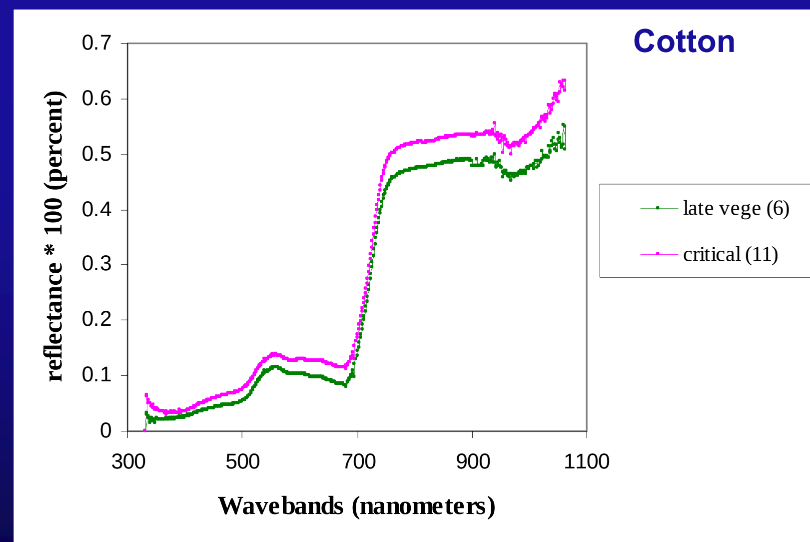

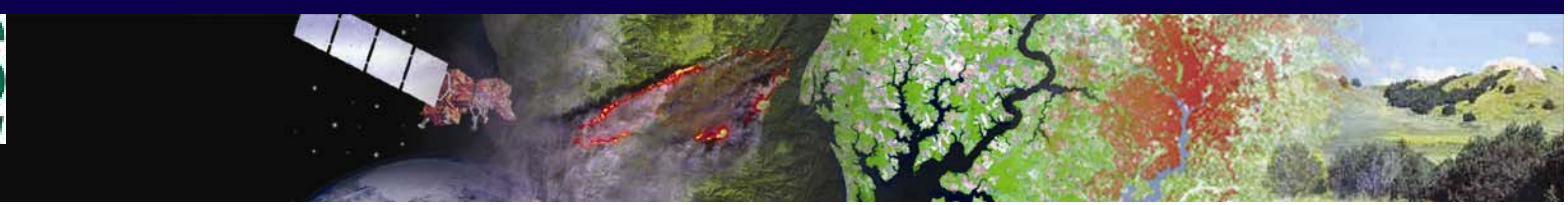

Hughes Phenomenon

(or Curse of High Dimensionality of Data) and

overcoming data redundancy through Data Mining

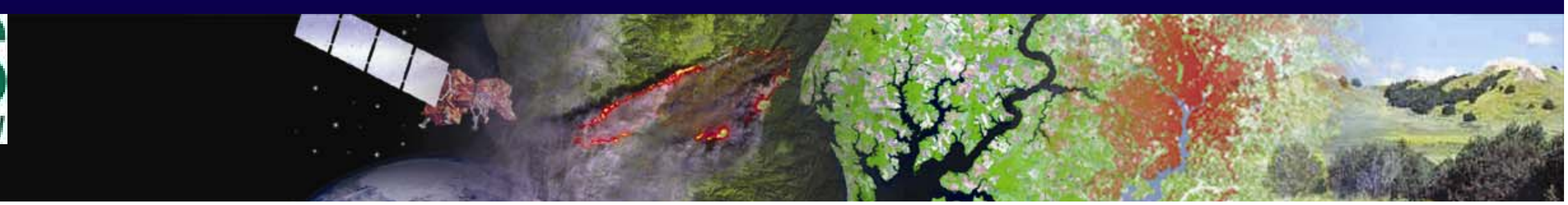

science for a changing world
U.S. Geological Survey
U.S. Department of Interior

Hyperspectral Data (Imaging Spectroscopy data)
Not a Panacea!

For example, hyperspectral systems collect large volumes of data in a short time. Issues include:

- data storage volume;
- data storage rate;
- downlink or transmission bandwidth;
- computing bottle neck in data analysis; and
- new algorithms for data utilization (e.g., atmospheric correction more complicated).

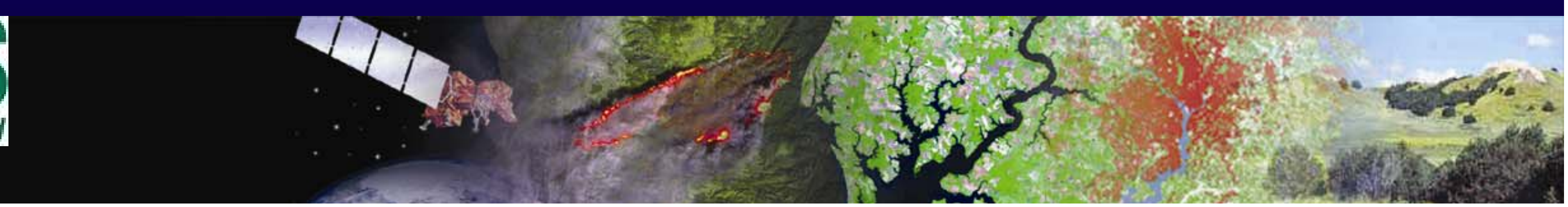

Data Mining Methods and Approaches in Vegetation Studies

Lambda by Lambda R-square Contour Plots: Identifying Least Redundant Bands

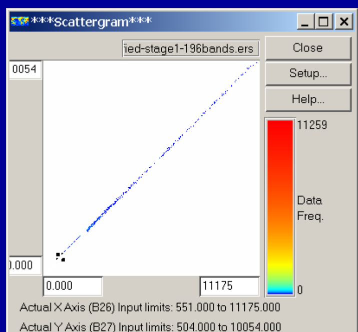

Highly redundant: bands centered at 680 nm and 690 nm

Hyperion rainforest vegetation: Least redundant bands

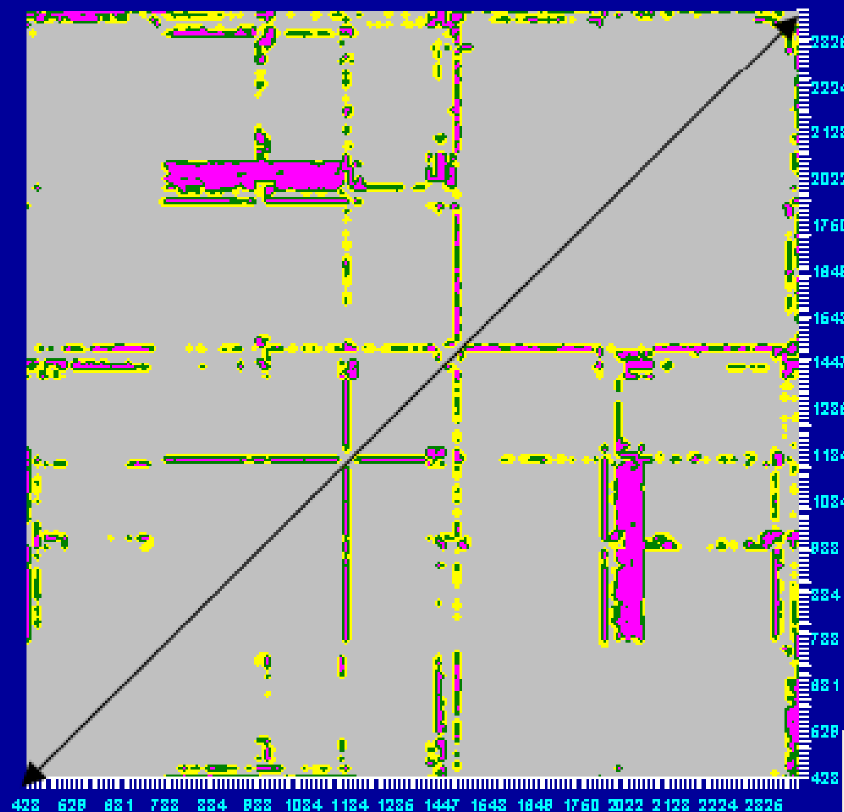

R^2 values between wavebands (lesser the R^2 value lesser the redundancy)

- 0.009-0.01
- 0.008-0.009
- 0.007-0.008
- 0.006-0.007
- 0.005-0.006
- 0.004-0.005
- 0.003-0.004
- 0.002-0.003
- 0.001-0.002
- 0-0.001

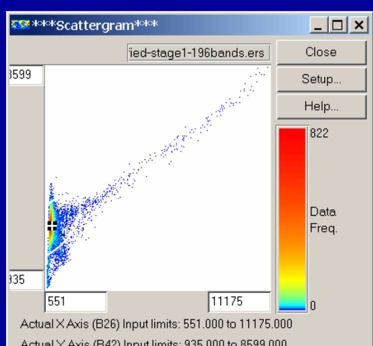

Significantly different: bands centered at 680 nm and 890 nm

Lambda vs. Lambda Correlation plot for African rainforest Vegetation

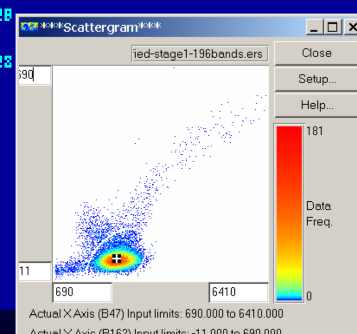

Distinctly different: bands centered at 920 nm and 2050 nm

Data Mining Methods and Approaches in Vegetation Studies
Feature selection\extraction and Information Extraction

Feature selection is necessary in any data mining effort. Feature selection reduces the dimensionality of data by selecting only a subset of measured features (predictor variables). Feature selection methods recommendation based on:

(a) Information Content (e.g., Selection based on Theoretical Knowledge, Band Variance, Information Entropy),
(b) Projection-Based methods (e.g., Principal Component Analysis or PCA, Independent Component Analysis or ICA),
(c) Divergence Measures (e.g., Distance-based measures),
(d) Similarity Measures (e.g., Correlation coefficient, Spectral Derivative Analysis), and
(e) Other Methods (e.g., wavelet Decomposition Method).

Note: see chapter 4

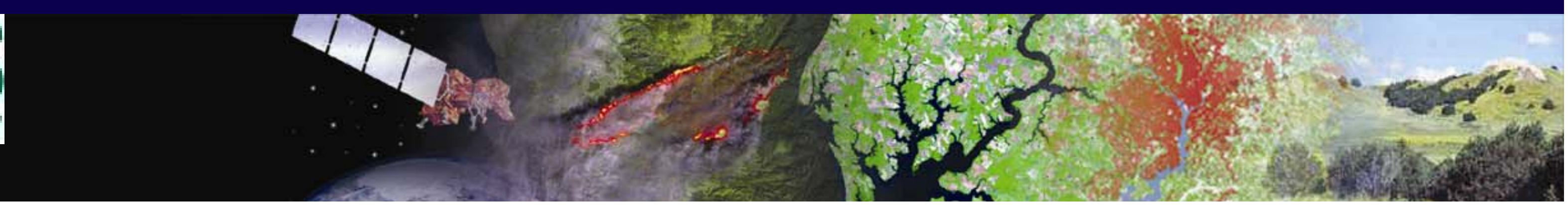

Data Mining Methods and Approaches in Vegetation Studies

Principal Component Analysis: Identifying Most useful Bands

Wavebands with Highest Factor Loadings

Principal component analysis for crop species											
Crops	Band centers (nm) with first 20 highest factor loadings					% variability explained					
	PCA1	PCA2	PCA3	PCA4	PCA5	PCA 1	PCA 2	PCA 3	PCA 4	PCA 5	5 cumulative PCAs
Cassava	1725;1715;1705;1575;1695;1605;1735;1585;1555;1595;1565;1685;1625;1655;1545;1615;1665;1635;1675;1645	635;625;695;615;645;605;595;655;585;705;575;685;665;515;525;565;535;555;545;715	2002;2342;2322;2282;2312;2312;2272;1455;1380;2012;2332;2022;2222;2292;2262;1465;1982;2252;1445;2132	2002;1245;1255;1235;1275;1265;1285;1992;2042;2032;2262;2062;2292;1225;2322;1982;2072;2232;2012;2282	2332;2342;2322;1982;2312;2312;1445;2292;2022;1992;2262;865;875;855;775;885;785; 845;795;805	63.9	18.9	5.6	2.6	1.9	92.7
Dominating bands	EMIR	Green; Red	MIR; MMIR; FMI	R;EMIR;MMIR;FN	; EMIR; MMIR; FMIR						
Corn	1675;1665;1645;1655;1685;1695;1635;1705;1625;1715;1725;1615;1735;1605;1745;1595;1755;1585;1765;1575	2032;2052;2042;2082;2072;2062;2092;2102;1982;2112;1465;2122;2022;1455;2132;1992;1475;2142;1485;2252	2002;2012;2342;1992;2022;1982;2332;2322;2032;2072;1255;1245;2042;1275;1285;1265;2062;1235;2052;1380	355;365;375;385;395;405;415;425;435;1445;1245;445;1255;1235;1275;1265;1285;1225; 1135;1455	2342;2002;2012;1992;1982;2332;2022;355;375;2052;365;2322;385;395;405;2042;2062;2312;2312;415	67.0	16.1	7.8	2.2	1.9	94.9
Dominating bands	EMIR	MIR; MMIR; FMI	FNIR; EMIR; MMIR; FMIR	UV; Blue; FNIR; EMIR	UV; Blue; EMIR; MMIR; FMIR						

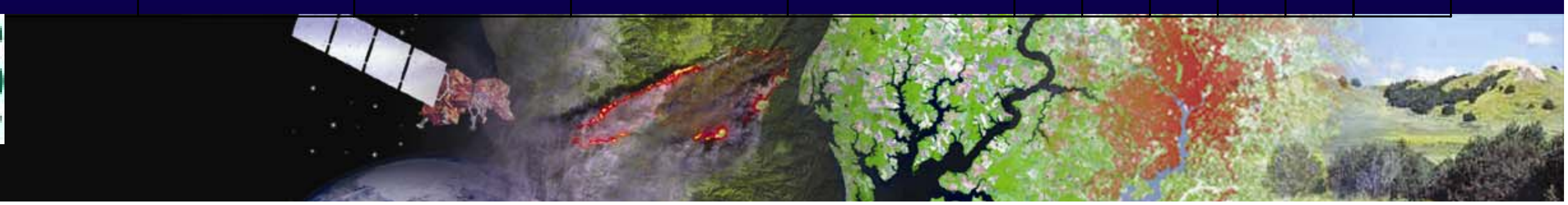

Methods of
Modeling Vegetation Characteristics using
Hyperspectral Vegetation Indices (HVIs)

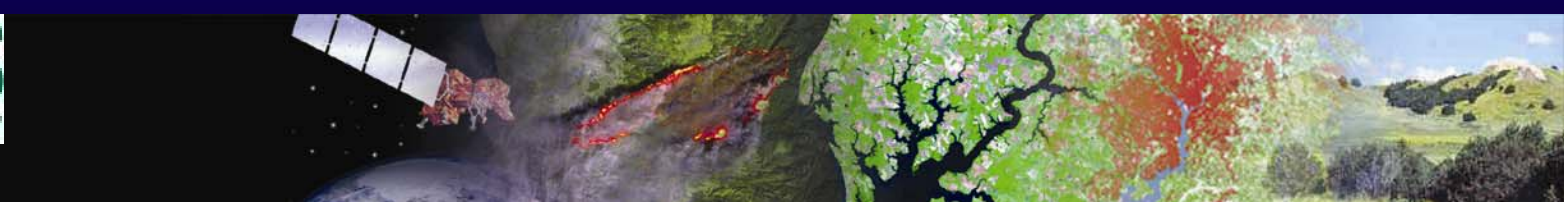

Hyperspectral Data (Imaging Spectroscopy data)

Hyperspectral Vegetation Indices (HVIs)

Unique Features and Strengths of HVIs

1. **Eliminates redundant bands**

   removes highly correlated bands

2. **Physically meaningful HVIs**

   e.g., Photochemical reflective index (PRI) as proxy for light use efficiency (LUE)

3. **Significant improvement over broadband indices**

   e.g., reducing saturation of broadbands, providing greater sensitivity (e.g., an index involving NIR reflective maxima @ 900 nm and red absorption maxima @680 nm

4. **New indices not sampled by broadbands**

   e.g., water-based indices (e.g., involving 970 nm or 1240 nm along with a nonabsorption band)

5. **multi-linear indices**

   indices involving more than 2 bands

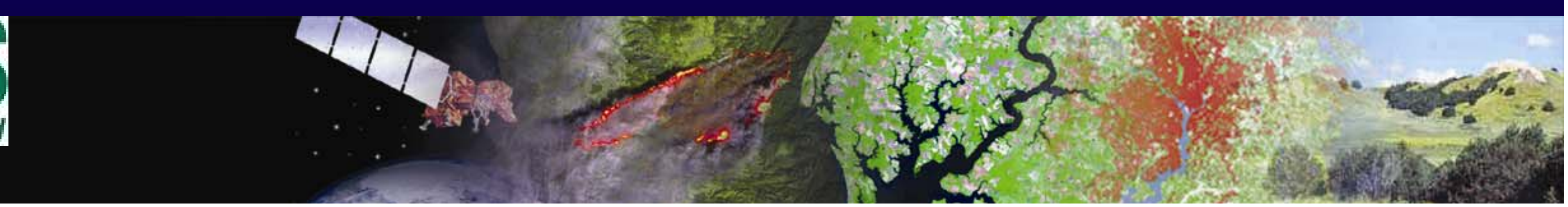

Methods of Modeling Vegetation Characteristics using Hyperspectral Indices

Hyperspectral Two-band Vegetation Indices (TBVIs) = 12246 unique indices for 157 useful Hyperion bands of data

$$HTBVI_{ij} = \frac{(R_j - R_i)}{(R_j + R_i)}$$

- **Hyperion**:
- **A. acquired over 400-2500 nm in 220 narrow-bands each of 10-nm wide bands. Of these there are 196 bands that are calibrated. These are: (i) bands 8 (427.55 nm) to 57 (925.85 nm) in the visible and near-infrared; and (ii) bands 79 (932.72 nm) to band 224 (2395.53 nm) in the short wave infrared.**
- **B. However, there was significant noise in the data over the 1206–1437 nm, 1790– 1992 nm, and 2365–2396 nm spectral ranges. When the Hyperion bands in this region were dropped, 157 useful bands remained.**

- **Spectroradiometer**:
- **A. acquired over 400-2500 nm in 2100 narrow-bands each of 1-nm wide. However, 1-nm wide data were aggregated to 10-nm wide to coincide with Hyperion bands.**
- **B. However, there was significant noise in the data over the 1350-1440 nm, 1790-1990 nm, and 2360-2500 nm spectral ranges. was seriously affected by atmospheric absorption and noise. The remaining good noise free data were in 400-1350 nm, and 1440-1790 nm, 1990-2360 nm.**

- **……..So, for both Hyperion and Spectroradiometer we had 157 useful bands, each of 10-nm wide, over the same spectral range.**

- **where, i,j = 1, N, with N=number of narrow-bands= 157 (each band of 1 nm-wide spread over 400 nm to 2500 nm), R=reflectance of narrow-bands.**

Model algorithm: two band NDVI algorithm in Statistical Analysis System (SAS). Computations are performed for all possible combinations of λ_1 (wavelength 1 = 157 bands) and λ_2 (wavelength 2 = 157 bands) = a total of 24,649 possible indices. It will suffice to calculate Narrow-waveband NDVI's on one side (either above or below) the diagonal of the 157 by 157 matrix as values on either side of the diagonal are the transpose of one another.

Methods of Modeling Vegetation Characteristics using Hyperspectral Indices

Lambda vs. Lambda R-square contour plot on non-linear biophysical quantity (e.g., biomass) vs. HTBVI models

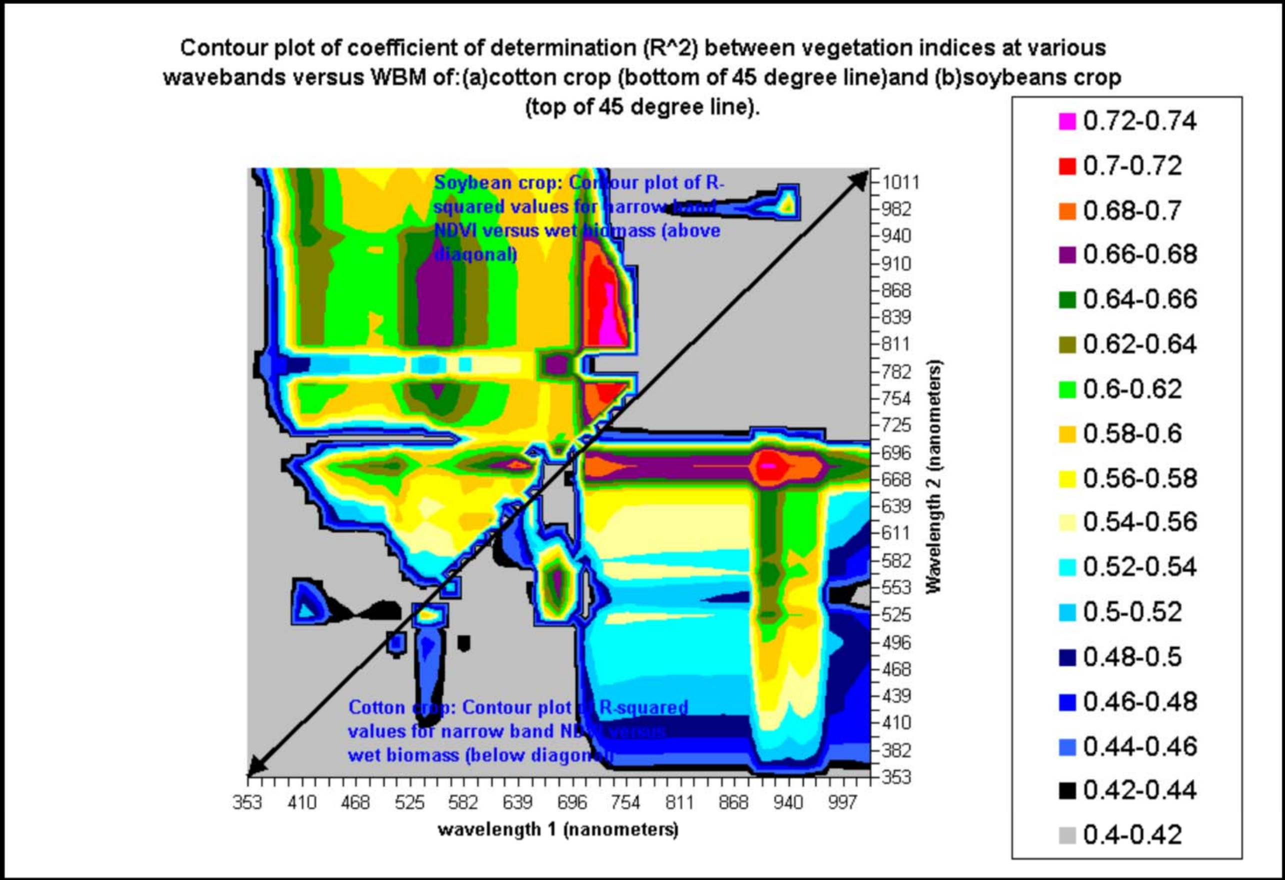

Illustrated for 2 crops here

Methods of Modeling Vegetation Characteristics using Hyperspectral Indices

Non-linear biophysical quantities (e.g., biomass, LAI) vs.:(a)Broadband models (top two), & (b)Narrowband HTBVI models (bottom two)

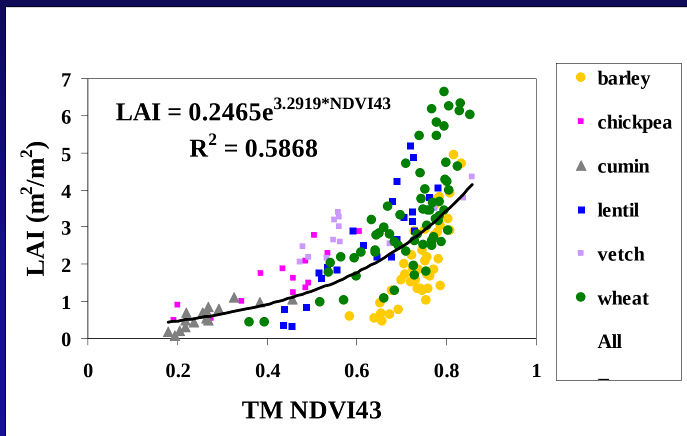

broad-band NDVI43 vs. LAI

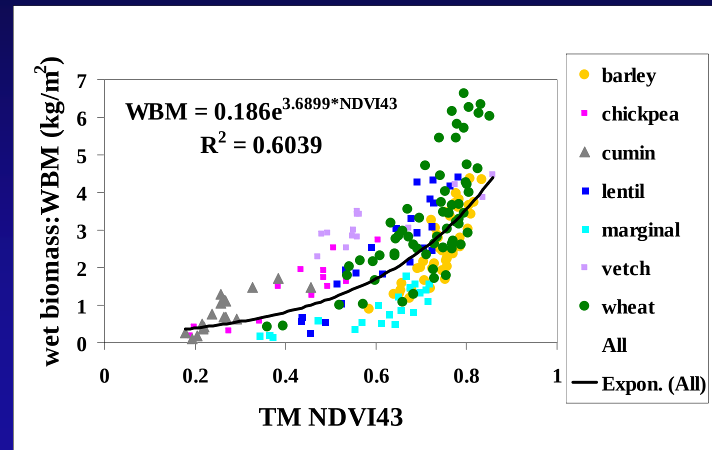

broad-band NDVI43 vs. WBM

HTBVIs explain about 13 percent Greater Variability than Broad-band TM indices in modeling LAI and biomass

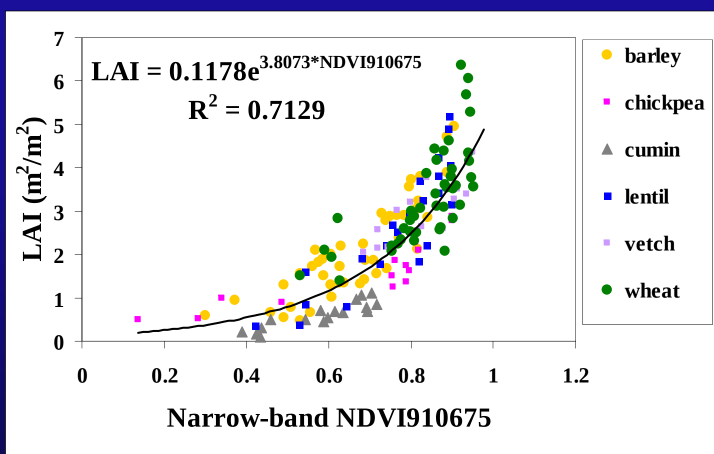

narrow-band NDVI43 vs. LAI

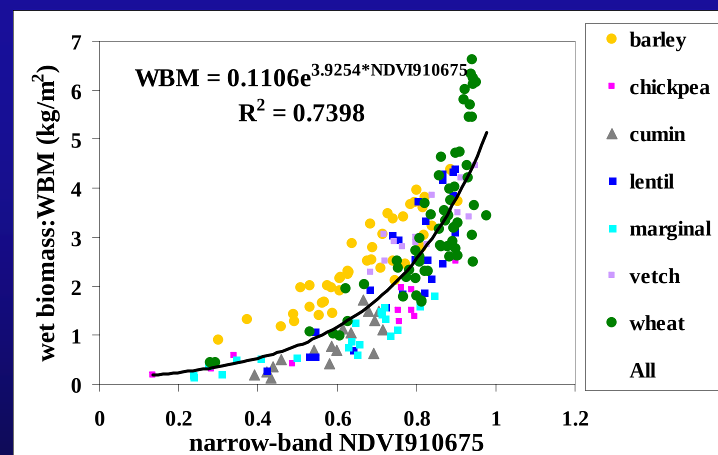

narrow-band NDVI43 vs. WBM

Developing Allometric Equations

in African Rainforests

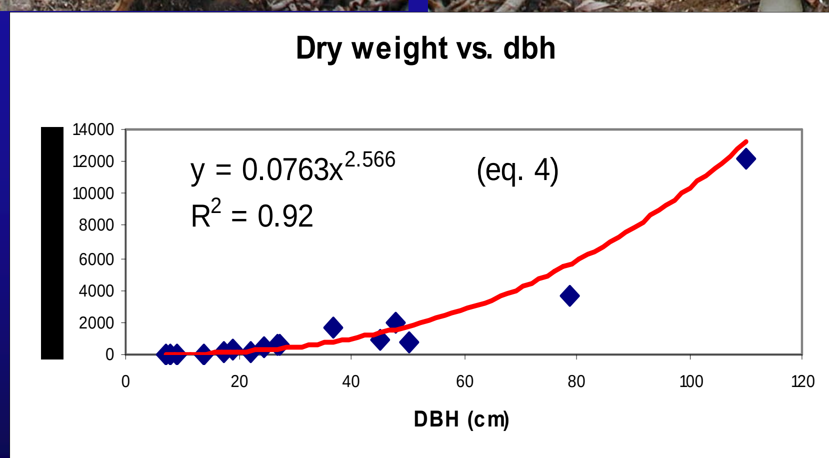

science for a changing world

U.S. Geological Survey
U.S. Department of Interior

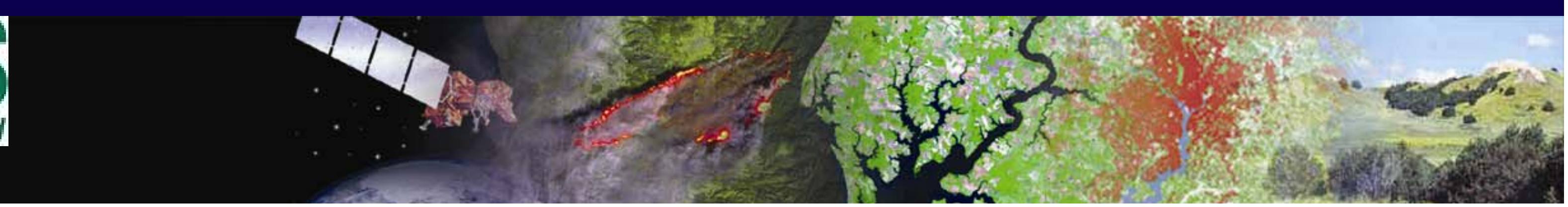

Methods of Modeling Vegetation Characteristics using Hyperspectral Indices

Lambda vs. Lambda R-square contour plot on non-linear biophysical quantity (e.g., biomass) vs. HTBVI models

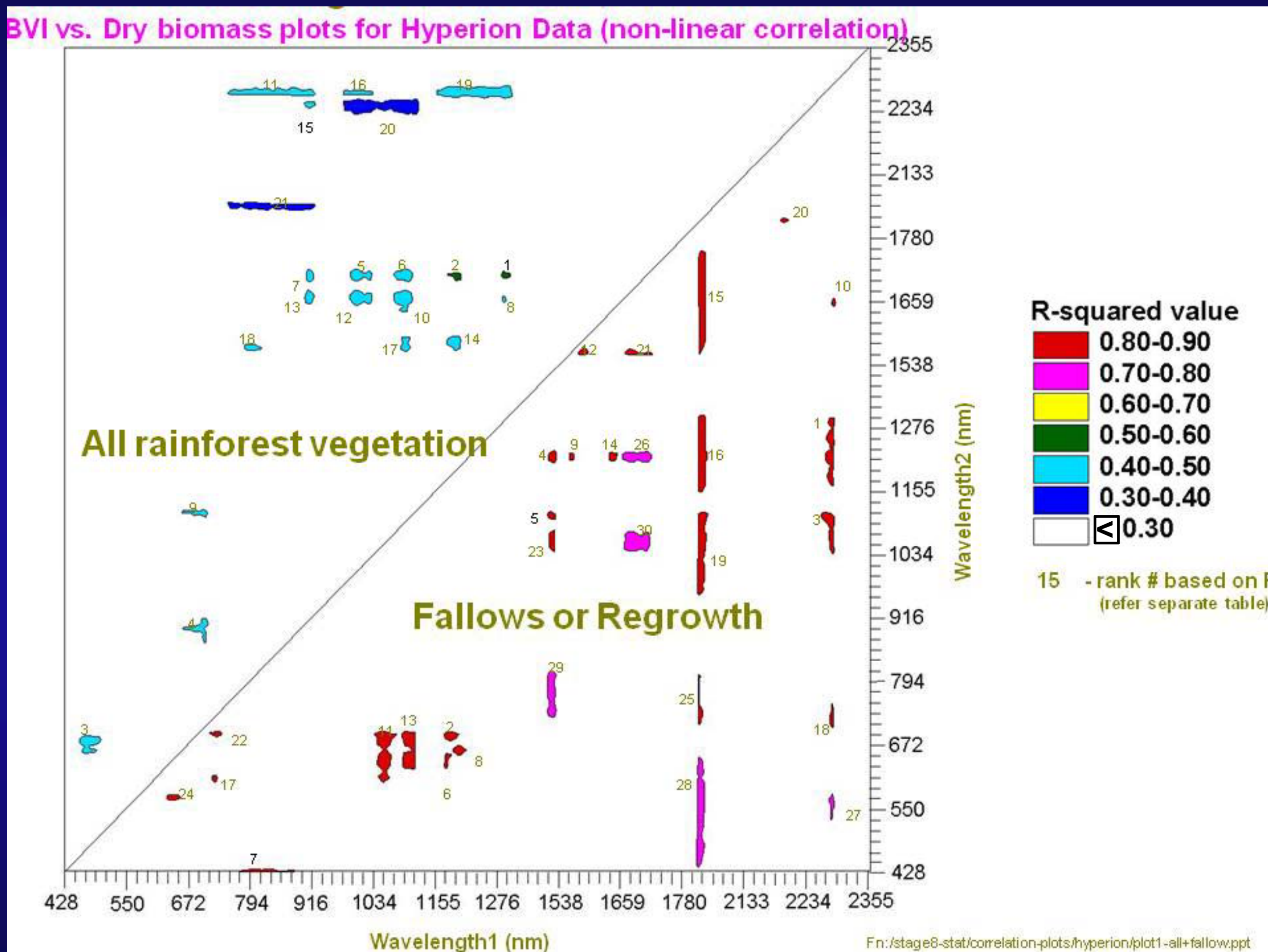

Waveband combinations with greatest R^2 values Greater are ranked…….bandwidths can also be determined.

U.S. Geological Survey
U.S. Department of Interior

Rainforest Vegetation Studies: biomass, tree height, land cover, species in African Rainforests

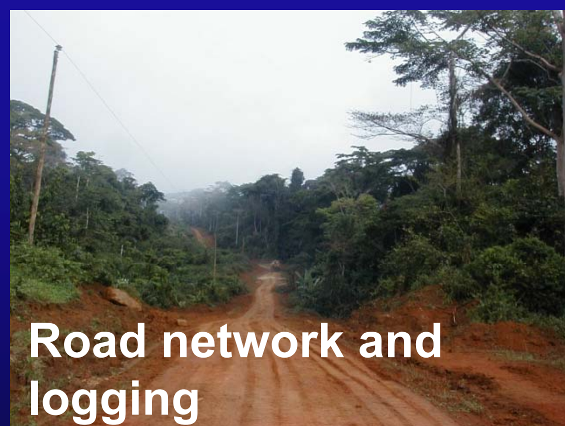

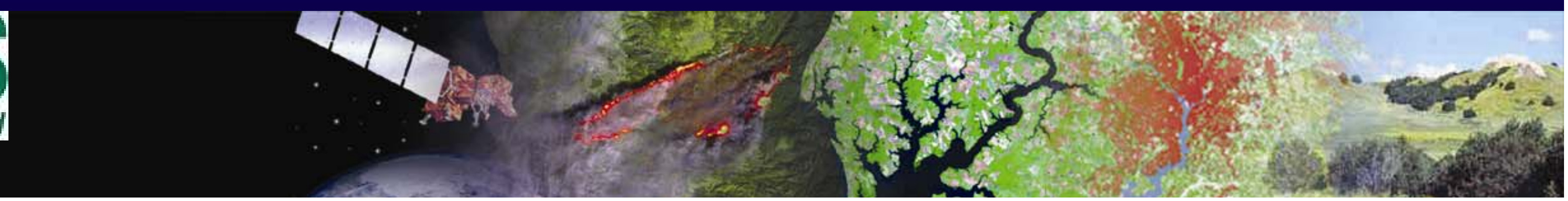

Methods of Modeling Vegetation Characteristics using Hyperspectral Indices

Hyperspectral Multi-band Vegetation Indices (HMBVIs)

$$HMBVI_i = \sum_{J=1}^{N} a_{ij} R_j$$

where, OMBVI = crop variable i, R = reflectance in bands j (j= 1 to N with N=157; N is number of narrow wavebands); a = the coefficient for reflectance in band j for i th variable.

Model algorithm: MAXR procedure of SAS (SAS, 1997) is used in this study. The MAXR method begins by finding the variable (R_j) producing the highest coefficient of determination (R^2) value. Then another variable, the one that yields the greatest increase in R^2 value, is added…………….and so on…….so we will get the best 1-variable model, best 2-variable model, and so on to best n-variable model………………..when there is no significant increase in R^2-value when an additional variable is added, the model can stop.

Methods of Modeling Vegetation Characteristics using Hyperspectral Indices

Predicted biomass derived using MBVI's involving various narrowbands in African Rainforests

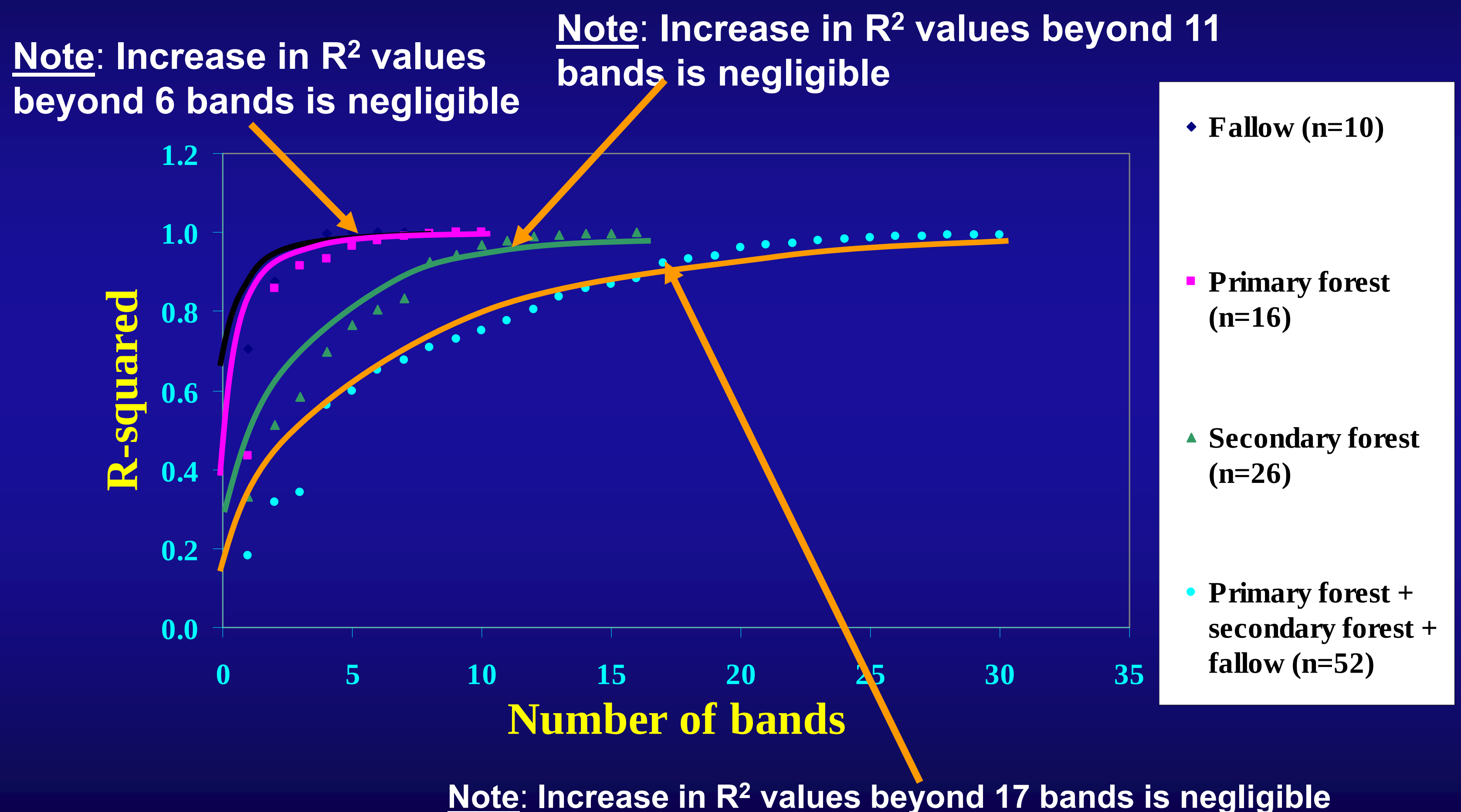

Methods of Modeling Vegetation Characteristics using Hyperspectral Indices

Hyperspectral Derivative Greenness Vegetation Indices (DGVIs)

First Order Hyperspectral Derivative Greenness Vegetation Index (HDGVI) (Elvidge and Chen, 1995): These indices are integrated across the (a) chlorophyll red edge:.626-795 nm, (b) Red-edge more appropriately 690-740 nm……and other wavelengths.

$$DGVI1 = \sum_{\lambda_1}^{\lambda_n} \frac{(\rho'(\lambda_i) - (\rho'(\lambda j)}{\Delta\lambda_I}$$

Where, I and j are band numbers,

λ = center of wavelength,

$\lambda_1 = 0.626\ \mu m$,

$\lambda_n = 0.795\ \mu m$,

ρ' = first derivative reflectance.

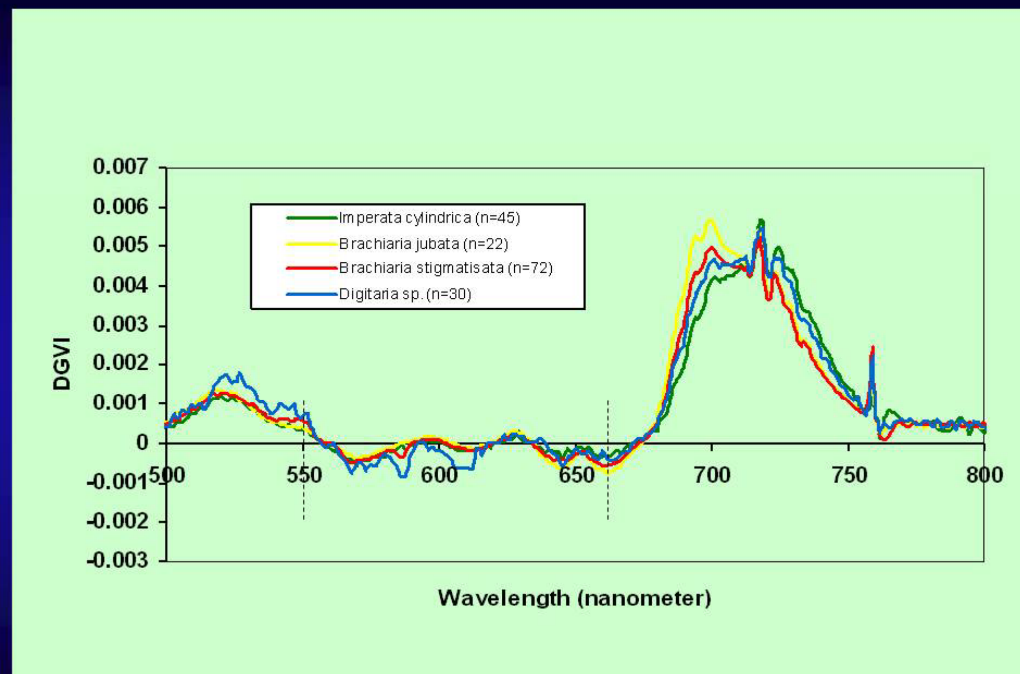

Note: HDGVIs are near-continuous narrow-band spectra integrated over certain wavelengths

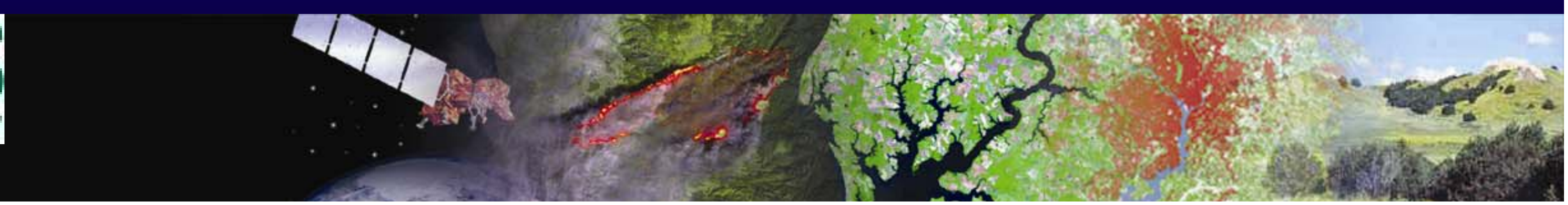

Methods of Modeling Vegetation Characteristics using Hyperspectral Indices

Hyperspectral Derivative Greenness Vegetation Indices (DGVIs) vs. Forest Biomass

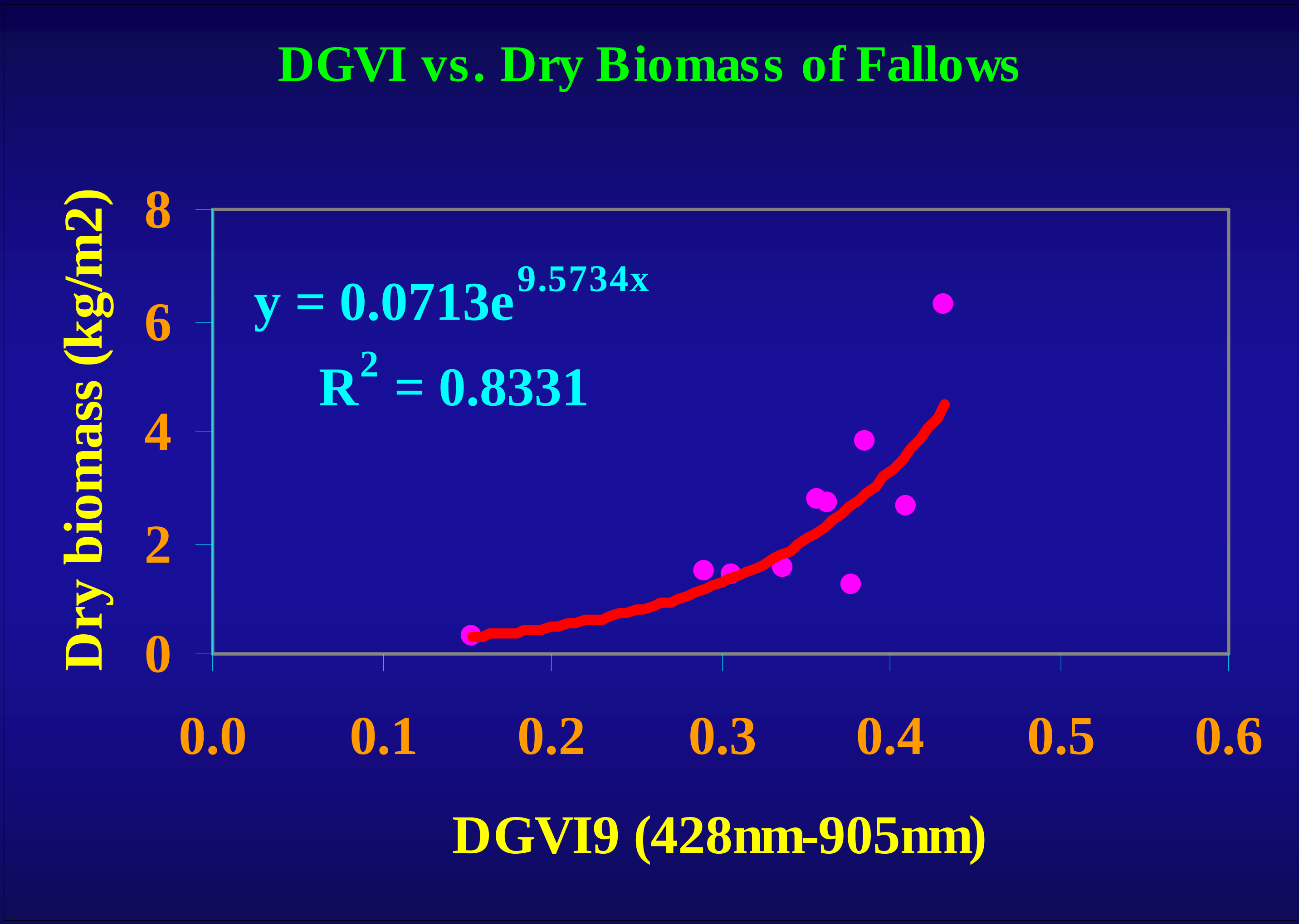

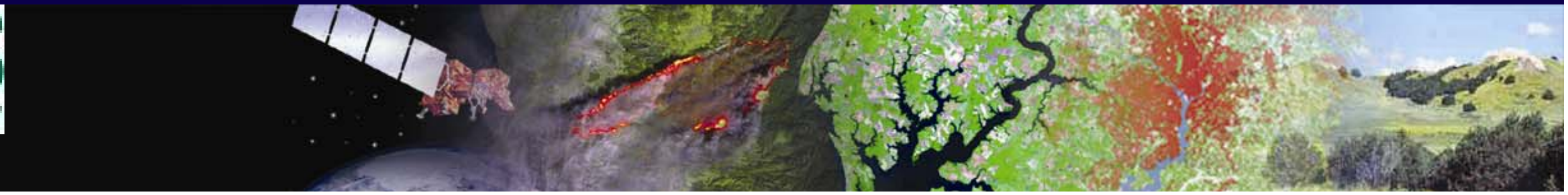

USGS
science for a changing world
U.S. Geological Survey
U.S. Department of Interior

Hyperspectral Data (Imaging Spectroscopy data)

HVIs: Biophysical, Biochemical, Pigment, Water, Lignin and cellulose, and Physiology

Major Hyperspectral Vegetation Indices, Including Relevant Formulas and Key Citations

Index	Equation	Reference
Structure (LAI, green biomass, fraction)		
*NDVI	$(R_{NIR}-R_{red})/(R_{NIR}+R_{red})$	Rouse et al.[15]
*SR	R_{NIR}/R_{red}	Jordan [3]
*EVI	$2.5*(R_{NIR}-R_{red})/(R_{NIR}+6*R_{red}-7.5*R_{blue}+1)$	Huete et al.[23]
*NDWI	$(R_{857}-R_{1241})/(R_{857}+R_{1241})$	Gao [29]
**WBI	R_{900}/R_{970}	Peñuelas et al.[28]
*ARVI	$(R_{NIR}-[R_{red}-\gamma*(R_{blue}-R_{red})])/(R_{NIR}+[R_{red}-\gamma*(R_{blue}-R_{red})])$	Kaufman & Tanré [22]
*SAVI	$[(R_{NIR}-R_{red})/(R_{NIR}+R_{red}+L)]*(1+L)$	Huete [21]
**1DL_DGVI	$\sum_{\lambda_{626\ nm}}^{\lambda_{795\ nm}} \lvert R'(\lambda_i) - R'(\lambda_{626\ nm}) \rvert \Delta\lambda_i$	Elvidge & Chen [1]
**1DZ_DGVI	$\sum_{\lambda_{626\ nm}}^{\lambda_{795\ nm}} \lvert R'(\lambda_i) \rvert \Delta\lambda_i$	Elvidge & Chen [1]
*VARI	$(R_{green}-R_{red})/(R_{green}+R_{red}-R_{blue})$	Gitelson et al.[13]
*VIgreen	$(R_{green}-R_{red})/(R_{green}+R_{red})$	Gitelson et al.[13]
Biochemical		
Pigments		
**SIPI	$(R_{800}-R_{445})/(R_{800}-R_{680})$	Peñuelas et al. [31]
**PSSR	(R_{800}/R_{675}); (R_{800}/R_{650})	Blackburn [30]
**PSND	$[(R_{800}-R_{675})/(R_{800}+R_{675})]$; $[(R_{800}-R_{650})/(R_{800}+R_{650})]$	Blackburn [32]
**PSRI	$(R_{680}-R_{500})/R_{750}$	Merzlyak et al. [33]
Chlorophyll		
**CARI	$[(R_{700}-R_{670})-0.2*(R_{700}-R_{550})]$	Kim [34]
**MCARI	$[(R_{700}-R_{670})-0.2*(R_{700}-R_{550})]*(R_{700}/R_{670})$	Daughtry et al. [35]
**$CI_{red\ edge}$	$R_{NIR}/R_{red\ edge}-1$	Gitelson et al. [36]
Anthocyanins		
**ARI	$(1/R_{green})-(1/R_{red\ edge})$	Gitelson et al.[40]
**mARI	$[(1/R_{green})-(1/R_{red\ edge})]*R_{NIR}$	Gitelson et al. [36]
**RGRI	R_{red}/R_{green}	Gamon & Surfus [7]
**ACI	R_{green}/R_{NIR}	Van den Berg & Perkins [41]
Carotenoids		
**CRI1	$(1/R_{510})-(1/R_{550})$	Gitelson et al.[42]
**CRI2	$(1/R_{510})-(1/R_{700})$	Gitelson et al. [42]
Water		
*NDII	$(R_{NIR}-R_{SWIR})/(R_{NIR}+R_{SWIR})$	Hunt & Rock [12]
*NDWI, **WBI	See Above	See Above
*MSI	R_{SWIR}/R_{NIR}	Rock et al. [43]
Lignin &Cellulose/Residues		
**CAI	100*[0.5*(R2031+R2211)-R2101]	Daughtry [47]
**NDLI	$[\log(1/R_{1754})-\log(1/R_{1680})]/[\log(1/R_{1754})+\log(1/R_{1680})]$	Serrano et al. [48]
Nitrogen		
**NDNI	$[\log(1/R_{1510})-\log(1/R_{1680})]/[\log(1/R_{1510})+\log(1/R_{1680})]$	Serrano et al. [48]
Physiology		
Light Use Efficiency		
**RGRI, **SIPI	See Above	See Above
**PRI	$(R_{530}-R_{570})/(R_{530}+R_{570})$	Gamon et al. [9]
Stress		
*MSI	See Above	See Above
**REP	l(max first derivitive: 680-750 nm)	Horler et al. [10]
**RVSI	$[(R_{714}+R_{752})/2-R_{733}$	Merton & Huntington [52]

Note: see chapter 14, Roberts et al.

science for a changing world

U.S. Geological Survey
U.S. Department of Interior

Hyperspectral Data (Imaging Spectroscopy data)

HVIs: Biophysical, Biochemical, Pigment, Water, Lignin and cellulose, and Physiology

Spectral index	Characteristics & functions	Definition	Reference
Multiple bioparameters:			
LI, Lepidium Index	To be sensitive to the uniformly bright reflectance displayed by *Lepidium* in the visible range.	R_{630}/R_{586}	[20]
NDVI, Normalized Difference Vegetation Index	Respond to change in the amount of green biomass and more efficiently in vegetation with low to moderate density.	$(R_{NIR}-R_R)/(R_{NIR}+R_R)$	[74]
PSND, Pigment-Specific Normalized Difference	Estimate LAI and carotenoids (Cars) at leaf or canopy level	$(R_{800}-R_{470})/(R_{800}+R_{470})$	[74]
SR, Simple Ratio	Same as **NDVI**	R_{NIR}/R_R	[76,77]
Pigments:			
Chl_{green}, Chlorophyll Index Using Green Reflectance	Estimate chlorophylls (Chls) content in anthocyanin-free leaves if NIR is set	$(R_{760-800}/R_{540-560})-1$	[78]
$Chl_{red-edge}$, Chlorophyll Index Using Red Edge Reflectance	Estimate Chls content in anthocyanin-free leaves if NIR is set	$(R_{760-800}/R_{690-720})-1$	[78]
LCI, Leaf Chlorophyll Index	Estimate Chl content in higher plants, sensitive to variation in reflectance caused by Chl absorption	$(R_{850}-R_{710})/(R_{850}+R_{680})$	[79]
mND_{680}, Modified Normalized Difference	Quantify Chl content and sensitive to low content at leaf level.	$(R_{800}-R_{680})/(R_{800}+R_{680}-2R_{445})$	[80]
mND_{705}, Modified Normalized Difference	Quantify Chl content and sensitive to low content at leaf level. **mND_{705}** performance better than **mND_{680}**	$(R_{750}-R_{705})/(R_{750}+R_{705}-2R_{445})$	[80,81]
mSR_{705}, Modified Simple Ratio	Quantify Chl content and sensitive to low content at leaf level.	$(R_{750}-R_{445})/(R_{705}-R_{445})$	[80]

Note: see chapter 19, Pu et al.

USGS
science for a changing world
U.S. Geological Survey
U.S. Department of Interior

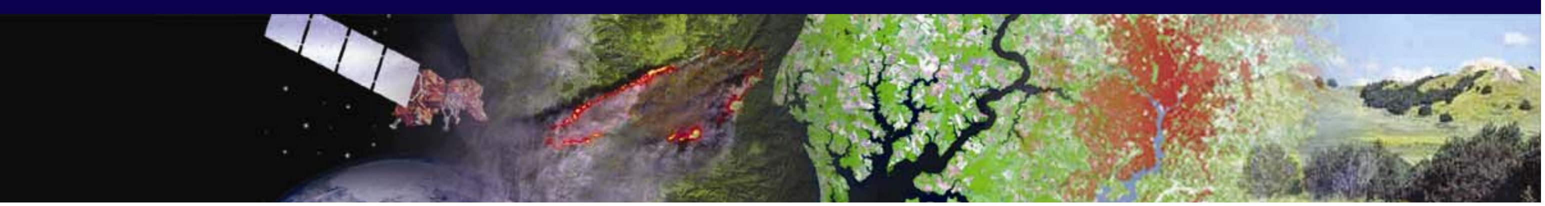

Hyperspectral Data (Imaging Spectroscopy data)

HVIs: Biophysical, Biochemical, Pigment, Water, Lignin and cellulose, and Physiology

mSR_{705}, Modified Simple Ratio	Quantify Chl content and sensitive to low content at leaf level.	$(R_{750}-R_{445})/(R_{705}-R_{445})$	[80]
NPCI, Normalized Pigment Chlorophyll ratio Index	Assess Cars/Chl ratio at leaf level	$(R_{680}-R_{430})/(R_{680}+R_{430})$	[82]
PBI, Plant Biochemical Index	Retrieve leaf total Chl and nitrogen concentrations from satellite hyperspectral data	R_{810}/R_{560}	[83]
PRI, Photochemical / Physiological Reflectance Index	Estimate Car pigment contents in foliage	$(R_{531}-R_{570})/(R_{531}+R_{570})$	[84]
PI2, Pigment index 2	Estimate pigment content in foliage	R_{695}/R_{760}	[85]
RGR, Red:Green Ratio	Estimate anthocyanin content with a green and a red band	R_{683}/R_{510}	[80,86]
SGR, Summed Green Reflectance	Quantify Chl content	Sum of reflectances from 500 to 599 nm	[81]
Floliar chemistry:			
CAI, Cellulose Absorption Index	Cellulose & lignin absorption features, discriminates plant litter from soils	$0.5(R_{2020}+R_{2220})-R_{2100}$	[87]
NDLI, Normalized Difference Lignin Index	Quantify variation of canopy lignin concentration in native shrub vegetation	$[\log(1/R_{1754})-\log(1/R_{1680})]$ / $[\log(1/R_{1754})+\log(1/R_{1680})]$	[88]
NDWI, ND Water Index	Improving the accuracy in retrieving the vegetation water content at both leaf and canopy levels	$(R_{860}-R_{1240})/(R_{860}+R_{1240})$	[89,90]
RVI_{hyp}, Hyperspectral Ratio VI	Quantify LAI and water content at canopy level.	R_{1088}/R_{1148}	[91]
WI, Water Index	Quantify relative water content at leaf level	R_{900}/R_{970}	[92]

Note: see chapter 19, Pu et al.

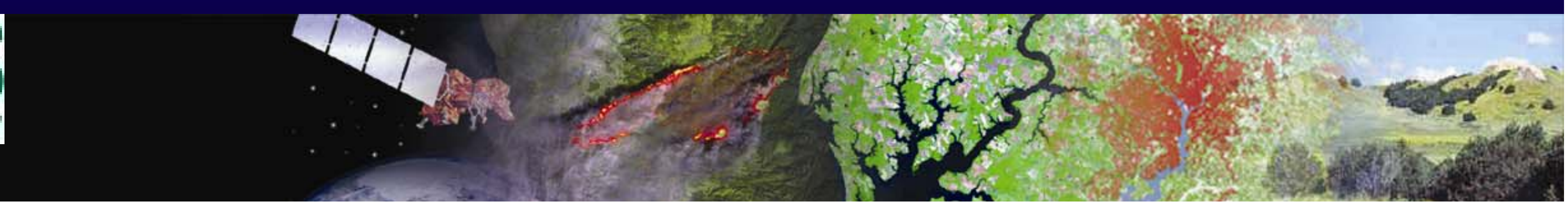

Hyperspectral Remote Sensing of Vegetation

Study of Pigments: chlorophyll

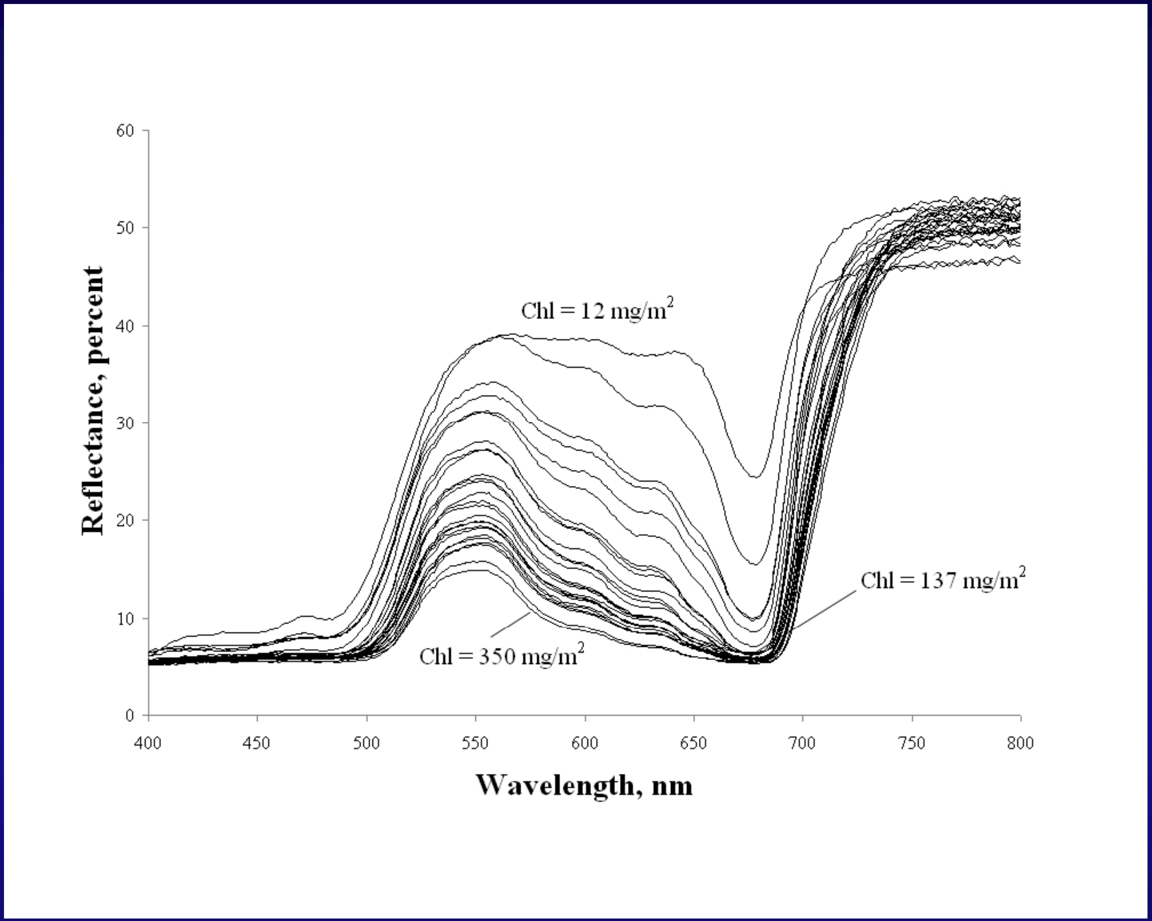

e.g., Reflectance spectra of beech leaves…red-edge (700-740 nm) one of the best.

Note: see chapter 6; Gitelson et al.

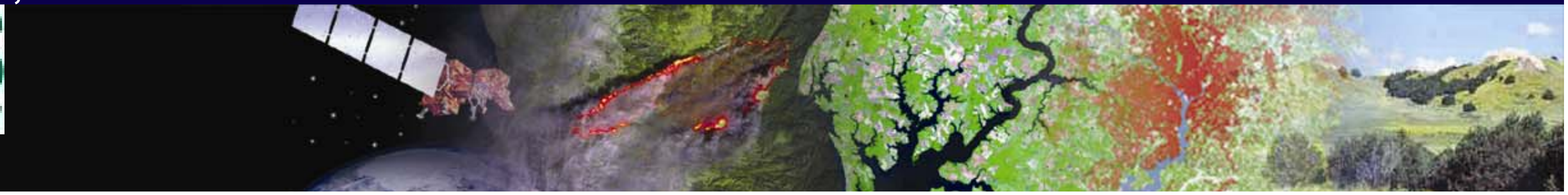

U.S. Geological Survey
U.S. Department of Interior

Hyperspectral Remote Sensing of Vegetation

Study of Pigments: carotenoids/chlorophyll

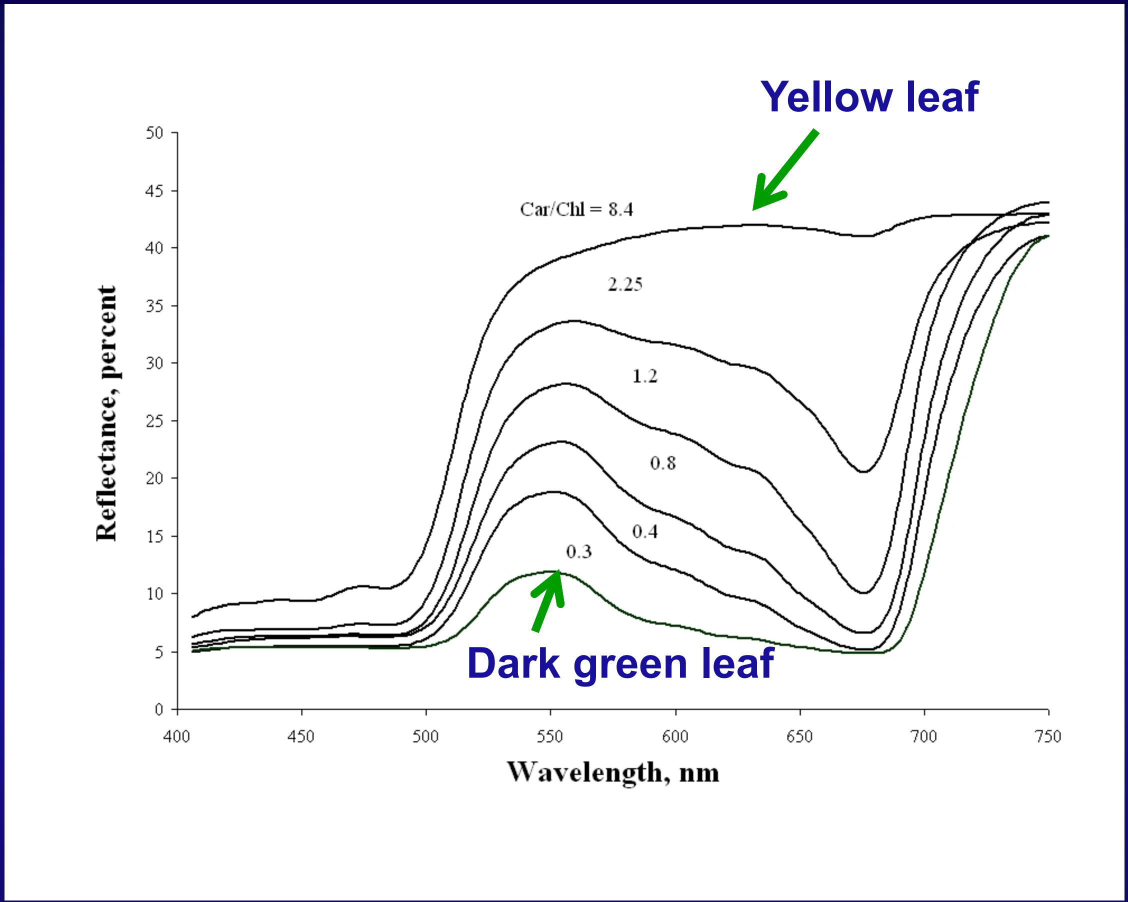

e.g., Reflectance spectra of chestnut leaves…difference reflectance of (680-500 nm)/750 nm quantitative measurement of plant senescence

Note: see chapter 6; Gitelson et al.

Methods of

Classifying Vegetation Classes or categories

Increased Accuracies over Broadband Data

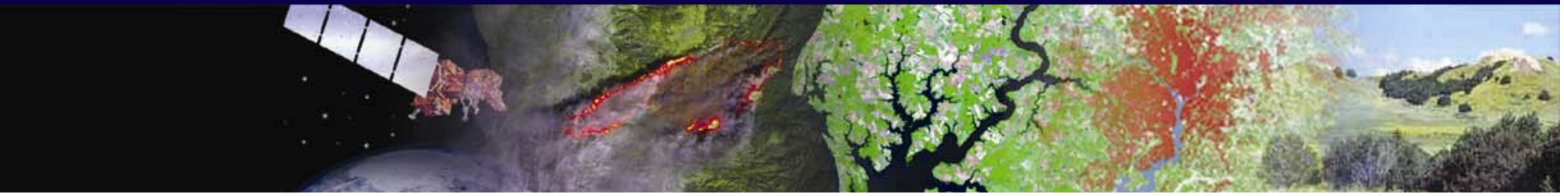

Methods of Classifying Vegetation Classes or Categories
Using hyperspectral narrowband data

1. Multivariate and Partial Least Square Regression,
2. Discriminant analysis
3. unsupervised classification (e.g., Clustering),
4. supervised approaches

A. Spectral-angle mapping or SAM,
B. Maximum likelihood classification or MLC,
C. Artificial Neural Network or ANN,
D. Support Vector Machines or SVM,

4. Spectral Matching Technique (SMT)

Excellent for full spectral analysis…..but needs good spectral library

………All these methods have merit; it remains for the user to apply them to the situation of interest.

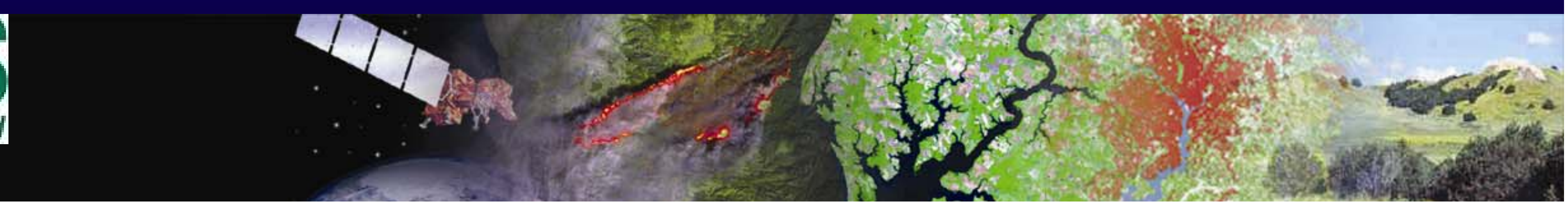

Methods of Classifying Vegetation Classes or Categories

Discriminant Model or Classification Criterion (DM) to Test

How Well 12 different Vegetation are Discriminated using different Combinations of Broadbands vs. Narrowbands?

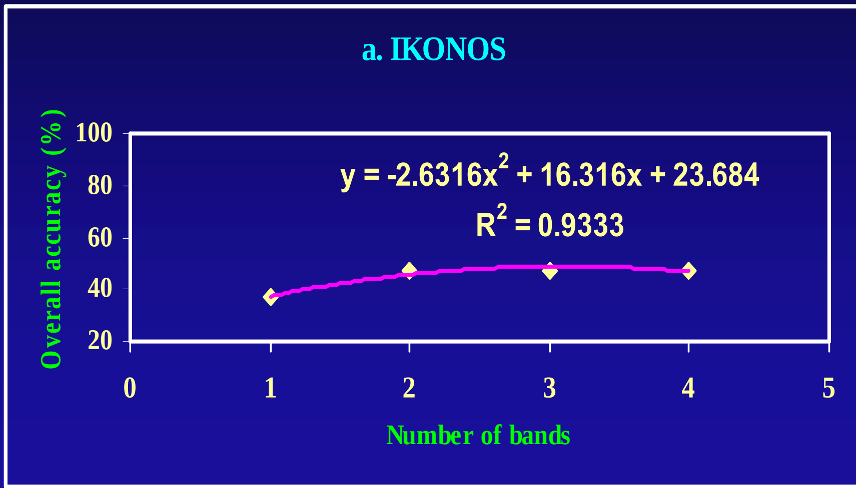

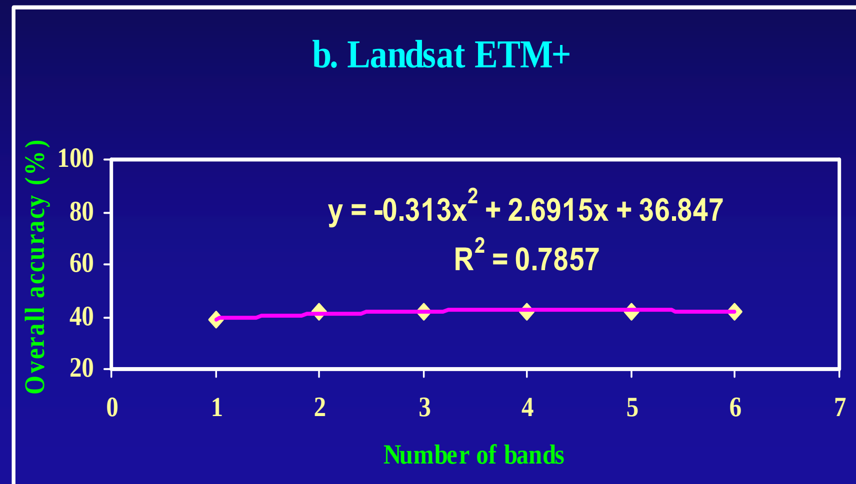

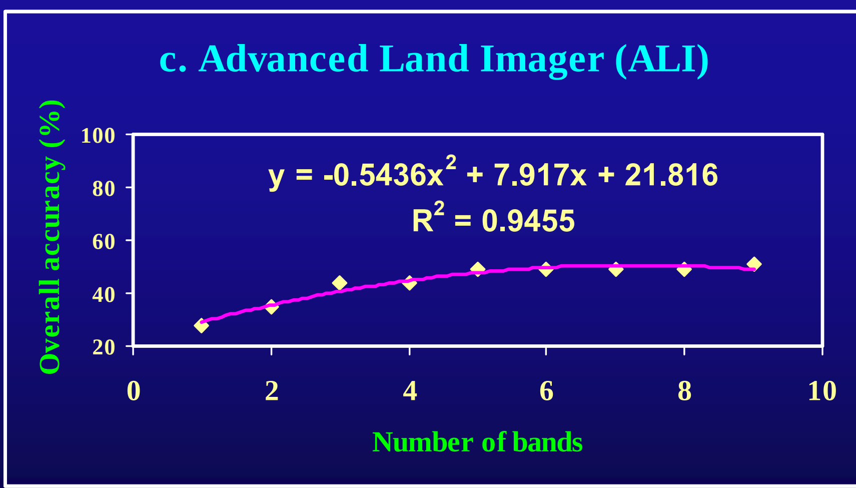

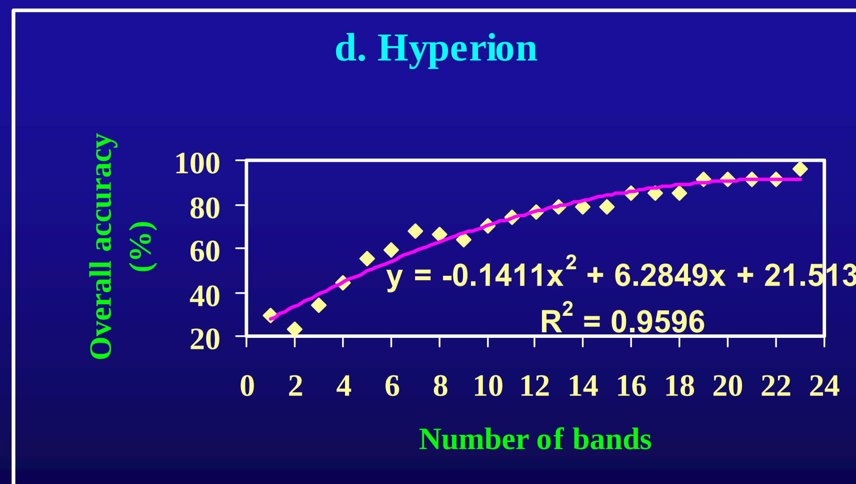

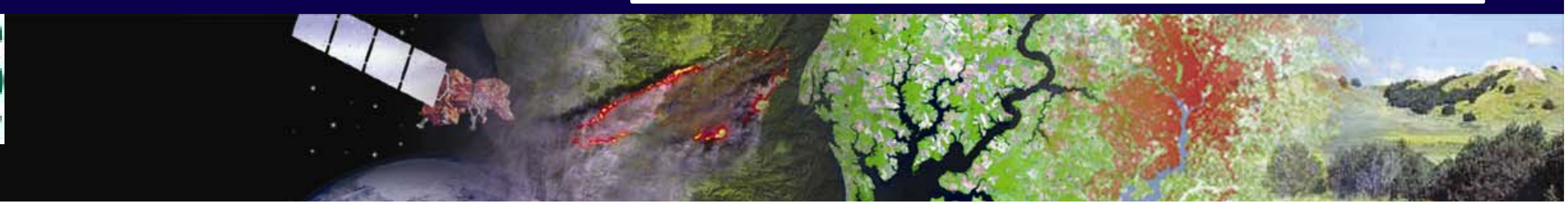

USGS
science for a changing world

U.S. Geological Survey
U.S. Department of Interior

Concluding Thoughts I

Hyperspectral (imaging Spectroscopy)

Knowledge Gain in Study of Vegetation

Hyperspectral Remote Sensing of Vegetation
Knowledge Gain and Knowledge Gap After 40 years of Research

1. Hyperspectral narrowbands when compared with broadbands data can significantly improve in:

1.1. Discriminating\Separating vegetation and crop types and their species;

1.2. Explaining greater variability in modeling vegetation and crop biophysical, yield, and biochemical characteristics;

1.3. Increasing accuracies (reducing errors and uncertainties) in vegetation\land cover classification; and

1.4. Enabling the study of specific biophysical and biochemical properties from specific targeted portion of the spectrum.

2. About 33 narrowbands, in 400-2500 nm, provide optimal information in vegetation studies. These waveband centers are identified in this study. A nominal 3 to 5 nm wide bandwidth is recommended for all wavebands;

3. Advances in methods and approaches of hyperspectral data analysis in vegetation studies.

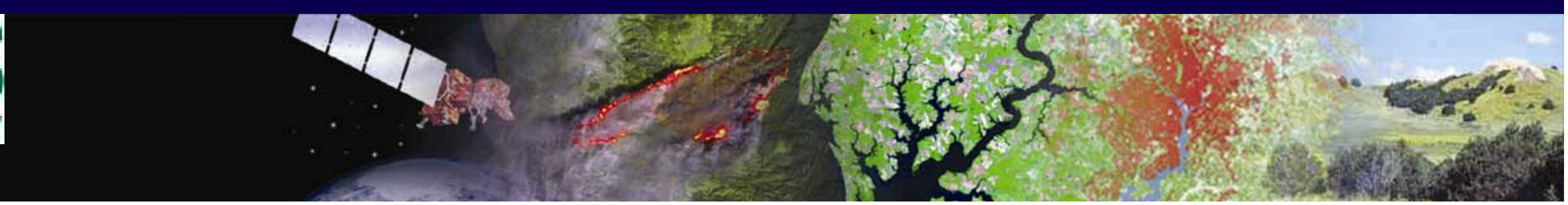

U.S. Geological Survey
U.S. Department of Interior

Knowledge Gain in using Hyperspectral Narrowband Data in Study of Vegetation

1.1a. Discriminating\Separating Vegetation Types

Note: Distinct separation of vegetation or crop types or species using distinct narrowbands

Broad-band (Landsat-5 TM) NIR vs. Red

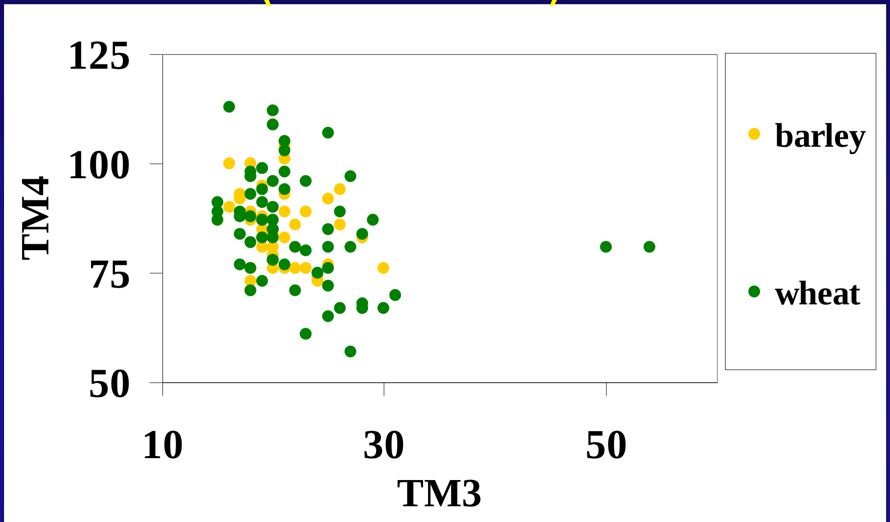

Narrow-band NIR vs. Red

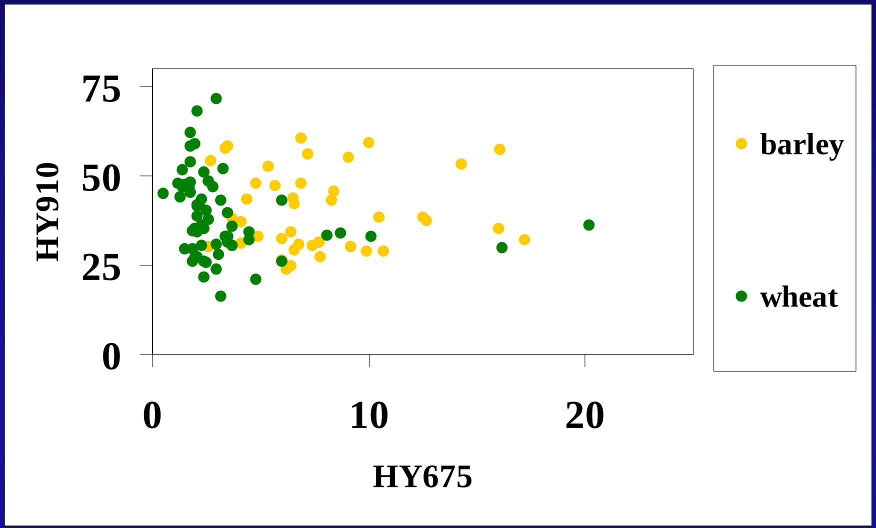

Numerous narrow-bands provide unique opportunity to discriminate different crops and vegetation.

Methods of Separating Vegetation Classes or Categories

Hyperion Narrowbands in Separating Vegetation\Crop Types (e.g., Crops in Brazil)

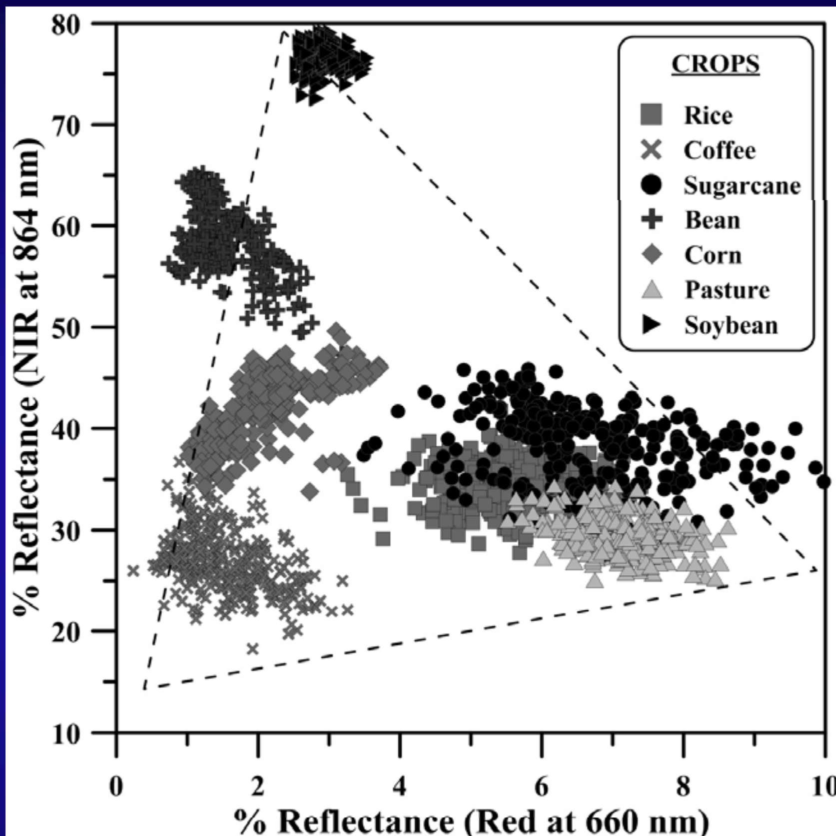

Relationships between red and near infrared (NIR) Hyperion bands for the studied crop types. The triangle is discussed in the text.

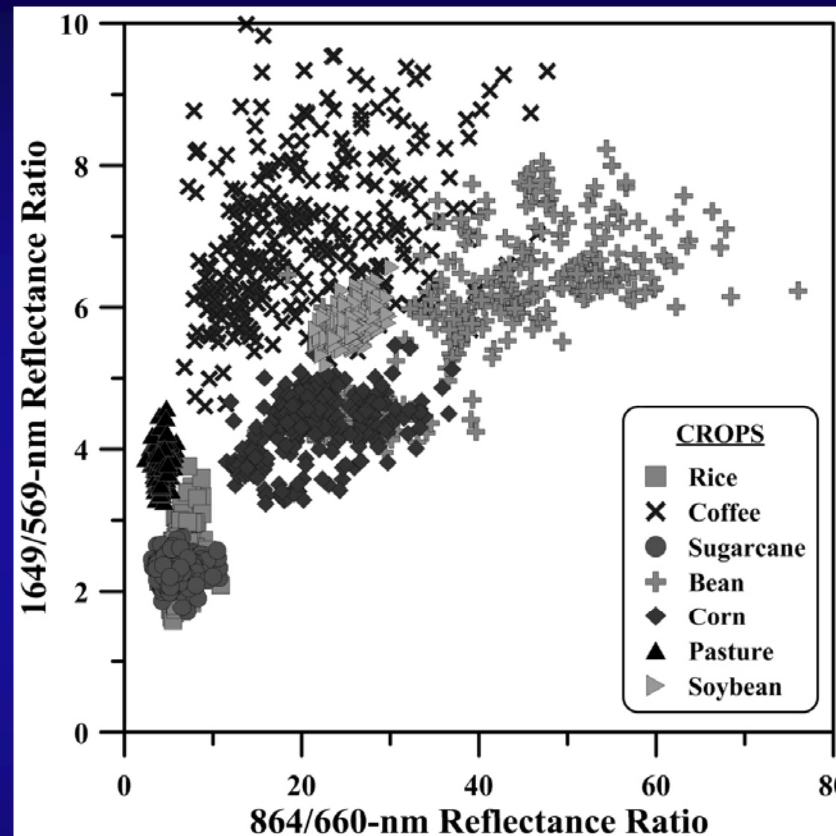

Variation in NIR-1/red and SWIR-1/green reflectance ratios for the crop types under study.

Note: see chapter 17

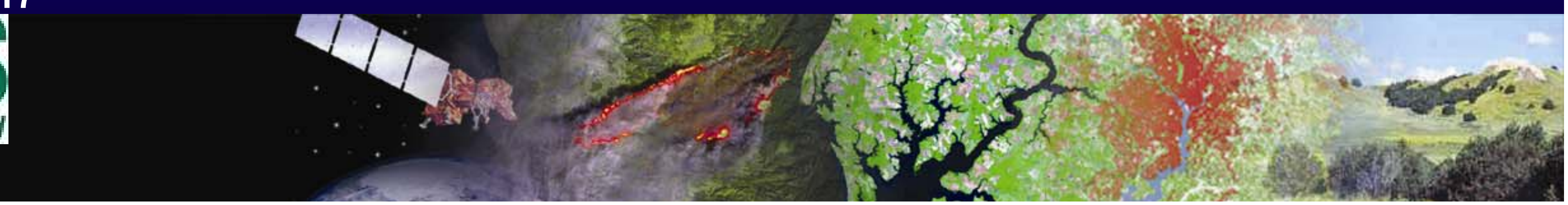

USGS
science for a changing world
U.S. Geological Survey
U.S. Department of Interior

Knowledge Gain in using Hyperspectral Narrowband Data in Study of Vegetation

1.2a. Improved biophysical and biochemical models of Vegetation

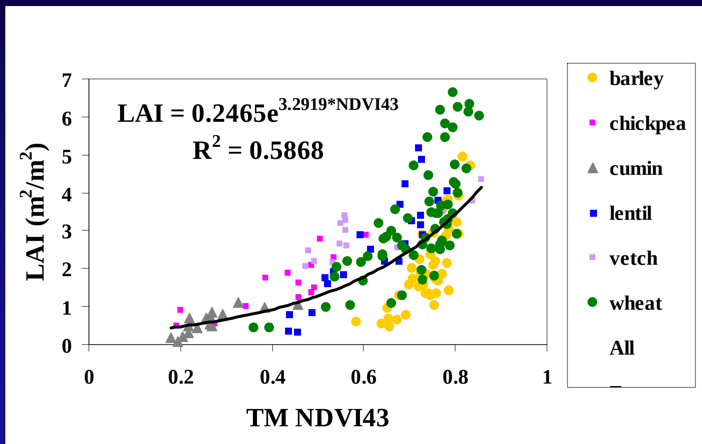

Broad-band NDVI43 vs. LAI

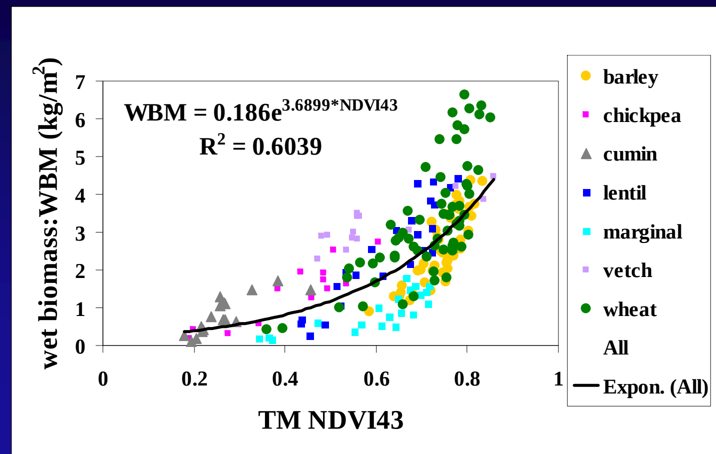

Broad-band NDVI43 vs. WBM

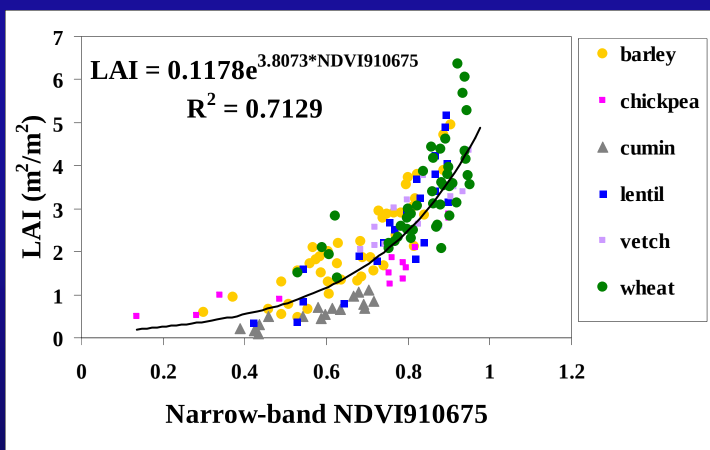

Narrow-band NDVI43 vs. LAI

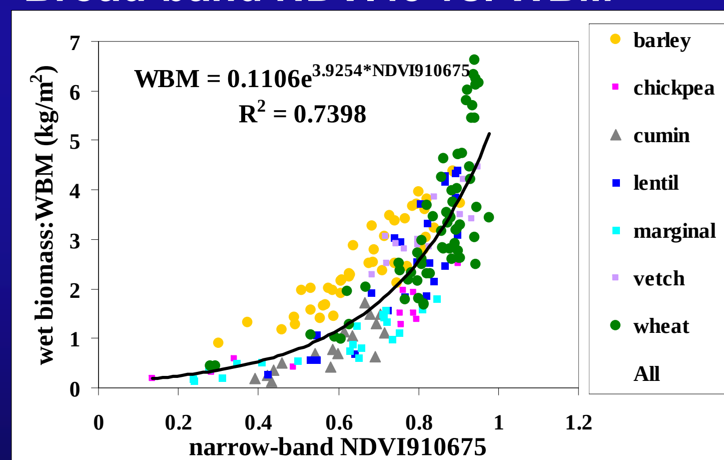

Narrow-band NDVI43 vs. WBM

Note: Improved models of vegetation biophysical and biochemical variables: The combination of wavebands in Table 28.1 or HVIs derived from them provide us with significantly improved models of vegetation variables such as biomass, LAI, net primary productivity, leaf nitrogen, chlorophyll, carotenoids, and anthocyanins. For example, stepwise linear regression with a dependent plant variable (e.g., LAI, Biomass, nitrogen) and a combination of "N" independent variables (e.g., chosen by the model from Table 28.1) establish a combination of wavebands that best model a plant variable

Narrow-band indices explain about 13 percent greater variability in modeling crop variables.

USGS
science for a changing world

U.S. Geological Survey
U.S. Department of Interior

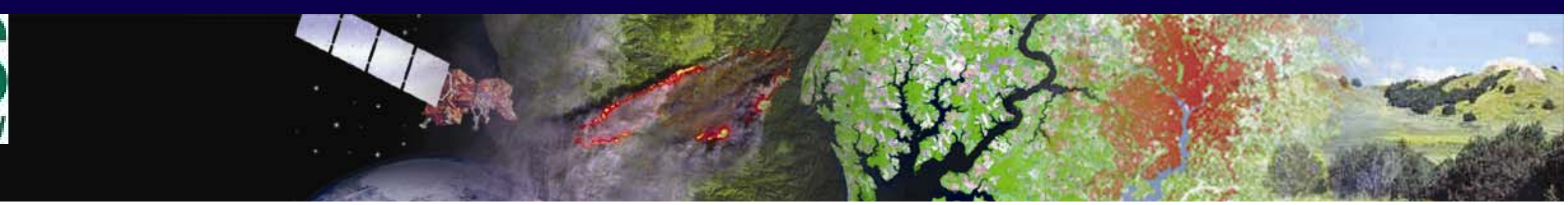

Knowledge Gain in using Hyperspectral Narrowband Data in Study of Vegetation

1.3a. Improved Classification Accuracies (and reduced errors and uncertainties)

Note: Overall Accuracies and K_{hat} Increase by about 30 % using 20 narrow-bands compared 6 non-thermal TM broad-bands in classifying 12 classes

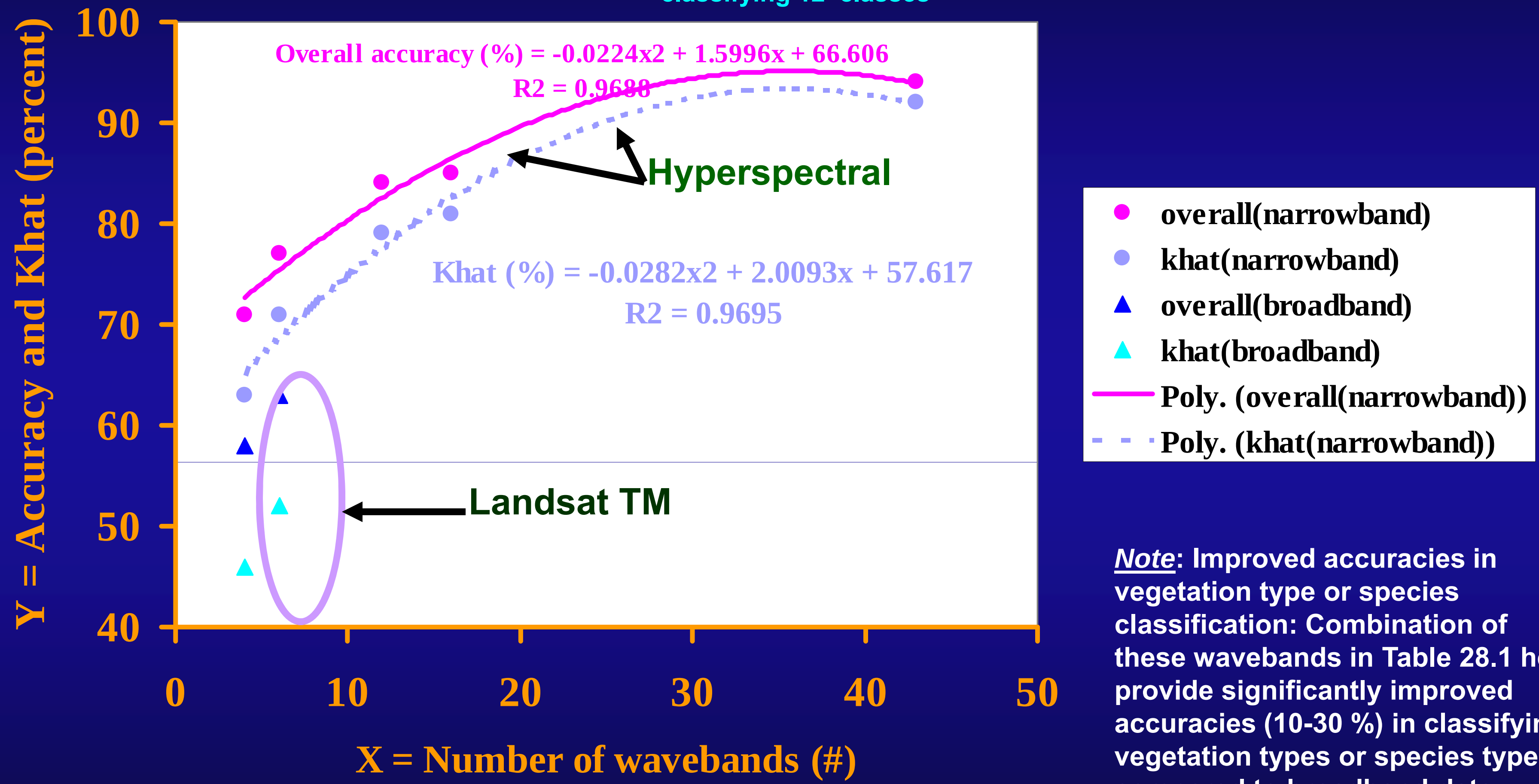

***Note*: Improved accuracies in vegetation type or species classification: Combination of these wavebands in Table 28.1 help provide significantly improved accuracies (10-30 %) in classifying vegetation types or species types compared to broadband data;**

Knowledge Gain in using Hyperspectral Narrowband Data in Study of Vegetation

1.3b. Improved Classification Accuracies (and reduced errors and uncertainties)

Stepwise Discriminant Analysis (SDA)- Wilks' Lambda to Test : How Well Different Forest Vegetation are Discriminated from One Another

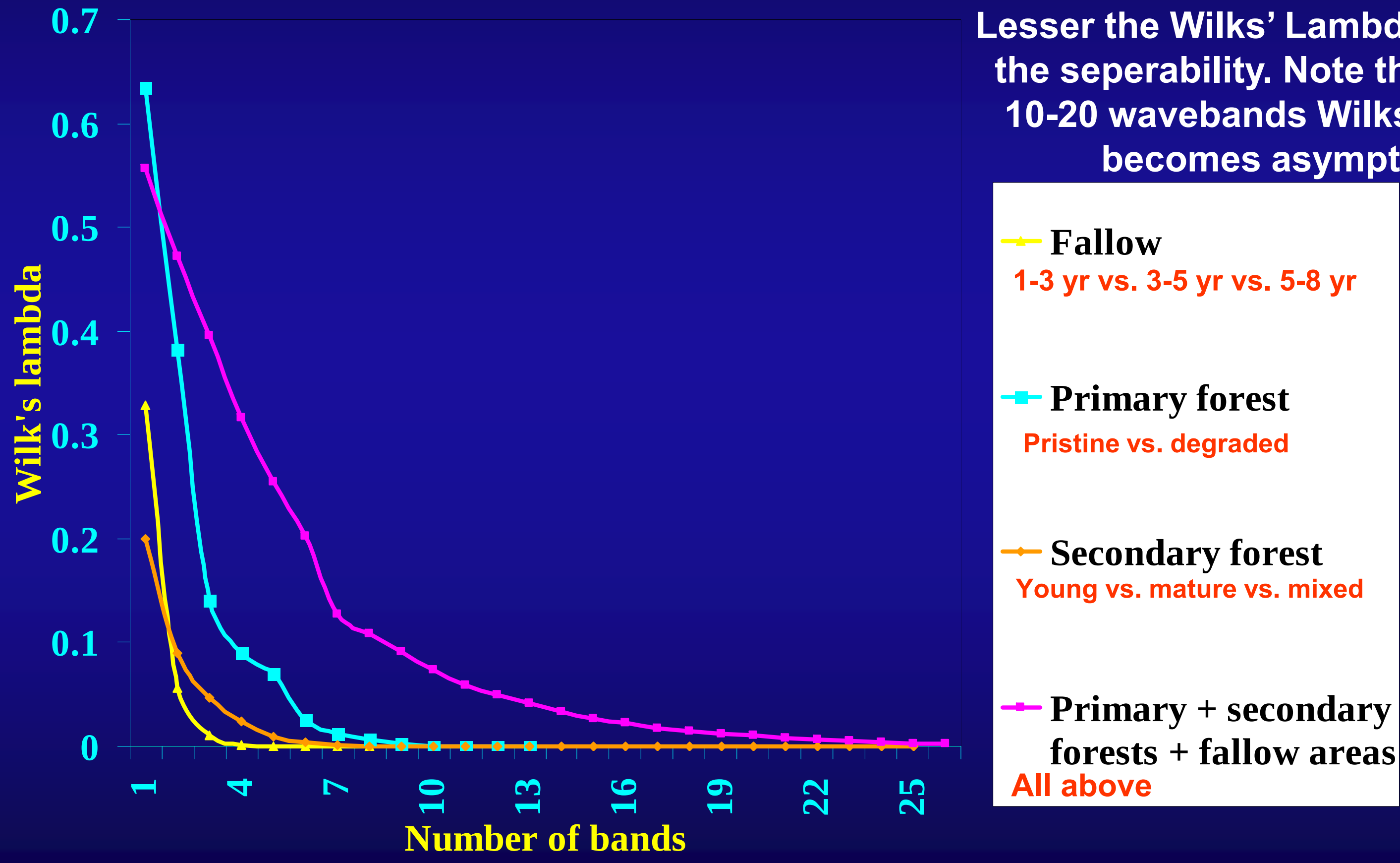

Lesser the Wilks' Lambda greater is the seperability. Note that beyond 10-20 wavebands Wilks' Lambda becomes asymptotic.

Knowledge Gain in using Hyperspectral Narrowband Data in Study of Vegetation

1.2b. Improved biophysical and biochemical models of Vegetation

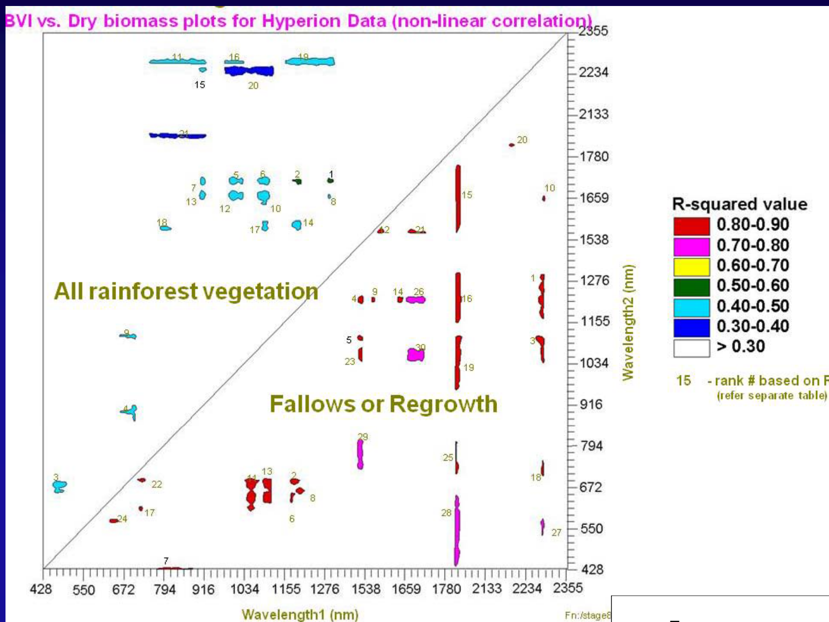

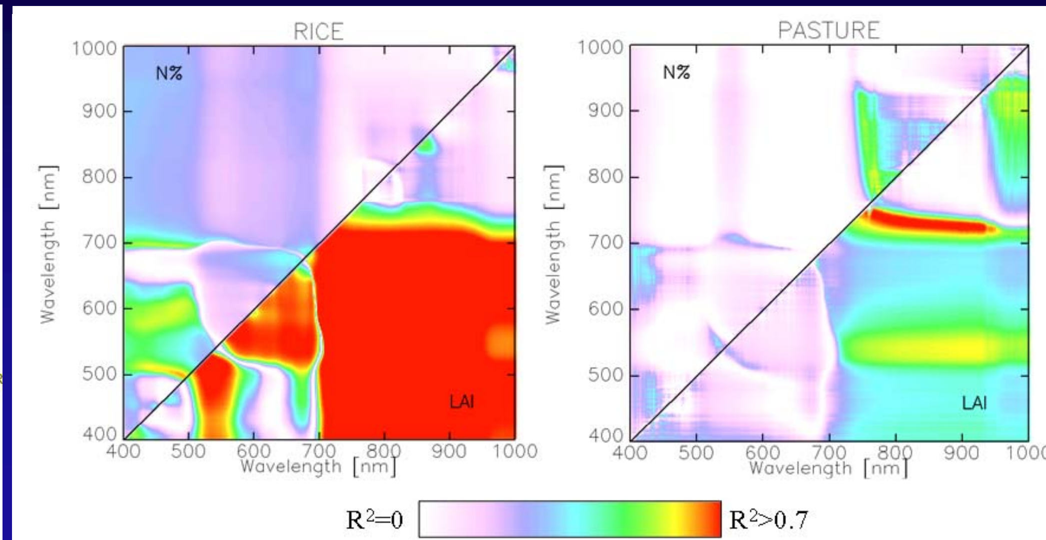

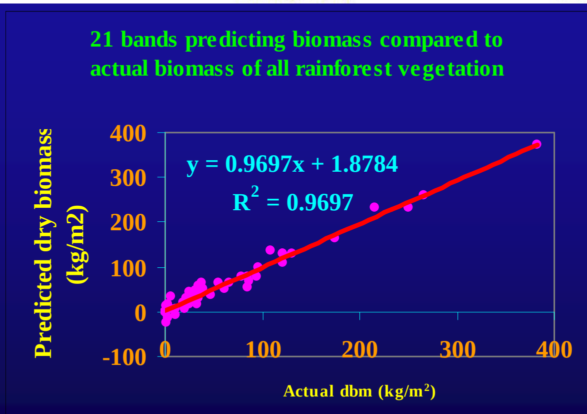

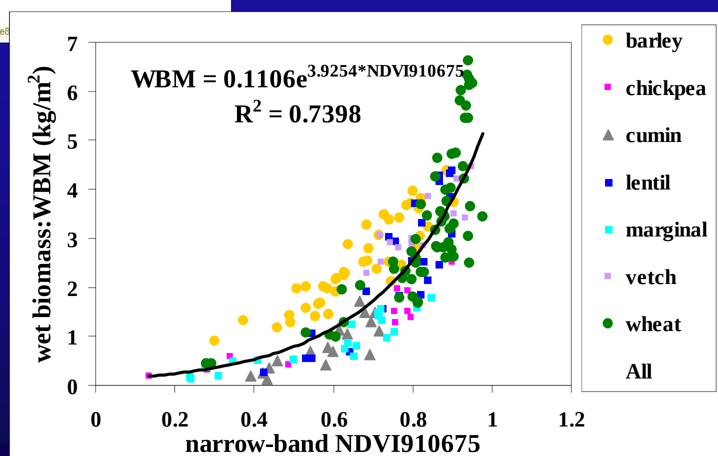

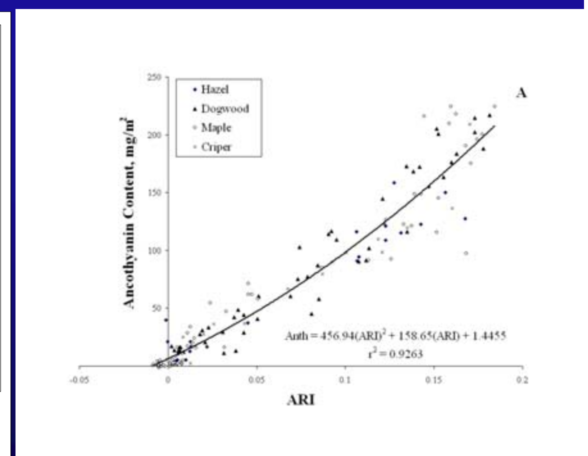

science for a changing world

U.S. Geological Survey
U.S. Department of Interior

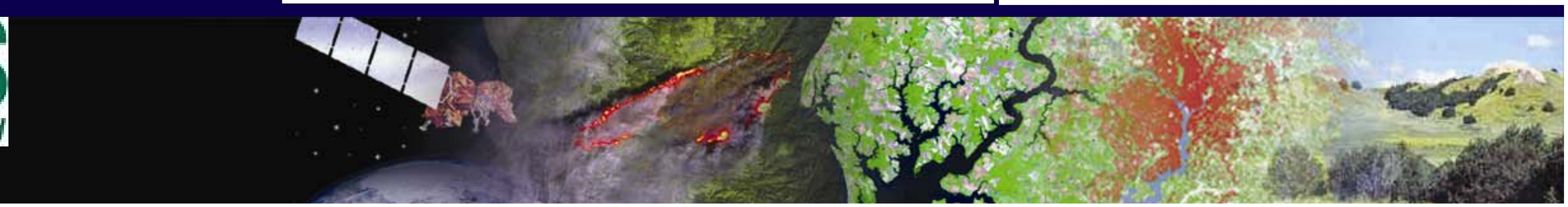

Concluding Thoughts II

Hyperspectral (imaging Spectroscopy)

Potential Products in Study of Vegetation

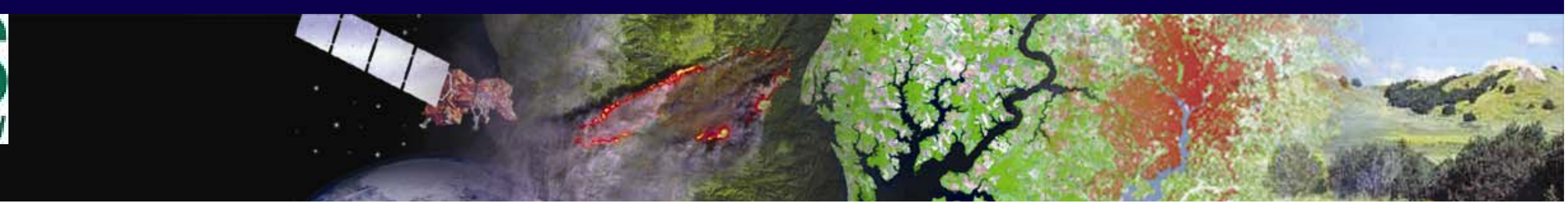

Hyperspectral (Imaging Spectroscopy) Products

6. Spectral Signature Data Bank of Vegetation Species (e.g., *P. Africana*)

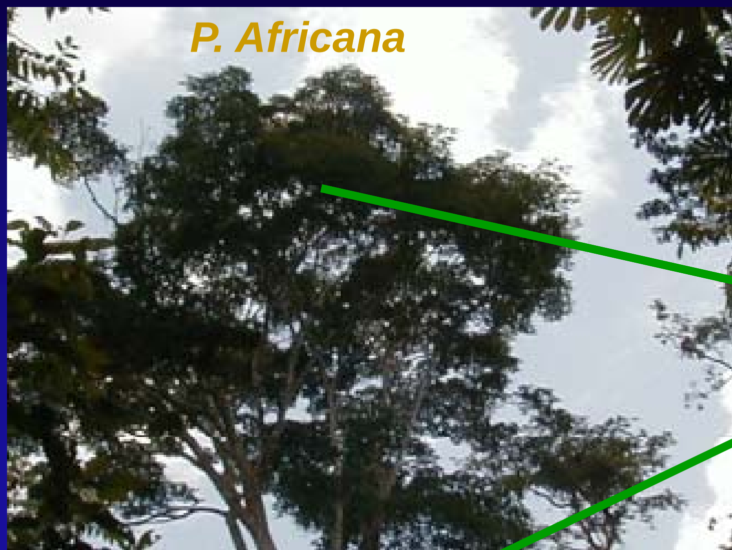

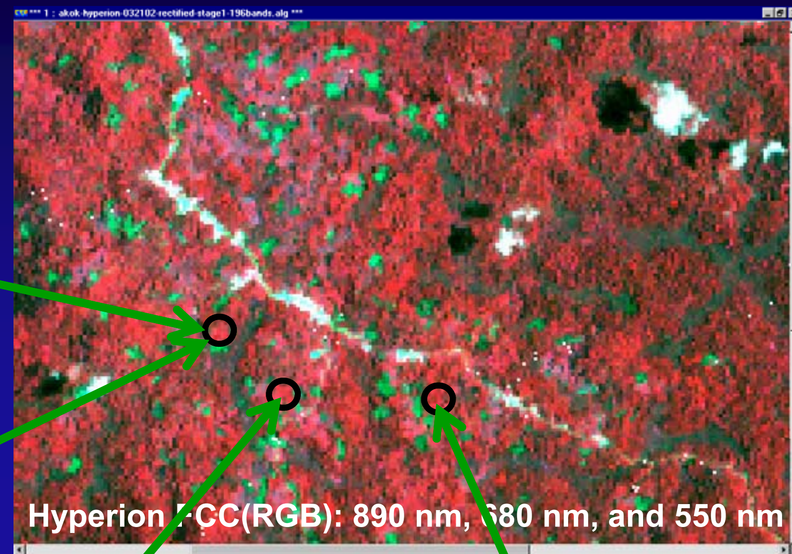

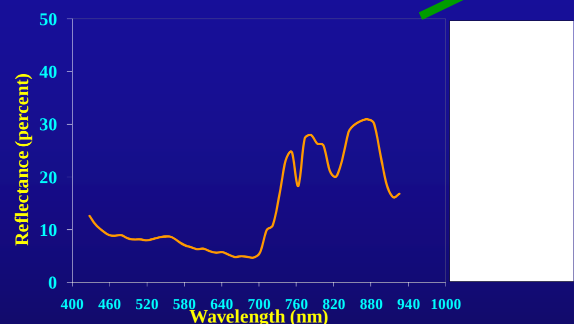

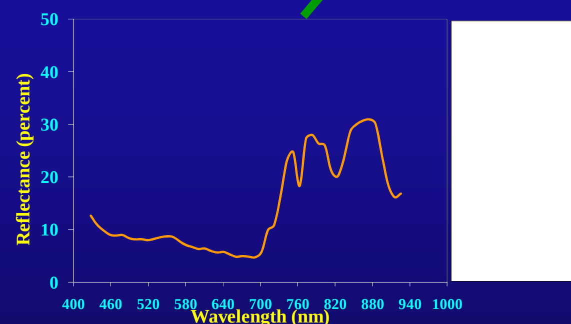

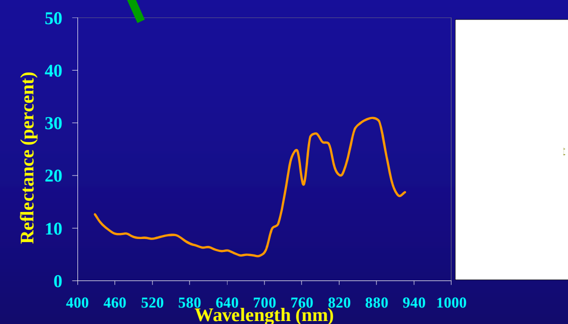

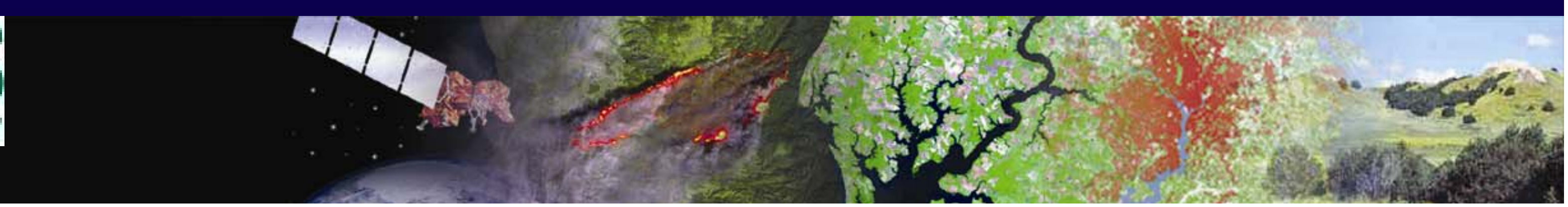

Hyperspectral (Imaging Spectroscopy) Products

5a. Specific Targeted Portion of the Spectrum to Study Specific Biophysical and Biochemical Property

Index	Equation	Reference
	Structure (LAI, green biomass, fraction)	
*NDVI	$(R_{NIR}-R_{red})/(R_{NIR}+R_{red})$	Rouse et al.[15]
*SR	R_{NIR}/R_{red}	Jordan [3]
*EVI	$2.5*(R_{NIR}-R_{red})/(R_{NIR}+6*R_{red}-7.5*R_{blue}+1)$	Huete et al.[23]
*NDWI	$(R_{857}-R_{1241})/(R_{857}+R_{1241})$	Gao [29]
**WBI	R_{900}/R_{970}	Peñuelas et al.[28]
*ARVI	$(R_{NIR}-[R_{red}-\gamma*(R_{blue}-R_{red})])/(R_{NIR}+[R_{red}-\gamma*(R_{blue}-R_{red})])$	Kaufman & Tanré [22]
*SAVI	$[(R_{NIR}-R_{red})/(R_{NIR}+R_{red}+L)]*(1+L)$	Huete [21]
**1DL_DGVI	$\sum_{\lambda_{626\,nm}}^{\lambda_{795\,nm}} \lvert R'(\lambda_i)-R'(\lambda_{626\,nm})\rvert \Delta\lambda_i$	Elvidge & Chen [1]
**1DZ_DGVI	$\sum_{\lambda_{626\,nm}}^{\lambda_{795\,nm}} \lvert R'(\lambda_i)\rvert \Delta\lambda_i$	Elvidge & Chen [1]
*VARI	$(R_{green}-R_{red})/(R_{green}+R_{red}-R_{blue})$	Gitelson et al.[13]
*VIgreen	$(R_{green}-R_{red})/(R_{green}+R_{red})$	Gitelson et al.[13]
	Biochemical	
	Pigments	
**SIPI	$(R_{800}-R_{445})/(R_{800}-R_{680})$	Peñuelas et al. [31]
**PSSR	(R_{800}/R_{675}); (R_{800}/R_{650})	Blackburn [30]
**PSND	$[(R_{800}-R_{675})/(R_{800}+R_{675})]$; $[(R_{800}-R_{650})/(R_{800}+R_{650})]$	Blackburn [32]
**PSRI	$(R_{680}-R_{500})/R_{750}$	Merzlyak et al. [33]
	Chlorophyll	
**CARI	$[(R_{700}-R_{670})-0.2*(R_{700}-R_{550})]$	Kim [34]
**MCARI	$[(R_{700}-R_{670})-0.2*(R_{700}-R_{550})]*(R_{700}/R_{670})$	Daughtry et al. [35]
**$CI_{red\ edge}$	$R_{NIR}/R_{red\ edge}-1$	Gitelson et al. [36]
	Anthocyanins	
**ARI	$(1/R_{green})-(1/R_{red\ edge})$	Gitelson et al.[40]
**mARI	$[(1/R_{green})-(1/R_{red\ edge})]*R_{NIR}$	Gitelson et al. [36]
**RGRI	R_{red}/R_{green}	Gamon & Surfus [7]
**ACI	R_{green}/R_{NIR}	Van den Berg & Perkins [41]
	Carotenoids	
**CRI1	$(1/R_{510})-(1/R_{550})$	Gitelson et al.[42]
**CRI2	$(1/R_{510})-(1/R_{700})$	Gitelson et al. [42]
	Water	
*NDII	$(R_{NIR}-R_{SWIR})/(R_{NIR}+R_{SWIR})$	Hunt & Rock [12]
*NDWI, **WBI	See Above	See Above
*MSI	R_{SWIR}/R_{NIR}	Rock et al. [43]
	Lignin &Cellulose/Residues	
**CAI	100*[0.5*(R2031+R2211)-R2101]	Daughtry [47]
**NDLI	$[\log(1/R_{1754})-\log(1/R_{1680})]/[\log(1/R_{1754})+\log(1/R_{1680})]$	Serrano et al. [48]
	Nitrogen	
**NDNI	$[\log(1/R_{1510})-\log(1/R_{1680})]/[\log(1/R_{1510})+\log(1/R_{1680})]$	Serrano et al. [48]
	Physiology	
	Light Use Efficiency	
RGRI,SIPI	See Above	See Above
**PRI	$(R_{530}-R_{570})/(R_{530}+R_{570})$	Gamon et al. [9]
	Stress	
*MSI	See Above	See Above
**REP	l(max first derivitive: 680-750 nm)	Horler et al. [10]
**RVSI	$[(R_{714}+R_{752})/2-R_{733}$	Merton & Huntington [52]

Specific structural indices

Specific biochemical indices

Specific physiological indices

Hyperspectral (Imaging Spectroscopy) Products

2. Generating Broadbands (e.g., Landsat, IKONOS) from Narrowbands (e.g., HyspIRI)

Hyperspectral image data cube

Hyperspectral image spectra

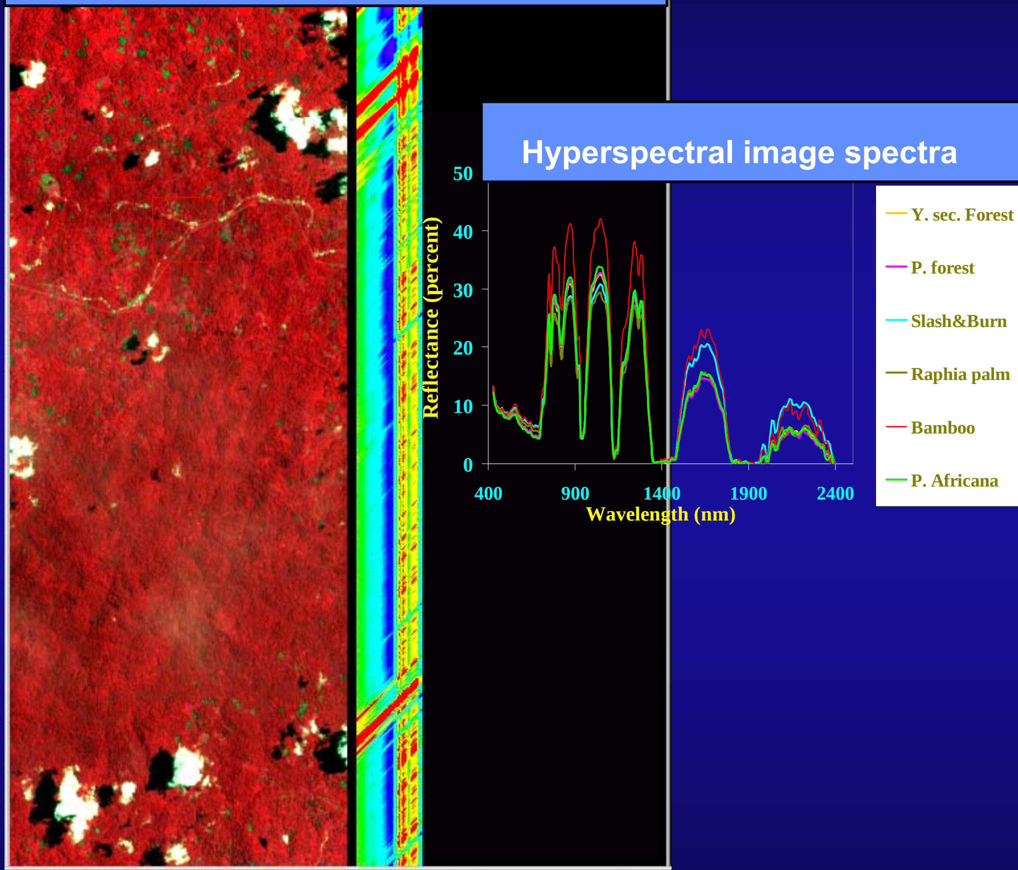

Generated Landsat ETM+ for data continuity: 6 non-thermal broadbands at 30 m of Landsat ETM+ Generated from a Hyperspectral Sensor

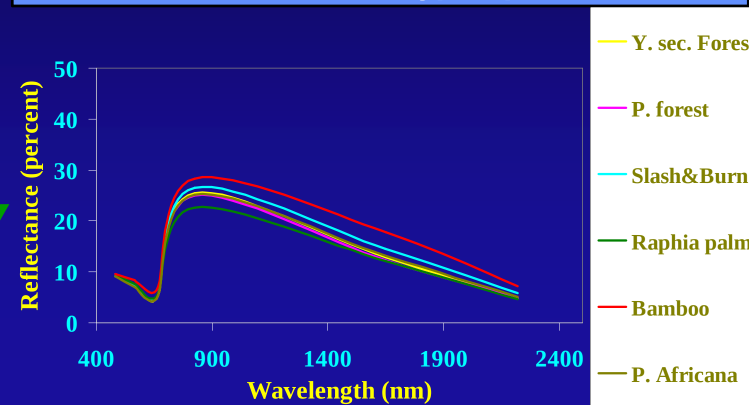

Generated IKONOS 4 m data: 4 broadbands at 4 m of IKONOS Generated from a Hyperspectral Sensor

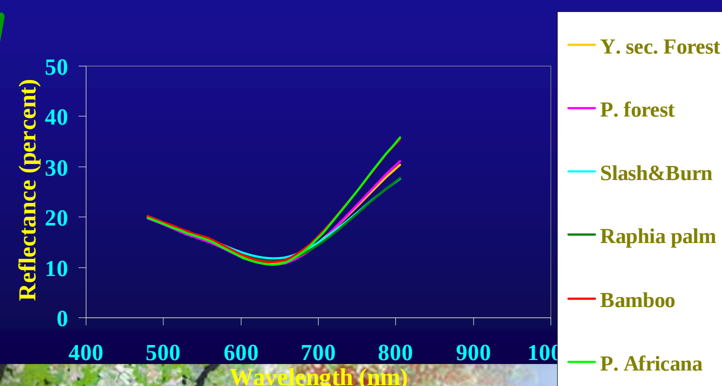

Imaging spectroscopy: 242 hyperspectral bands, each of 5 or 10 nm wide, in 400-2500 nm spectral range.

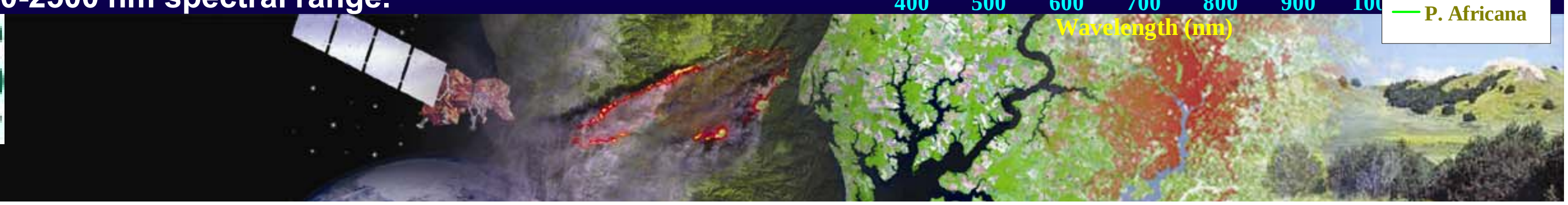

USGS
science for a changing world
U.S. Geological Survey
U.S. Department of Interior

Hyperspectral (Imaging Spectroscopy) Products

5b. Specific Targeted Portion of the Spectrum to Study Specific Biophysical and Biochemical Property

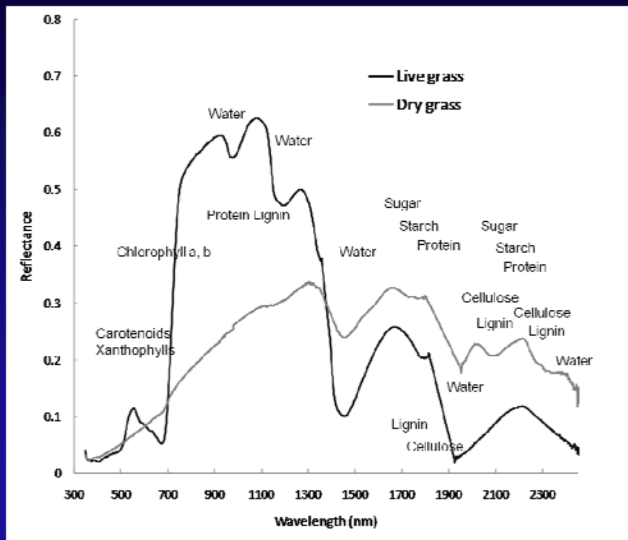

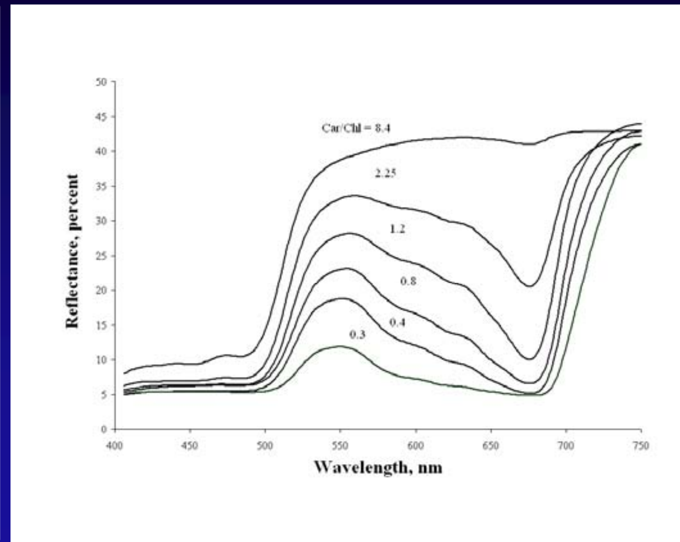

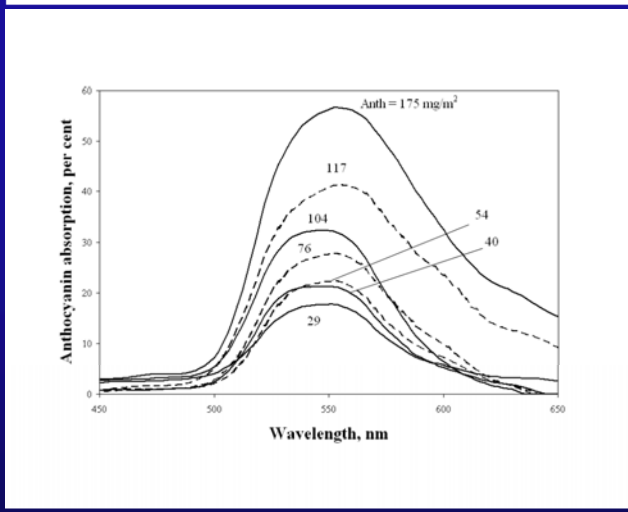

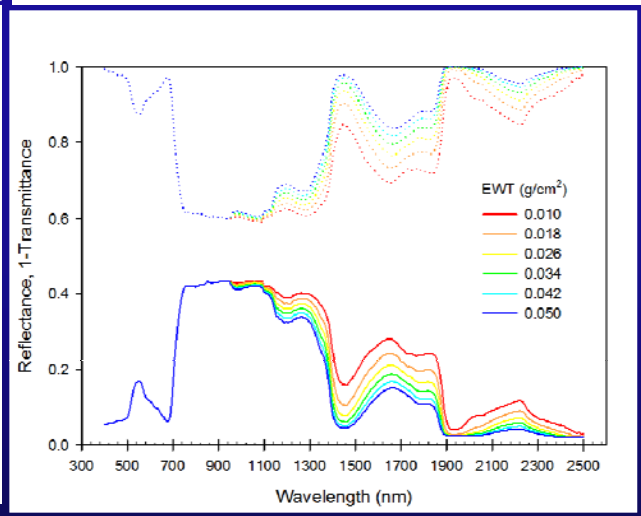

It is also important to know what specific wavebands are most suitable to study particular biophysical and/or biochemical properties. As examples, plant moisture sensitivity is best studied using a narrowband (5 nm wide or less) centered at 970 nm, while plant stress assessments are best made using a red-edge band centered at 720 nm (or an first order derivative index derived by integrating spectra over 700-740 nm range), and biophysical variables are best retrieved using a red band centered at 687 nm. These bands are, often, used along with a reference band to produce an effective index such as a two-band normalized difference vegetation index involving a near infrared (NIR) reference band centered at 890 nm and a red band centered at 687 nm.

Gitelson et al.

Knowledge Gain in using Hyperspectral Narrowband Data in Study of Vegetation

2.1a. Thirty-three (33) Optimal Bands in Study of Vegetation

A. Blue bands		
1	405	Nitrogen, Senescing
2	450	Chlorophyll, carotenoids, senescing
3	490	Carotenoid, Light use efficiency (LUE), Stress in vegetation
B. Green bands		
4	515	Pigments (Carotenoid, Chlorophyll, anthocyanins), Nitrogen, Vigor
5	531	Light use efficiency (LUE), Xanophyll cycle, Stress in vegetation, pest and disease
6	550	Anthocyanins, Chlorophyll, LAI, Nitrogen, light use efficiency
7	570	Pigments (Anthrocyanins, Chlorophyll), Nitrogen
C. Red bands		
8	650	Pigment, nitrogen
9	687	Biophysical quantities, chlorophyll, solar induced chlorophyll Floroscense
D. Red-edge bands		
10	705	Stress in vegetation detected in red-edge, stress, drought
11	720	Stress in vegetation detected in red-edge, stress, drought
12	700-740	Chlorophyll, senescing, stress, drought
E. Near infrared (NIR) bands		
13	760	Biomass, LAI, Solar-induced passive emissions
14	855	Biophysical\biochemical quantities, Heavy metal stress
15	970	Water absorption band
16	1045	Biophysical and biochemical quantities

Note 1: Overcomes data redundancy and yet retains optimal solution.

Note 2: for each band, a bandwidth of 3 nm will be ideal, 5 nm maximum to capture the best characteristics of vegetation.

Note:

* = wavebands were selected based on research and discussions in the chapters;

** = when there were close wavebands (e.g., 960 nm, 970 nm), only one waveband (e.g., 970 nm) was selected based on overwhelming eveidence as reported in various chapters. This would avoid redundancy.

*** = a nominal 5 nm waveband width can be considered optimal for obtaining best results with above wavebands as band centers. So, for 970 nm waveband center, we can have a band of range of 968-972 nm.

**** = The above wavebands can be considered as optimal for studying vehetation. Adding more waveband will only add to redundancy. Vegetation indices can be computed using above wavebands.

***** = 33 wavebands lead to a matrix of 33 x 33 = 1089 two band vehetation indices (TBVIs). Given that the indices above the diagonal and below diagonal replicate and indices along diagonal are redundant, there are 5

science for a changing world

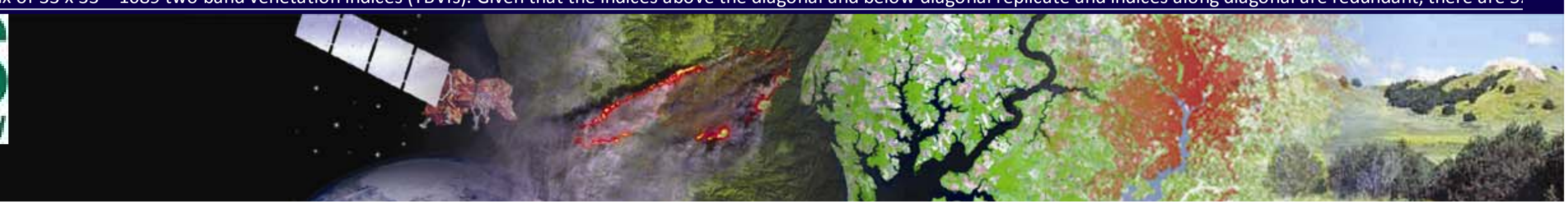

Knowledge Gain in using Hyperspectral Narrowband Data in Study of Vegetation

2.1b. Thirty-three (336) Optimal Bands in Study of Vegetation

E. Far near infrared (FNIR) bands		
17	1100	Biophysical quantities
18	1180	Water absorption band
19	1245	Water sensitivity
F. Early short-wave infrared (ESWIR) bands		
20	1450	Water absorption band
21	1548	Lignin, cellulose
22	1620	Lignin, cellulose
23	1650	Heavy metal stress, Moisture sensitivity
24	1690	Lignin, cellulose, sugar, starch, protein
25	1760	Water absorption band, senescence, lignin, cellulose
G. Far short-wave infrared (FSWIR) bands		
26	1950	Water absorption band
27	2025	Litter (plant litter), lignin, cellulose
28	2050	Water absorption band
29	2133	Litter (plant litter), lignin, cellulose
30	2145	Water absorption band
31	2173	Water absorption band
32	2205	Litter, lignin, cellulose, sugar, startch, protein; Heavy metal stress
33	2295	Stress and soil iron content

Note 1: Overcomes data redundancy and yet retains optimal solution.

Note 2: for each band, a bandwidth of 3 nm will be ideal, 5 nm maximum to capture the best characteristics of vegetation.

Note:

* = wavebands were selected based on research and discussions in the chapters;

** = when there were close wavebands (e.g., 960 nm, 970 nm), only one waveband (e.g., 970 nm) was selected based on overwhelming eveidence as reported in various chapters. This would avoid redundancy.

*** = a nominal 5 nm waveband width can be considered optimal for obtaining best results with above wavebands as band centers. So, for 970 nm waveband center, we can have a band of range of 968-972 nm.

**** = The above wavebands can be considered as optimal for studying vehetation. Adding more waveband will only add to redundancy. Vegetation indices can be computed using above wavebands.

***** = 33 wavebands lead to a matrix of 33 x 33 = 1089 two band vehetation indices (TBVIs). Given that the indices above the diagonal and below diagonal replicate and indices along diagonal are redundant, there are 5

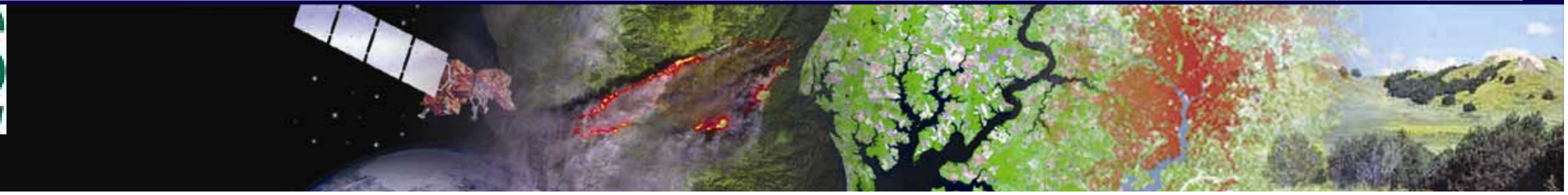

Hyperspectral Data on Tropical Forests

Advances in Combining Hyperspectral and LIDAR over Tropical Forests

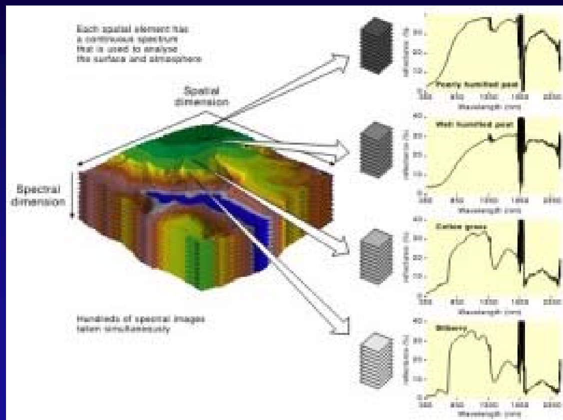

Hyperspectral for

canopy

biochemistry

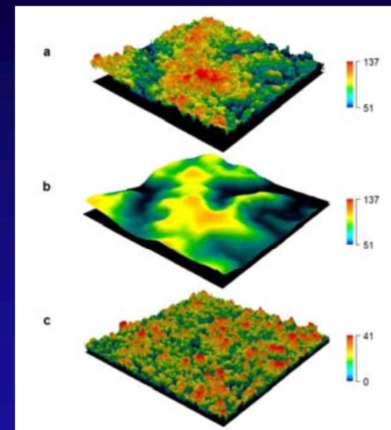

LIDAR for

canopy structure including

height,
crown shape,
leaf area,
biomass, and
basal area

Hyperspectral + LIDAR for

characterize parameters such as

height
canopy cover
leaf area
canopy chlorophyll content, and
canopy water content

Note: see chapter 20, Thomas et al.

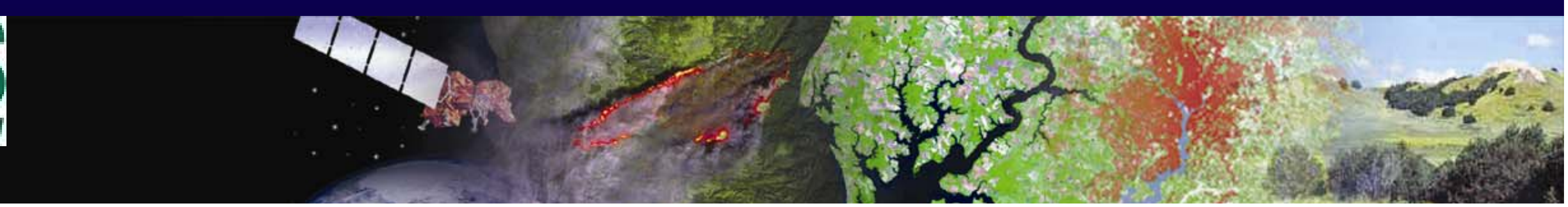

Publications

Hyperspectral Remote Sensing of Vegetation

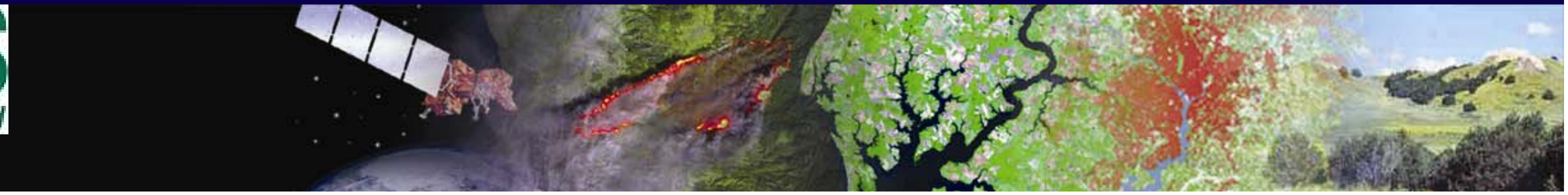

Hyperspectral Remote Sensing Vegetation

References Pertaining to this Presentation

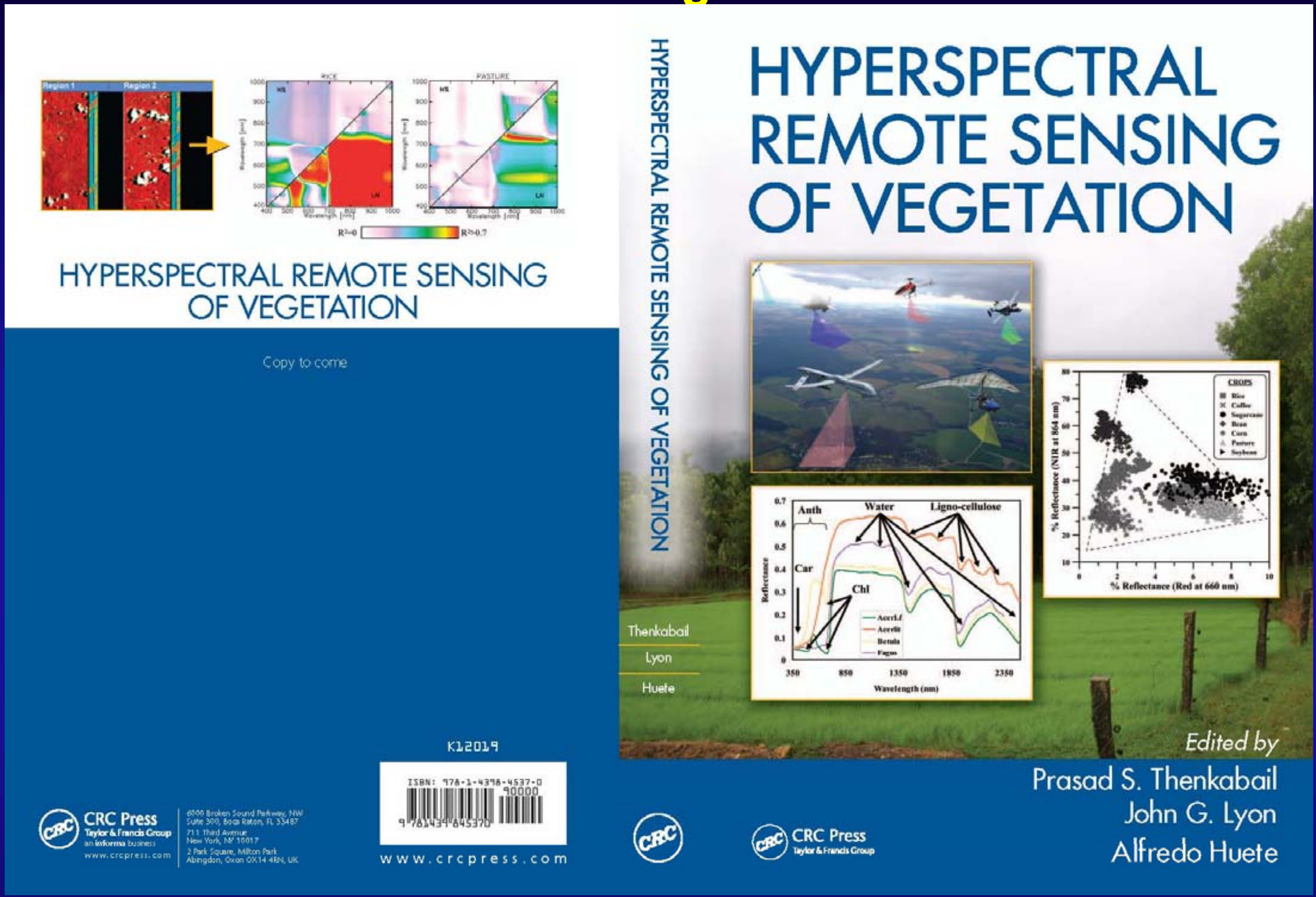

Thenkabail, P.S., Lyon, G.J., and Huete, A. 2011. Book entitled: "Hyperspectral Remote Sensing of Vegetation". 28 Chapters. CRC Press- Taylor and Francis group, Boca Raton, London, New York. Pp. 700+ (80+ pages in color). To be published by October 31, 2011.

Hyperspectral Remote Sensing Vegetation

References Pertaining to this Presentation

1. Thenkabail, P.S., Enclona, E.A., Ashton, M.S., Legg, C., Jean De Dieu, M., 2004. Hyperion, IKONOS, ALI, and ETM+ sensors in the study of African rainforests. Remote Sensing of Environment, 90:23-43.

2. Thenkabail, P.S., Enclona, E.A., Ashton, M.S., and Van Der Meer, V. 2004. Accuracy Assessments of Hyperspectral Waveband Performance for Vegetation Analysis Applications. Remote Sensing of Environment, 91:2-3: 354-376.

3. Thenkabail, P.S. 2003. Biophysical and yield information for precision farming from near-real time and historical Landsat TM images. International Journal of Remote Sensing. 24(14): 2879-2904.

4. Thenkabail P.S., Smith, R.B., and De-Pauw, E. 2002. Evaluation of Narrowband and Broadband Vegetation Indices for Determining Optimal Hyperspectral Wavebands for Agricultural Crop Characterization. Photogrammetric Engineering and Remote Sensing. 68(6): 607-621.

5. Thenkabail, P.S., 2002. Optimal Hyperspectral Narrowbands for Discriminating Agricultural Crops. Remote Sensing Reviews. 20(4): 257-291.

6. Thenkabail P.S., Smith, R.B., and De-Pauw, E. 2000b. Hyperspectral vegetation indices for determining agricultural crop characteristics. Remote sensing of Environment. 71:158-182.

7. Thenkabail P.S., Smith, R.B., and De-Pauw, E. 1999. Hyperspectral vegetation indices for determining agricultural crop characteristics. CEO research publication series No. 1, Center for earth Observation, Yale University. Pp. 47. Book:ISBN:0-9671303-0-1. (Yale University, New Haven).